



Università
Ca'Foscari
Venezia

**Scuola Dottorale di Ateneo
Graduate School**

**Dottorato di ricerca
in Scienze chimiche
Ciclo XXIX**

Life in Hydrocarbons: typical micelles in oil

**SETTORE SCIENTIFICO DISCIPLINARE DI AFFERENZA: Chim/06
Tesi di Dottorato di Manuela Facchin, matricola 819274**

Coordinatore del Dottorato

Prof. Maurizio Selva

Supervisore del Dottorando

**Prof. Alvise Perosa
Prof. Pietro Riello**

Estratto per riassunto della tesi di dottorato

Studente: Facchin Manuela matricola: 819274

Dottorato: Scienze Chimiche

Ciclo: XXIX°

Titolo della tesi : Life in Hydrocarbons: typical micelles in oil

Abstract:

La scoperta dei laghi di idrocarburi presenti sulla superficie di Titano ha sollevato la questione dell'esistenza di membrane in grado di auto-assemblarsi in idrocarburi che potrebbero essere alla base della vita extraterrestre.

In questa tesi vengono descritti design, sintesi e aggregazione di una nuova classe di anfifili inversi in solventi idrocarburici. Questi anfifili inversi di neo sintesi hanno una geometria simile a quella dei surfattanti tradizionali ma con configurazione topologica opposta, vale a dire testa lipofila e coda lipofobica.

La loro aggregazione in idrocarburi è stata studiata mediante una serie di tecniche diverse, tra le quali ¹H DOSY-NMR, SAXS, SANS, DSC, DLS. È stato dimostrato che gli anfifili inversi sintetizzati in questa tesi hanno la capacità di aggregarsi in solventi idrocarburici e di formare strutture micellari.

Abstract

The hydrocarbon lakes discovered on Titan prompted the question on the existence of membranes able to self-assemble in hydrocarbons that would be at the basis of life in such extra-terrestrial environments.

This thesis describes the design, synthesis and the self-assembly behavior of a new class of reverse amphiphiles in a hydrocarbon solvent. The synthesised reverse amphiphilic molecules possess a geometry similar to conventional amphiphiles but with an opposite topological configuration: lipophilic heads and lipophobic tails. Their self-assembly in hydrocarbons was studied by using a number of techniques, including ¹H DOSY-NMR, SAXS, SANS, DSC, DLS. It was demonstrated that the reverse amphiphiles synthesized in this project are capable of self-assembly in a hydrocarbon solvent and that they form organized micellar-like structures.

Firma dello studente

Manuela Facchin

Summary

1.1.	Preface	i
1.2.	Life on Titan	i
1.3.	References and notes	v
2.	Introduction: self-assembly of conventional surfactants	1
2.1.	Conventional surfactants	1
2.2.	The Hydrophobic effect	2
2.3.	Thermodynamics of micelle formation	3
2.4.	Critical Micelle Concentration.....	5
2.5.	Typical and reverse micelles	6
2.6.	Aim and structure of the thesis.....	7
	References and notes	11
3.	Results: Syntheses of the reverse amphiphiles.....	13
3.1.	The Geometric Packing Parameter	13
3.2.	Single-tail reverse amphiphiles.....	15
3.3.	Double-headed reverse amphiphiles.....	18
3.4.	Double-tailed reverse amphiphiles.....	19
3.5.	Experimental procedures:.....	27
	References and notes	33
4.	Introduction: Aggregates analysis methods.....	34
4.1.	Diffusion Ordered Nuclear Magnetic Resonance Spectroscopy (NMR-DOSY)	34
4.2.	Scattering techniques	35
4.3.	Dynamic light scattering	42
4.4.	Differential Scanning microCalorimetry (nano DSC).....	45
	References and Notes.....	47
5.	Results: Measurement of phase behaviour	48
5.1.	Dynamic Light Scattering (DLS)	48
5.1.1.	<i>DLS data discussion</i>	51
5.2.	Nano DSC	52
5.2.1.	<i>Nano DSC data discussions</i>	54
4.3.	2D-Diffusion Ordered Spectroscopy Nuclear Magnetic Resonance (2D-DOSY NMR)	55
4.3.1.	<i>2D-DOSY experiments acquisition and processing</i>	55
4.3.2.	<i>2D-DOSY results</i>	56
4.3.3.	<i>2D-DOSY data Discussions</i>	58
4.4.	Small Angle X-ray Scattering (SAXS) results	59

4.4.2.	<i>Solvent effect</i>	65
4.4.3.	<i>Addition of water effect</i>	68
4.4.4.	<i>SAXS Data discussions</i>	72
4.5.	Small Angle Neutron Scattering (SANS) results.....	75
4.5.1.	<i>Micelle detection: water and temperature effect</i>	75
4.5.2.	<i>SANS: Micelles in liquid methane</i>	82
4.5.3.	<i>SANS data discussion</i>	84
	References and notes	86
6.	Conclusions	87
	References and notes	95
	Appendix A.....	96
	A.1 <i>Chemical Potential</i>	96
	Appendix B	97
	Appendix C	98
	Abbreviations List	103

1. Introduction: self-assembly of conventional surfactants

1.1. Conventional surfactants

Surfactant science has seen great developments in its theoretical and applied fronts since the 1950's. Surfactants are among the most versatile products of the chemical industry and find wide uses as pharmaceuticals or detergents.

The last decades have seen the extension of surfactant applications to such high-technology areas as electronic printing, magnetic recording, biotechnology, micro-electronics, and viral research^[1].

Conventional surfactants (from surf(ace)-act(ive)) are amphiphilic molecules, composed by a hydrophilic part called head group and a hydrophobic part, called tail, that is capable of reducing the surface tension of a liquid.^[1] The head group may be ionic, zwitterionic or nonionic while the tail is usually a linear hydrocarbon. Examples of common, conventional surfactants are reported in figure 1.1. In this thesis, our interest is addressed to non-ionic surfactants.

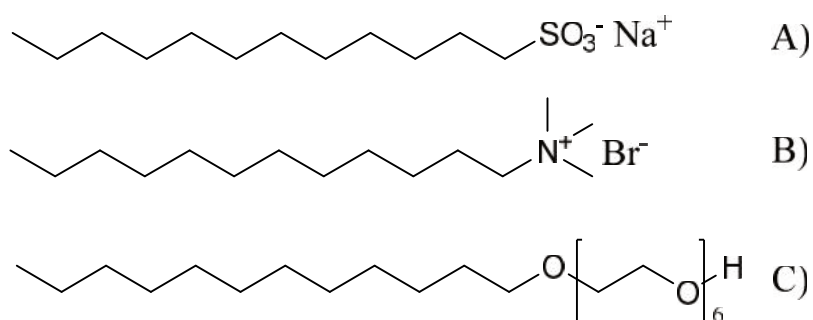


Figure 0.1 Examples of conventional surfactants, a) anionic surfactant sodium dodecyl sulfate (SDS), b) cationic surfactant trimethyl ammonium bromide (TTAB) and c) non-ionic surfactant hexaethylene glycol monododecyl ether (C12E6).

Non-ionic surfactants are excellent emulsifiers. They can be synthesised with a variety of head groups, such as sugar esters, alkanol amides and amine oxides^[2].

When dissolved in aqueous solution surfactants can self-assemble in the bulk into different structures.

Both these processes are driven by the hydrophobic effect. ^[3-4]

1.2. The Hydrophobic effect

Water is such an unusual substance that it has been reviewed extensively in the literature, not only because it is the most important liquid on Earth, but also because it has such interesting and anomalous properties that it is still a poorly understood liquid.

Although water has a low molecular weight, it has unexpectedly high melting and boiling point and high latent heat of vaporization. Also, its density maximum is at 4°C with ice being less dense than the liquid. All these properties are thought to arise from the ability of water to form tetrahedrally coordinated hydrogen bonds. These interactions are stronger than that expected even for ordinary highly polar liquids.

The literature on this subject is vast, and it was mainly developed around the '70s by Tanford,^[3] Israelachvili,^[5-6] Mitchell and Ninham^[5] who pioneered two of the most important ideas that explain water behaviour: the hydrophobic effect and intermolecular and surface forces.

The phenomenological definition of the hydrophobic effect begins with the fact that hydrocarbons have a much higher solubility in apolar organic solvents than they do in water^[3]. The common mechanism of solvation is based mainly on solute-solvent attractive forces. In the case of alkyl chains, solute-solvent attractive forces are weak both in hydrocarbon environment and in aqueous medium. The dipole-induced dipole attraction between H₂O and CH₂ groups may be slightly stronger than the attractive dispersion forces between CH₂ groups. On the other hand, water is characterized by a strong cohesive forces between water molecules and by the fact that the H₂O-H₂O bonds network is isotropic. Alkyl chains are literally squeezed out of the aqueous medium^[7-9].

1.3. Thermodynamics of micelle formation

Micelle formation is one of the most important characteristics of surfactants in solution and therefore it is important to understand its driving force and the mechanism of formation. In this paragraph, thermodynamics of micellization will be discussed from a general point of view. For a more detailed explanation, including charged surfactants, please refer to literature.^[7, 10-16]

Micellization is a dynamic process in which n monomeric surfactants S associate to form micelles^[17]



One of the thermodynamic parameters used to monitor micelle formation is critical micelle concentration (CMC, paragraph 2.3). Micelle formation can be associated to the formation of a separate phase, in fact when the aggregation has started, it becomes more and more favourable to add monomers until a large aggregation number is reached.^[18]

To calculate CMC, it is necessary to know the standard free energy of micelle formation (ΔG°), which is the energy required to take one mole of surfactant from solution and place it into micelles (at 25 degrees Celsius and 100 kilopascals). At equilibrium ΔG° is

$$\Delta G^\circ = \mu_B^\circ - \mu_A^\circ \quad (1.b)$$

where μ_B° and μ_A° are the standard state chemical potentials for a surfactant in state A and B respectively (see Appendix A).

Once ΔG° has been defined, this quantity can be reformulated in terms of an equilibrium constant describing micelle formation^[19-20] (eq 2.3):

$$\Delta G_{mic}^\circ = -RT \ln K \quad (1.c)$$

From this point two models can be used to derive ΔG_{mic}° , the micelle equilibrium model^[7, 12-13] and the pseudo-phase model^[12, 17, 19, 21]; they relate to the chemical potentials of the composition in two different ways.

The *equilibrium model* assumes that surfactants aggregate into micelles with a single, well-defined aggregation number in a reversible equilibrium process. Hence, this model has the disadvantage that monodispersity of the micellar aggregation number is assumed in spite of the fact that polydispersity exists^[19, 22]. The association-dissociation equilibrium constant (K_m) between surfactant monomers and micelles is given in eq 1.4

$$K_m = [S_n]/[S]^n \quad 1.4$$

where S is a surfactant molecule, n is the number of surfactants per micelle and square brackets represent the concentration.

The standard free energy per monomer is given by:

$$-\Delta G_{mic}^\circ = -\Delta G/n = (RT/n) \ln K_m = (RT/n) \ln [S_n] - RT \ln [S] \quad 1.5$$

for many micellar systems n is high enough to make the first term on the right negligible, resulting in Eq 1.6

$$\Delta G_{mic}^\circ = RT \ln [S] = RT \ln CMC \quad 1.6$$

As can be seen, ΔG_{mic}° is proportional to $\ln CMC$ and not CMC . Thus, ΔG_{mic}° increases exponentially with a decrease of CMC ^[12].

The *Pseudo-phase model* or *Phase separation model* assumes micelles as a single phase and the micelle formation as a phase separation phenomenon. In this case the CMC is the saturation concentration of the amphiphile in the monomeric state in which micelle constitute a separate pseudo phase^[17, 19, 21].

The chemical potential of the surfactant in the micellar state is assumed constant and may be adopted as standard chemical potential μ_{mic}° in analogy to a pure liquid. Taking into account the equilibrium between micelle and monomer, then,

$$\mu_{mic}^\circ = \mu_1^\circ + RT \ln a_1 \quad 1.7$$

where μ_1° is the standard potential of the single monomer and a_1 is the activity of that monomer. The free energy of micellization per mol of monomer is given by

$$\Delta G_{mic}^\circ = \mu_{mic}^\circ - \mu_1^\circ = RT \ln a_1 \quad 1.8$$

At high dilution the activity can be assumed equal to the mole fraction, and the CMC may be identified with the latter so that

$$\Delta G_{mic}^{\circ} = RT \ln CMC \quad 1.9$$

where the CMC is expressed in terms of molar fraction instead of concentration. It should be noticed that eq 1.9 is identical to the one derived for the equilibrium model^[17].

Although the Pseudo-phase model is much simpler than the Equilibrium model, its limitation is that it is applicable only to non-ionic surfactants.

1.4. Critical Micelle Concentration

Critical Micelle Concentration (CMC or C_M) is defined as the concentration of surfactants above which micelles form and all additional surfactants added to the system go to micelles^[23].

This definition is slightly misleading because of the singular form of the noun "concentration": the formation of micelles is a rapid and dynamic equilibrium, that implies dissociation and association processes. Experimentally, it is found that micelles are undetectable at very low concentration of monomers, and become detectable only over a narrow range of concentration, above which all solutes added forms micelles.

The concentration at which the micelles became detectable depends on the sensitivity of the technique used to detect them^[24].

It is important to find the CMC value because it reflects the surface and interfacial activity of amphiphilic molecules. As we have explained in paragraph 1.2, the tendency to form micelle arises mainly from the interaction between the hydrophobic part of the surfactant with the aqueous medium. Similar factors are involved in the surface activity of the monomer. There is thus a good correspondence between the adsorbability of monomers, their ability to reduce surface and interfacial tensions, and the value of CMC^[24]: the more surface active

the monomer is, the higher is the tendency to form micelles, and the lower the CMC value.

1.5. Typical and reverse micelles

The attractive force between water molecules drive the organization of amphiphilic molecules if they are in a sufficiently high concentration. In water the opposite thermodynamic preferences of the two ends of such a molecule are satisfied by self-association to form an aggregate with the hydrocarbon chains in the core, avoiding the contact with water, and the polar (or charged) heads at the surface. The resulting aggregate is called micelle and it typically contains 100 molecules per particle^[4]. see figure 1.2

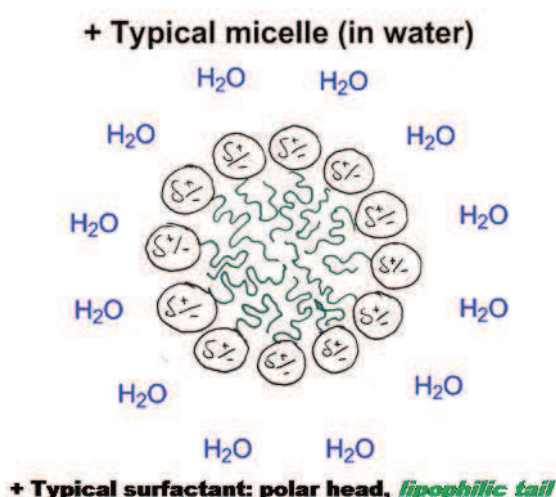


Figure 0.2 Cartoon representation of the association of surfactants to form micelles in water

Amphiphilic molecules can form micelles not only in water, but also in non-polar organic solvents, and these particles are called reverse micelles. In these type of aggregates the hydrocarbon tails are exposed to the solvent, while the polar heads point toward the core of the micelle to escape the contacts with the solvent.

Reverse micelles form a subset of structures that can exist in water-in-oil (w/o) microemulsions^[25].

In this case, reverse micelles form when an amphiphile delineates a nanoscale droplet of the aqueous phase from a non-polar medium, coating the surface of an

isolated water droplet in solution. These nanoscopic water pools have been applied in a wide range of processes from nanoparticle synthesis^[26-31], for the enhancement of chemical reaction rates^[32-35], to models for water in biological confinement^[36-40].

Inverse aggregate (e.g. micelle in hydrocarbon)

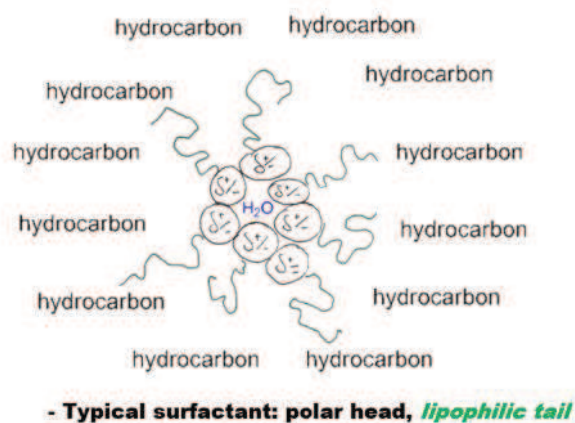


Figure 0.3 Cartoon representation of the association of surfactants to form reverse micelles

1.6. Aim and structure of the thesis

The work presented here is an experimental approach on the topic of how life could exist in an extra-terrestrial environment. We synthesized new amphiphile molecules, called reverse amphiphiles, with opposite electronic configuration to conventional surfactants, *i.e.* bearing lipophobic tails and lipophilic heads (see figure 1.4).

These reverse amphiphiles were designed to self-assemble in hydrocarbons in typical micellar structures. The geometry was based on a compact headgroup linked to a polar and linear tail.

The total length of amphiphiles was around 2nm, as for common surfactants in water. More details about the topologic conformation of reverse amphiphile will be presented in the following chapter.

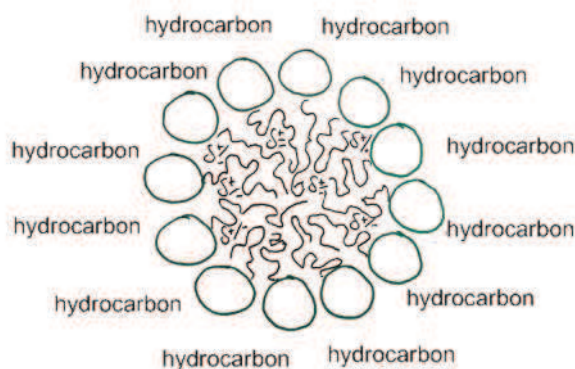
a) Conventional amphiphile b) Reverse amphiphile



Figure 0.4 cartoon representation of the structure of conventional amphiphiles (a) and reverse amphiphiles (b)

We thus proposed that typical kinds of aggregates are possible with a reverse surfactant whose lipophilic head faces out towards the hydrocarbon solvent (figure 1.5), similarly to what would be observed with a normal surfactant in water (figure 1.2).

Typical aggregate (e.g. micelle in hydrocarbon)



- Reverse surfactant: lipophobic tail, lipophilic head

Figure 0.5 Cartoon representation of the association of reverse amphiphiles to form typical micelles in hydrocarbons.

An explanation of the difference between the terms surfactant and amphiphile is due. A surfactant is a surface active agent^[1], or wetting agent, capable of reducing the surface tension of a liquid; typically organic compounds having a hydrophilic

"head" and a hydrophobic "tail"; an amphiphile is a chemical compound which has both hydrophilic and hydrophobic properties and many of such compounds show surface active properties. Amphiphilic molecules often exhibit self-assembly behaviour similar to conventional surfactants.^[41] Our interest is on amphiphilic molecules that can aggregate in micelles or membranes. In the first part of this thesis we will go through an overview of common surfactants properties in water and then we will focus on reverse amphiphiles. We will refer to the latter with the term amphiphiles, because we studied only their self-assembly behaviour.

A chapter will be dedicated to the design and synthesis of reverse amphiphiles, followed by the study of their aggregation behaviour in different hydrocarbon solvents.

Although we didn't obtain bilayer membranes, we here present the proof that reverse amphiphiles assemble in hydrocarbons. It must be stressed that the in this thesis the observed structures are not reverse micelles as expected by dissolving a normal surfactant in a hydrocarbon solvent (Figure 1.3).

This kind of amphiphilic molecules are feasible to obtain more complex structures, only changing their geometry.

References and notes

- [1] Milton J. R., Joy T. K., in *Sfatabad Interfacial Phenomena*, John Wiley & Sons, Inc., **2012**, pp. 1-38.
- [2] M. J. Schick, *Non-ionic surfactants*, Schick, M.J. ed., Marcel Dekker, New York, **1967**.
- [3] C. Tanford, *The hydrophobic effect: formation of micelles and biological membranes*, Wiley, New York, **1973**.
- [4] C Tanford, *Science* **1978**, 200, 1012-1018.
- [5] J. N. Israelachvili, D. J. Mitchell, B. W. Ninham, *Journal of the Chemical Society, Faraday Transactions 2: Molecular and Chemical Physics* **1976**, 72, 1525-1568.
- [6] J. N. Israelachvili, D. J. Mitchell, B. W. Ninham, *Biochimica et Biophysica Acta (BBA) - Biomembranes* **1977**, 470, 185-201.
- [7] G. S. Hartley, *Aqueous solutions of paraffin-chain salts; a study in micelle formation, ch7*, Hermann & cie, Paris, **1936**.
- [8] H. S. Frank, M. W. Evans, *The Journal of Chemical Physics* **1945**, 13, 507-532.
- [9] W. Kauzmann, in *Advances in Protein Chemistry*, Vol. Volume 14 (Eds.: M. L. A. K. B. C.B. Anfinsen, T. E. John, Academic Press, **1959**, pp. 1-63.
- [10] R. C. Murray, G. S. Hartley, *Transactions of the Faraday Society* **1935**, 31, 183-189.
- [11] M. J. Vold, *Journal of Colloid Science* **1950**, 5, 506-513.
- [12] J. N. Phillips, *Transactions of the Faraday Society* **1955**, 51, 561-569.
- [13] J. M. Corkill, J. F. Goodman, T. Walker, J. Wyer, *Proceedings of the Royal Society of London A: Mathematical, Physical and Engineering Sciences* **1969**, 312, 243-255.
- [14] G. Stainsby, A. E. Alexander, *Transactions of the Faraday Society* **1950**, 46, 587-597.
- [15] E. Matijevic, B. A. Pethica, *Transactions of the Faraday Society* **1958**, 54, 587-592.
- [16] K. Shinoda, E. Hutchinson, *The Journal of Physical Chemistry* **1962**, 66, 577-582.
- [17] T. F. Tadros, in *Applied Surfactants*, Wiley-VCH Verlag GmbH & Co. KGaA, **2005**, pp. 19-51.
- [18] E. Fiscaro, C. Compari, E. Duce, M. Biemmi, M. Peroni, A. Braibanti, *Phys Chem Chem Phys* **2008**, 10, 3903-3914.
- [19] M. J. Blandamer, P. M. Cullis, L. G. Soldi, J. B. F. N. Engberts, A. Kacperska, N. M. Van Os, M. C. S. Subha, *Advances in Colloid and Interface Science* **1995**, 58, 171-209.
- [20] J. R.; Goates, J. B. Ott, *Chemical Thermodynamics*, Elsevier Science & Technology Books New York, **1971**.
- [21] Y. Moroi, *J Colloid Interf Sci* **1988**, 122, 308-314.
- [22] P.A. FitzGerald, PhD thesis, *Solution behaviour of Polyethylene Oxide, Nonionic Gemini Surfactants*, The University of Sydney **2002**.

- [23] A. D. McNaught, A. Wilkinson, *IUPAC. Compendium of Chemical Terminology*, Blackwell Scientific Publications, Oxford, **1997**.
- [24] P. Mukherjee, K. J Mysels, *Critical micelle concentration of aqueous surfactant systems, Vol. NSRDS-NBS 36*, NIST National Institute of Standards and Technology:, Washington D.C., **1971**.
- [25] N. M. Correa, J. J. Silber, R. E. Riter, N. E. Levinger, *Chem Rev* **2012**, 112, 4569-4602.
- [26] M. P. Pileni, *The Journal of Physical Chemistry* **1993**, 97, 6961-6973.
- [27] M. P. Pileni, *Langmuir* **1997**, 13, 3266-3276.
- [28] Y. Xia, J. A. Rogers, K. E. Paul, G. M. Whitesides, *Chem Rev* **1999**, 99, 1823-1848.
- [29] H. Bönemann, R. M Richards, *Eur J Inorg Chem* **2001**, 2001, 2455-2480.
- [30] M. P. Pileni, *Nat Mater* **2003**, 2, 145-150.
- [31] J. Eastoe, M. J. Hollamby, L. Hudson, *Advances in Colloid and Interface Science* **2006**, 128–130, 5-15.
- [32] M. T. de Gómez-Puyou, A. Gómez-Puyou, *Critical Reviews in Biochemistry and Molecular Biology* **1998**, 33, 53-89.
- [33] C. M. L. Carvalho, J. M. S. Cabral, *Biochimie* **2000**, 82, 1063-1085.
- [34] K. Holmberg, *Curr Opin Colloid In* **2003**, 8, 187-196.
- [35] N. L. Klyachko, A. V. Levashov, *Curr Opin Colloid In* **2003**, 8, 179-186.
- [36] D. P. Siegel, *Biophys J* **1986**, 49, 1171-1183.
- [37] S. Fiori, C. Renner, J. Cramer, S. Pegoraro, L. Moroder, *J Mol Biol* **1999**, 291, 163-175.
- [38] N. Nandi, K. Bhattacharyya, B. Bagchi, *Chem Rev* **2000**, 100, 2013-2046.
- [39] S. Rasmussen, L. Chen, M. Nilsson, S. Abe, *Artificial Life* **2003**, 9, 269-316.
- [40] S. Kawamoto, M. Takasu, T. Miyakawa, R. Morikawa, T. Oda, S. Futaki, H. Nagao, *The Journal of Chemical Physics* **2011**, 134, 095103.
- [41] R. Nagarajan, in *Amphiphiles: Molecular Assembly and Applications*, Vol. 1070, American Chemical Society, **2011**, pp. 1-22.

Preface

Life on Titan

"As the search for life in the solar system expands, it is important to know what exactly to search for". ^[1] This statement has been the trigger of this project. The most established approach to the search for life is focused on planets where liquid water is possible and it emphasizes the search for water-based life-as-we-know-it-on-Earth ^[2-3]. Following the Cassini-Huygens mission on Saturn's moon Titan, the astrobiology community is now debating whether life forms are possible on such planetary systems where the surface temperature is 95 K and with abundant nitrogen (95-99% N₂) and gaseous methane (1-5% CH₄) as well as massive methane and ethane lakes in the vicinity of the polar regions^[4]. McKay and Smith^[5] and Shultze-Mackuch and Grispoon^[6] have proposed a scenario in which a microbial life could have developed in such lakes.

Titan possesses an atmospheric "hydrocarbon cycle"^[7-8] that creates complex organic molecules, potential precursors for prebiotic syntheses. For example, the photochemical conversion of methane present in Titan's troposphere generates hydrogen and acetylene ($2\text{CH}_4 \rightarrow \text{C}_2\text{H}_2 + 3\text{H}_2$), that eventually "rain" to the surface. In this model, acetylene would be available as a nutrient and energy source for hydrocarbon-based life forms, e.g. by recombining with hydrogen in the reverse reaction ($\text{C}_2\text{H}_2 + 3\text{H}_2 \rightarrow 2\text{CH}_4$). Coincidentally, depletion in the concentration of hydrogen between the upper atmosphere and the surface of Titan was observed^[9], although the reasons for its disappearance are still obscure.

One possible answer is that something on the surface of Titan uses H₂ to hydrogenate acetylene producing energy. This consumption could result either from the photochemical destruction of methane followed by the escape of Hydrogen to space^[8] or from an organism consuming acetylene and hydrogen to sustain itself ^[5-6].

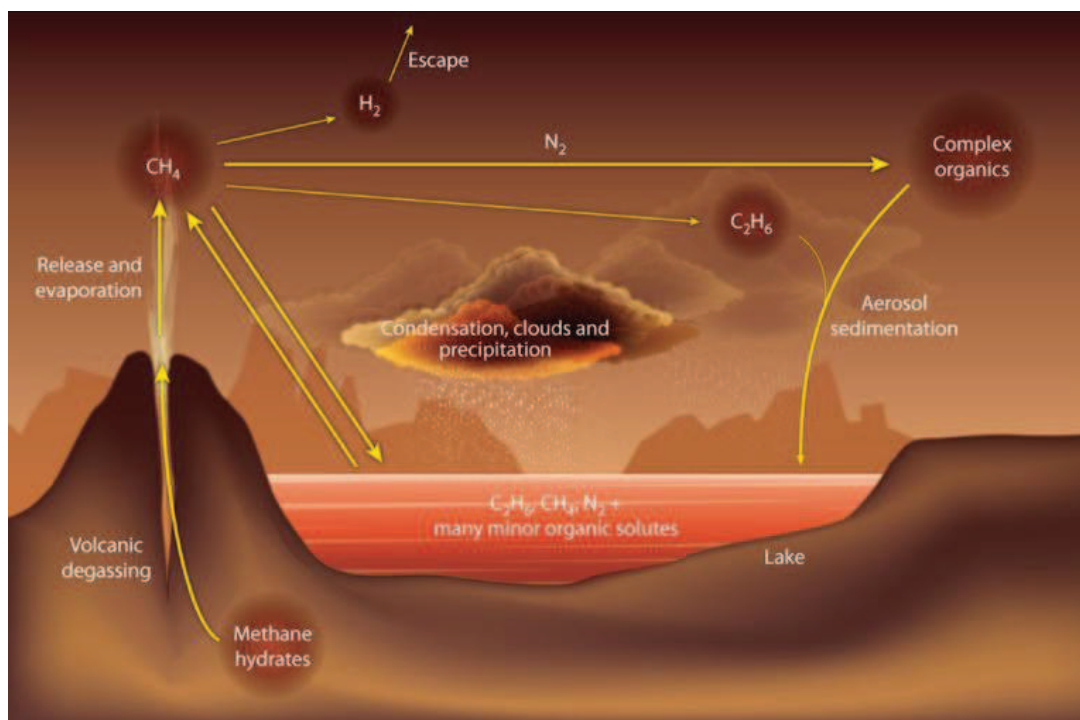


Figure P1: Scheme of Hydrocarbon cycle on Titan's atmosphere^[10]

The latter hypothesis implies a revision of the paradigm of life-as-we-know-it-on-Earth in order to adapt it to the hydrocarbon solvent. Life forms can be loosely defined as self-sustaining organized molecular aggregates compartmentalized by a boundary lipid bilayer which separates cellular components from the extracellular environmental and that are able to reproduce and evolve based on the following set of fundamental requirements:

- (i) A self-assembled structure to define the boundary layer of the organism, such as a permeable membrane that mediates transport between the outer environment and the inner core, *e.g.* cellular membranes on Earth.
- (ii) Energy to sustain the organism, either chemical or external, *e.g.* solar energy.
- (iii) Autocatalysis to provide accessible chemical pathways to transform nutrients into other chemicals (body constituents and waste products) and energy, *e.g.* photosynthesis on Earth.
- (iv) Finally, an organism must be able to store information in the form of an organized structure able to replicate itself, *e.g.* nucleic acids on Earth.

For Earth-like organisms, one must add two additional constraints: (v) carbon as the fundamental element and (vi) liquid water as a medium.^[1]

Based on the requirements outlined above, one can imagine two different types of life forms in the methane lakes of Titan.

The first kind would include Earth-like organisms with a lipid-based membrane that feed on hydrocarbons, e.g. similar to the ones on Earth that anaerobically oxidize methane to carbon dioxide^[11-12].

The second alternative implies reversing the paradigm of life. Compartmentalization in methane would occur by the self-assembly of reverse amphiphiles to form membranes in the hydrocarbon solvent. Such reverse amphiphiles should possess a lipophobic tail and a lipophilic head in order to be able to self-assemble in the hydrocarbon solvent by orienting their lipophilic heads outwards.

Previous reports of vesicle formation in non-aqueous environments already exist. Bryant, Atkin and Warr,^[13] proved that phospholipids self-assemble to form vesicles in a choline chloride-urea deep eutectic solvent system; again, Gayet and ^[14] and collaborators studied vesicle formation of 1,2-dipalmitoyl-sn-glycero-3-phosphocholine (DPPC) in ionic liquids. Both these reports demonstrated the possibility of aggregate formation in a non-aqueous environment but still involve typical amphiphiles and highly polar solvents. In this scenario, though, an important requirement is missing. With the rearrangement of phospholipids in reverse vesicles, the insertion of macromolecules that permits transport of chemical species across the membrane is not possible, due to the absence of the lipophilic micro-phase created by the surfactant tails. Our interest on this topic was born from this inconsistency, and by the fact that all the research for life activity in extreme environments is focused on the search for life-on-earth based molecules.

This project aims at providing evidence of the possibility of self-aggregation of reverse surfactants in hydrocarbons and at proposing a different way of thinking of life in non-aqueous media.

Theoretical support already exists and in fact Cornell scientists have recently offered computational support to life in Titan's methane lakes. Their theorised cell membranes, dubbed "azotosomes" in analogy to liposomes, are composed of small organic nitrogen compounds that were calculated to be capable of forming vesicles in liquid methane at 94 K. Modelling suggests that they would possess stability and flexibility similar to liposomes on Earth.^[15] Up to date, this represents the only attempt towards defining the parameters on the basis of the formation of self-assembled aggregates of non-conventional amphiphiles in hydrocarbons.

We here wish to give an experimental support of life developing in non-aqueous environments. The idea was born reading about the possibility of life on Titan's methane lakes^[16], but that hydrocarbon lakes exist in many other environments, including on Earth^[17]. Therefore, hydrocarbon solvents as for example cyclohexane, were used as a model solvent in order to demonstrate that our idea could be substantiated by experimental data.

References and notes

- [1] *The Limits of Organic Life in Planetary Systems*, Nature Publishing Group, **2007**.
- [2] I. Asimov, *Not as We Know it The Chemistry of Life, Vol. 3*, North American AstroPhysical Observatory (NAAPO), **1981**.
- [3] I. Asimov, *Isaac Asimov's Guide to Earth and Space*, Fawcett, **1992**.
- [4] E. R. Stofan, *Nature* **2007**, 445, 61-64.
- [5] C. P. McKay, H. D. Smith, *Icarus* **2005**, 178, 274-276.
- [6] Dirk Schulze-Makuch, David H. Grinspoon, *Astrobiology* **2005**, 5, 560-567.
- [7] S. K. Atreya, *Planet.Space Sci.* **2006**, 54, 1177-1187.
- [8] J. I. Lunine, S. K. Atreya, *Nature Geosci* **2008**, 1, 159-164.
- [9] D. F. Strobel, *Icarus* **2010**, 208, 878-886.
- [10] Francois Raulin, *Nature* **2008**, 454, 587-589.
- [11] C. R. Fisher, I. R. MacDonald, R. Sassen, C. M. Young, S. A. Macko, S. Hourdez, R. S. Carney, S. Joye, E. McMullin, *Naturwissenschaften* **2000**, 87, 184-187.
- [12] Jennifer B. Glass, Hang Yu, Joshua A. Steele, Katherine S. Dawson, Shulei Sun, Karuna Chourey, Chongle Pan, Robert L. Hettich, Victoria J. Orphan, *Environmental Microbiology* **2014**, 16, 1592-1611.
- [13] S. J. Bryant, R. Atkin, G. G. Warr, *Soft Matter* **2016**, 12, 1645-1648.
- [14] Florence Gayet, Jean-Daniel Marty, Annie Brûlet, Nancy Lauth-de Viguerie, *Langmuir* **2011**, 27, 9706-9710.
- [15] J. Stevenson, J. Lunine, P. Clancy, *Science Advances* **2015**, 1.
- [16] Lucy H Norman, *Astron Geophys* **2011**, 52, 1.39-31.42.
- [17] Felisa Wolfe-Simon, Jodi Switzer Blum, Thomas R. Kulp, Gwyneth W. Gordon, Shelley E. Hoefft, Jennifer Pett-Ridge, John F. Stolz, Samuel M. Webb, Peter K. Weber, Paul C. W. Davies, Ariel D. Anbar, Ronald S. Oremland, *Science* **2011**, 332, 1163-1166.

2. Results: Syntheses of the reverse amphiphiles

The design of new kinds of amphiphiles able to assemble in hydrocarbons to give typical micelles requires some preliminary considerations. The geometry of the molecules as well as the polarity of its constituents need to be considered.

2.1. The Geometric Packing Parameter

The possible aggregate shapes are basically three: spheres, rods or bilayers, all others can be considered as distortions of these. The size and shape of aggregates depend on thermodynamic factors and on the amphiphile properties^[1].

The packing geometry of the amphiphile depends on their optimal headgroup area a_0 , the volume of the chain v (or chains) and the maximum effective length that the chain l_c can assume. The latter is also called critical length and sets a limit on how far the chain can extend; smaller extensions are possible, but further extensions are not. The length of the surfactant determines the radius of the micelle or the thickness of the double layer.

Besides, repulsive headgroup forces and attractive hydrophobic interfacial forces determine the "optimal surface area" per headgroup (or optimal headgroup area) for which the total interaction free energy per lipid molecule is a minimum.^[2]

The repulsive contribution is too complex to formulate explicitly because it contains the steric contribution, a hydration force contribution, and an electrostatic double layer contribution if the headgroups are charged.

Once all these parameters are specified for a given molecule, it is possible to calculate the Geometric Packing Parameter (GPP)^[3] defined as the dimensionless number $GPP=v/a_0l_c$.

This number gives an indication of the limiting packing shapes that the molecule can adopt in the structure they assemble into (see fig 2.1).

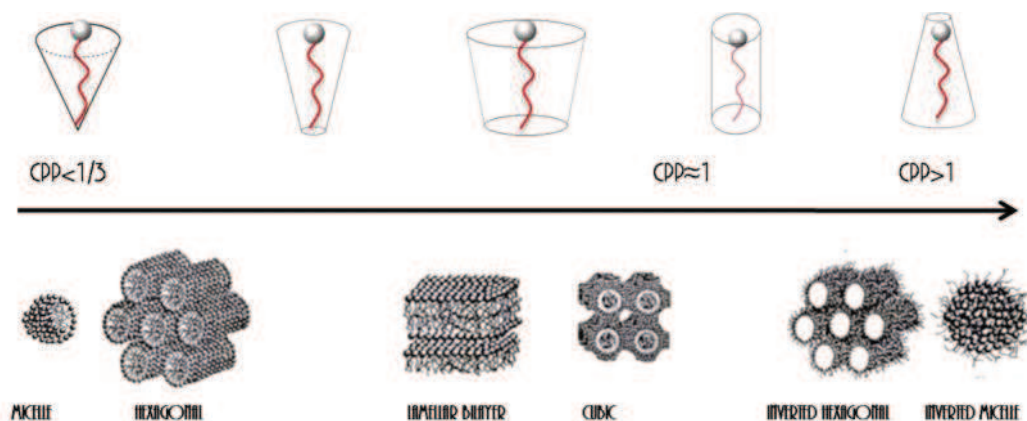


Figure 2.1 Relationship between surfactant GPP and aggregation behaviour

For micelles, changes in shape are determined solely by a_0 , if l_c and v are constant. Decreasing a_0 the packing parameter increases from one third (spherical micelles) to one half (rod-like micelles) to eventually one (bilayers). This transition from spherical micelles to bilayers can also be rationalised by considering the aggregate curvature: small GPPs lead to highly curved aggregates (e.g. spheres) whereas larger GPPs lead to aggregates with reduced curvature (e.g. vesicles or bilayers).^[4] The choice of the geometry of the new reverse amphiphiles was dictated in a first approximation by previous experience on analogous amphiphiles. For example, a large C60-fullerene head with a short aminoacidic tail^[5] has an excessively small GPP; at the other extreme we took triethylene glycol mono ethyl ether and attempted to measure its small angle x-ray scattering SAXS in solution and no aggregation was observed. The choice of the structure was further refined based on the observation that phospholipids have two lipophilic tails and a packing geometry suitable to form double layers in water typical of cell membranes (length ≈ 2 nm, GPP $\approx 0.5-0.8$). Self-assembly of amphiphiles of this size would lead to an overall bilayer thickness of 4 nm.^[6]

We therefore chose to synthesise amphiphiles with different geometries (different GPPs) in order to study their self-assembly in different kind of aggregates. We started with the synthesis of amphiphiles with one head and one tail (GPP ≈ 0.3) in order to obtain the simplest case. Once we observed aggregation of these

molecules to form micelles, we then started changing the geometry in order to get different aggregation such as lamellar phases or bilayer vesicles.

We thus synthesized several molecules bearing one head and one tail, one with two heads linked with one tail, and we started the synthesis of one bearing one head and two tails.

2.2. Single-tail reverse amphiphiles

In order to study the simplest aggregation form, that is the micelle, we started by synthesizing amphiphile molecules with a packing factor calculated to be approximately 0.3. This GPP is typical of amphiphiles bearing a small compact head and one linear tail. These reverse amphiphiles possess a polar tail and a lipophilic head and thus, based on their geometry, they were expected to form typical micellar structures in a hydrocarbon solvent. In such an arrangement they can expose a tightly packed lipophilic surface towards the hydrocarbon solvent, while reducing the interaction between the hydrophilic core and the hydrocarbon solvent. The driving force for assembly could be considered a sort of “lipophobic effect”. (see figure 1.5 in previous chapter)

The precursors were then chosen by taking into account different electronic properties. Table 2.1 shows all the single-tailed reverse amphiphiles synthesised. Each one is labelled with a number used throughout this thesis.

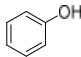
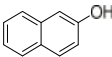
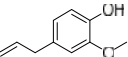
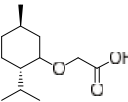
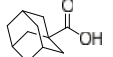
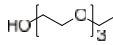
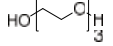
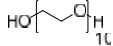
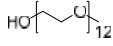
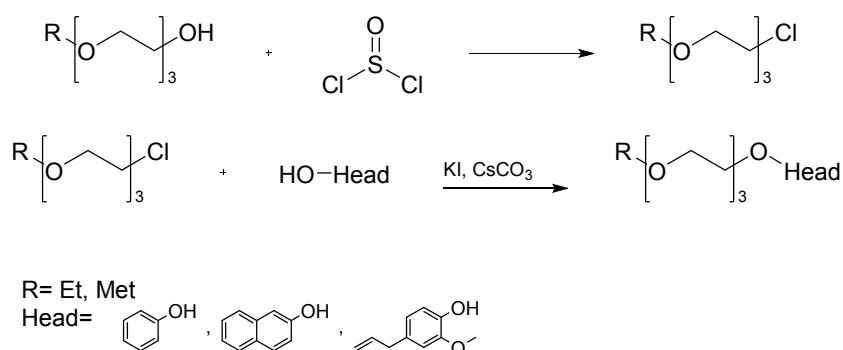
					
	1	2	3	4	5
				6	7
					8
				9	

Table 2.1 table of one-tailed reverse amphiphiles synthesised

Different approaches were adopted for the synthesis of single-tailed reverse amphiphiles based on the precursors used. In all cases our target was to bond the headgroup to the hydroxyl group of the polyethylene glycol (PEG) used. Therefore, the synthetic route was essentially based on the reactive group available on the headgroup.

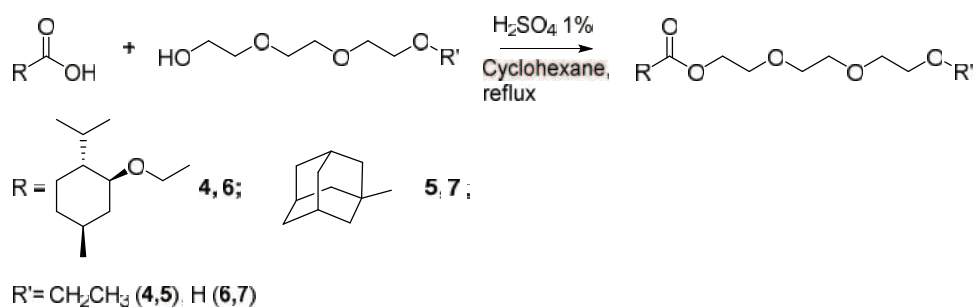
In Scheme 2.1 is reported the general synthetic route for surfactants **1-3**.



Scheme 2.1 general synthetic route adopted for amphiphiles 1-3

The first reaction step is the chlorination of PEG. This reaction allowed to obtain a better leaving group useful for the subsequent reaction step. The second step involves nucleophilic substitution of the PEG-chloride by the hydroxyl group functionalized head. Different bases were tested, all in stoichiometric excess. The best was Cs_2CO_3 that allowed reaching 50-70% conversion. All products were purified by Flash Column Chromatography (FCC), up to 80-90% purity.

Scheme 2.2, instead, shows the synthetic route adopted to synthesise amphiphiles **4-9**. The general reaction was an acid-catalysed esterification reaction between menthyloxyacetic acid or adamantanoic acid as head precursors, and triethylene glycol (TEG) or triethylene glycol monoethyl ether (TEGME) as tail precursors. This simple synthetic route have been applied under different condition depending on the polyethylene glycol used (details in experimental procedures).



Scheme 2.2 synthetic route for the single-tailed reverse surfactants.

Several features distinguish all these amphiphiles. The menthyl and the adamantane moieties were chosen because are non-polar and because of their compact geometry, that largely determines the GPP. The main difference between them is that the menthyl has a more “flat” geometry while the adamantane is more spherical.

For what concerns the tail, all the PEGs used are different in terms of length and polarity. With a longer chain (PEG 400 for compound **8** and PEG 550 for compound **9**) the v_c is bigger, and the GPP shifts in the range of lamellar phases or vesicles. On the other hand, at the same chain length (compounds **4-7**) the polarity of PEG dramatically change with an ethyl group at one extremity instead of the hydroxyl group, *i.e.* TEGME is soluble in cyclohexane while TEG is not.

For this reason, although the reaction pathway was the same, the operative conditions were different. The solubility of TEGME in cyclohexane allowed to operate in a homogeneous system for the synthesis of compounds **4** and **5**. In this case, the removal of the co-produced water was achieved by distillation of the azeotrope using a Dean Stark apparatus. On the contrary, in the synthesis of compounds **6** and **7** that involved the use of TEG, the water was confined in the PEG phase. For all these compounds we reached quantitative conversions. They were then extracted with diethyl ether (**4, 5**) or cyclohexane (**6, 7**), and isolated by FCC, reaching isolated yield between 75 and 90 %.

A first evidence of the different polarity between TEG and amphiphilic molecule (**6** and **7**) was that while TEG itself is not soluble in cyclohexane, the reverse amphiphiles **6** and **7** form clear colourless solutions up to a 50/50 volume ratio.

This behaviour will be discussed more in detail in the following chapters.

For what concerns amphiphiles **8** and **9**, the synthetic route adopted was the same as per amphiphiles **4** and **5**, but their high molecular weight didn't allow their characterisation by GC-MS and the high number of atoms with similar magnetic properties on the tail didn't allowed the characterisations by NMR. Because of the difficulties in the characterisation and in the isolation of the products, no further investigation were conducted.

2.3. Double-headed reverse amphiphiles

Among the aims of this project was to prove the possibility of typical aggregate formation in a non-polar system. We started synthesising reverse surfactants with a GPP suitable for micelle formation. We then proceeded with the synthesis of another amphiphilic molecule with a different geometry, *i.e.* a molecule bearing two apolar heads connected by a PEG chain.

The synthetic route adopted is the same used for the production of reverse amphiphile **6** and **7**, but with a different molar ratio. Although it was not optimised, the detailed synthesis is reported in the experimental session.

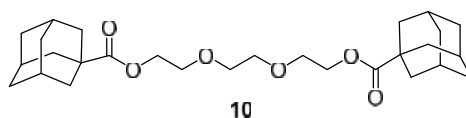


Figure 2.2 Chemical structure of the two-headed reverse amphiphile **10**

This geometry was inspired by bolaamphiphiles,^[7] that are molecules containing a hydrophobic skeleton (e.g., one, two, or three alkyl chains, a steroid, or a porphyrin) and two water-soluble groups on both ends. Synthetic bolaamphiphiles try to reproduce the unusual architecture of monolayered membranes found in

archaeobacteria but commonly do not use the same building blocks, which are difficult to synthesize. [8-10]

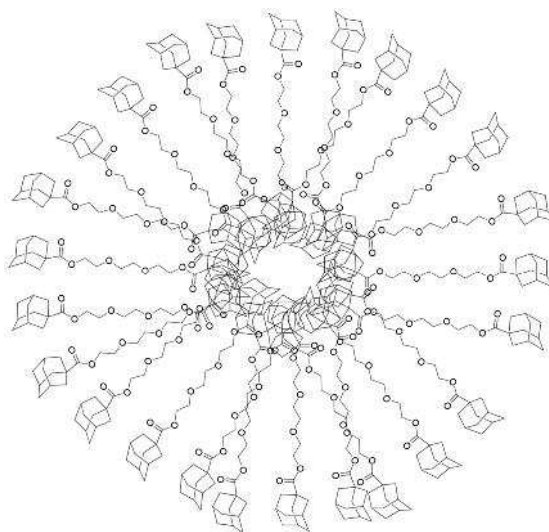


Figure 2.3 schematic structure of typical micelle composed by bolaamphiphile **10**

In water common synthetic bolas tend to form extended planar monolayers on the surface of water or of smooth solids. Multilayers may be formed by the combination of two bolas with two cationic or two anionic headgroups or, more common, by combination of a dianionic bola and a cationic polymer or vice versa. [11-13] Long-chain bolas produce vesicles, while short chain water-soluble bolas give micelles.

In this project, reverse bolas were synthesised using two apolar headgroups (*i.e.* adamantane moiety), and one short PEG tail. The resulting molecule was designed in order to obtain a double layer membrane or vesicles as speculated in figure 2.3.

2.4. Double-tailed reverse amphiphiles

Cell membranes are formed by phospholipids that are double-tailed surfactants with a GPP in the range of flexible double layer. In the preface we introduced the question of the possibility of life in Titan's methane lakes. In this context, we planned to synthesise a new reverse amphiphile that is, in terms of geometry, as much similar to phospholipids as possible.

To synthesise this reverse double tailed amphiphile we chose the adamantane and menthol moieties as headgroups and TEGME as precursor for the tails. We then needed a linker molecule that allowed the connection between the carboxylic group on the adamantane moiety and two molecules of TEGME. The molecules used for this purpose were Bicine and Solketal.

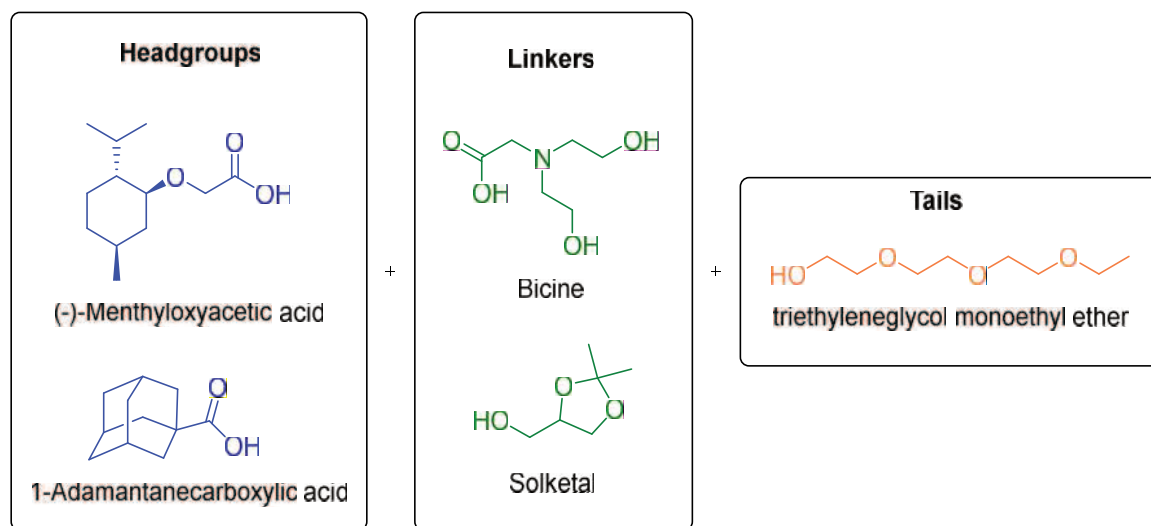
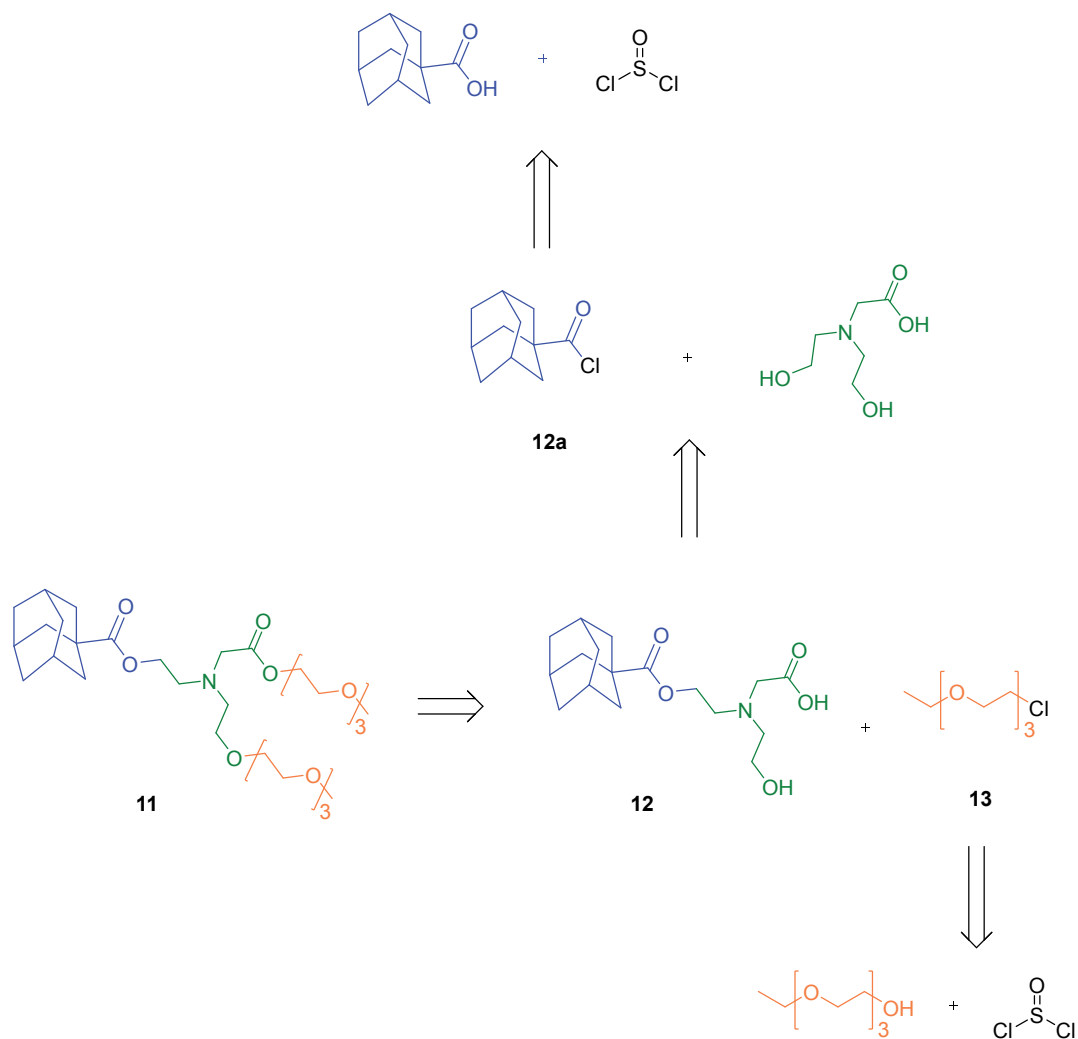


Figure 2.4 Chemical structure of reagents used for the synthesis of double tailed reverse amphiphiles

2.4.1. Bicine as linker

Bicine [N,N-Bis(2-hydroxyethyl)glycine, figure 2.4] is an α -amino acid in which the nitrogen is bonded to two aliphatic chains with a terminal hydroxyl group. This molecule possesses a carboxylic group suitable for the bond with the headgroup by esterification, and two hydroxyl groups that can be used to link the tails by etherification. This molecule was chosen because the presence of a nitrogen atom may increase the polarity of the tails in the final amphiphiles.

The first attempt was carried on between 1-adamantane carboxylic acid and bicine. In order to bond the two molecules, we first converted the former in the corresponding methyl ester or acyl chloride. The aim of this step was to enhance the reactivity towards the reaction with bicine.



*Scheme 2.3 Retrosynthetic route of double-tailed amphiphile **11***

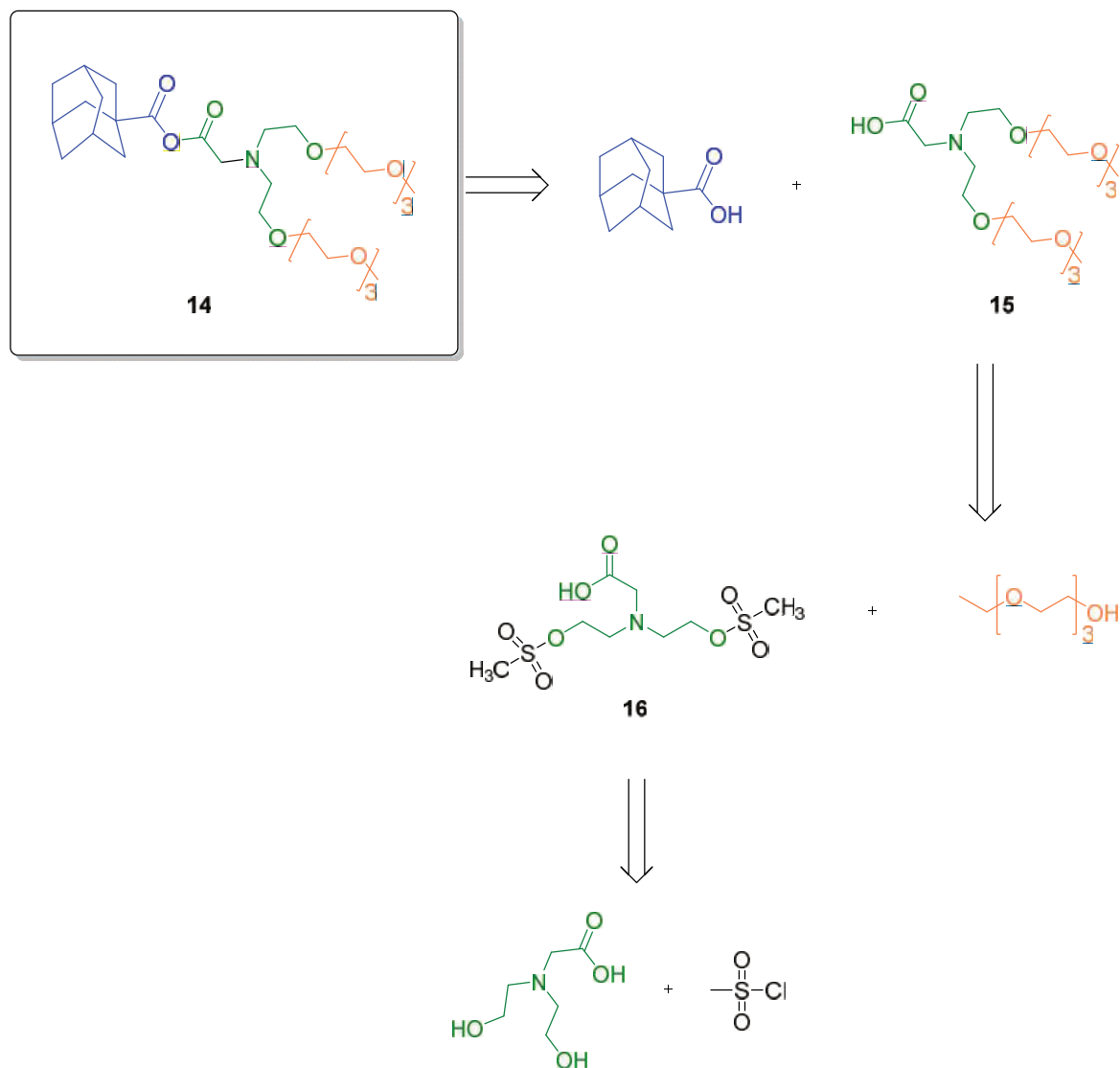
In scheme 2.3 is reported the retrosynthetic route for the synthesis of an amphiphile molecule bearing the adamantane moiety as head group, connected with two PEG chains using bicine as linker (**11**).

Adamantane carboxylic acid and triethylene glycol monoethyl ether were functionalised to the corresponding chloride. The chlorurations were performed to obtain a better leaving group in the subsequent nucleophilic substitution with one hydroxyl group of bicine and compound **12** respectively.

The reaction between compound **12a** and bicine didn't take place because of the poor solubility of bicine in almost all organic solvents.

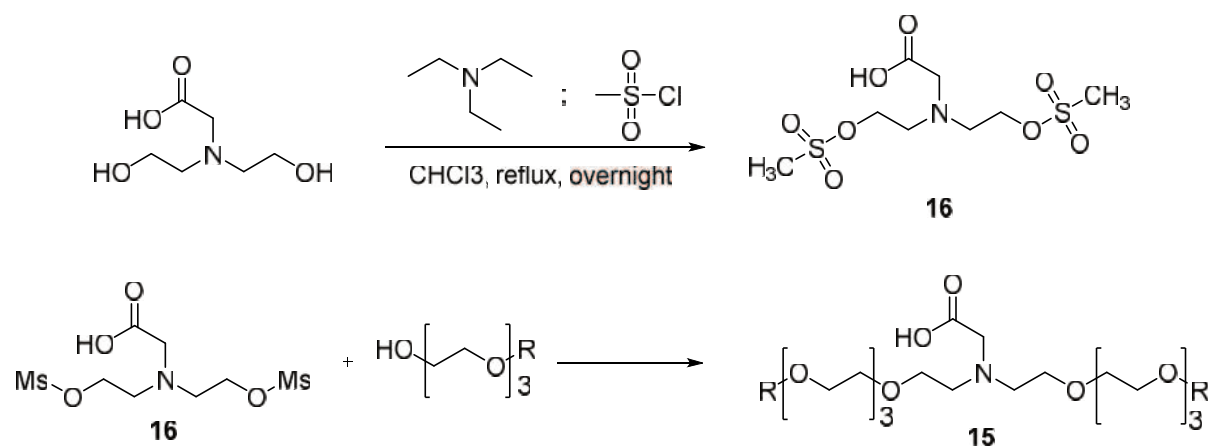
Thus, this scheme for the preparation of **11** proved unsuccessful.

A similar retrosynthetic route was proposed to synthesise compound **14**. To favour the solubilisation of bicine in organic solvents, we tried to functionalise its hydroxyl groups with mesyl groups (scheme 2.4).



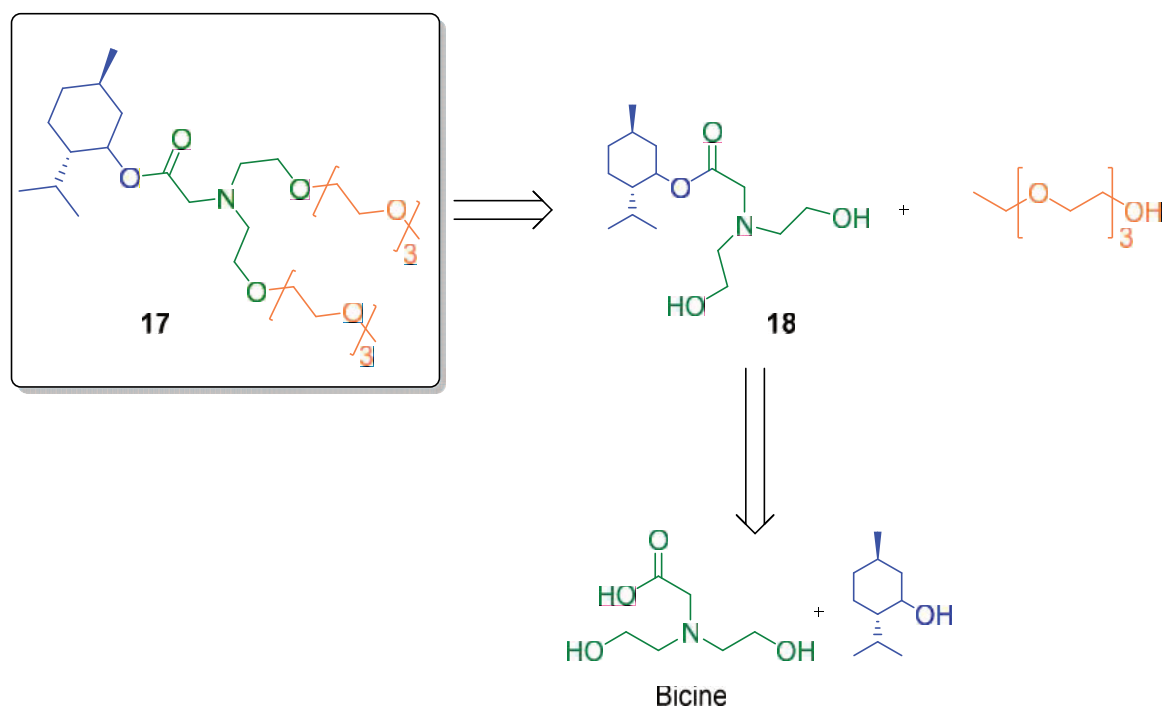
Scheme 2.4 Synthetic route for compound 14

The reaction was performed adding dropwise the mesylchloride to a solution of bicine and triethylamine in chloroform at reflux (scheme 2.5). We didn't observe the formation of compound **15**, thus the synthesis of compound **14** was abandoned.



Scheme 2.5 Synthetic route for compound **15**

We then attempted the synthesis of double tailed amphiphile using menthol as head precursor. In this case the headgroup bond through esterification of the hydroxyl group and the carboxylic group of the bicine.

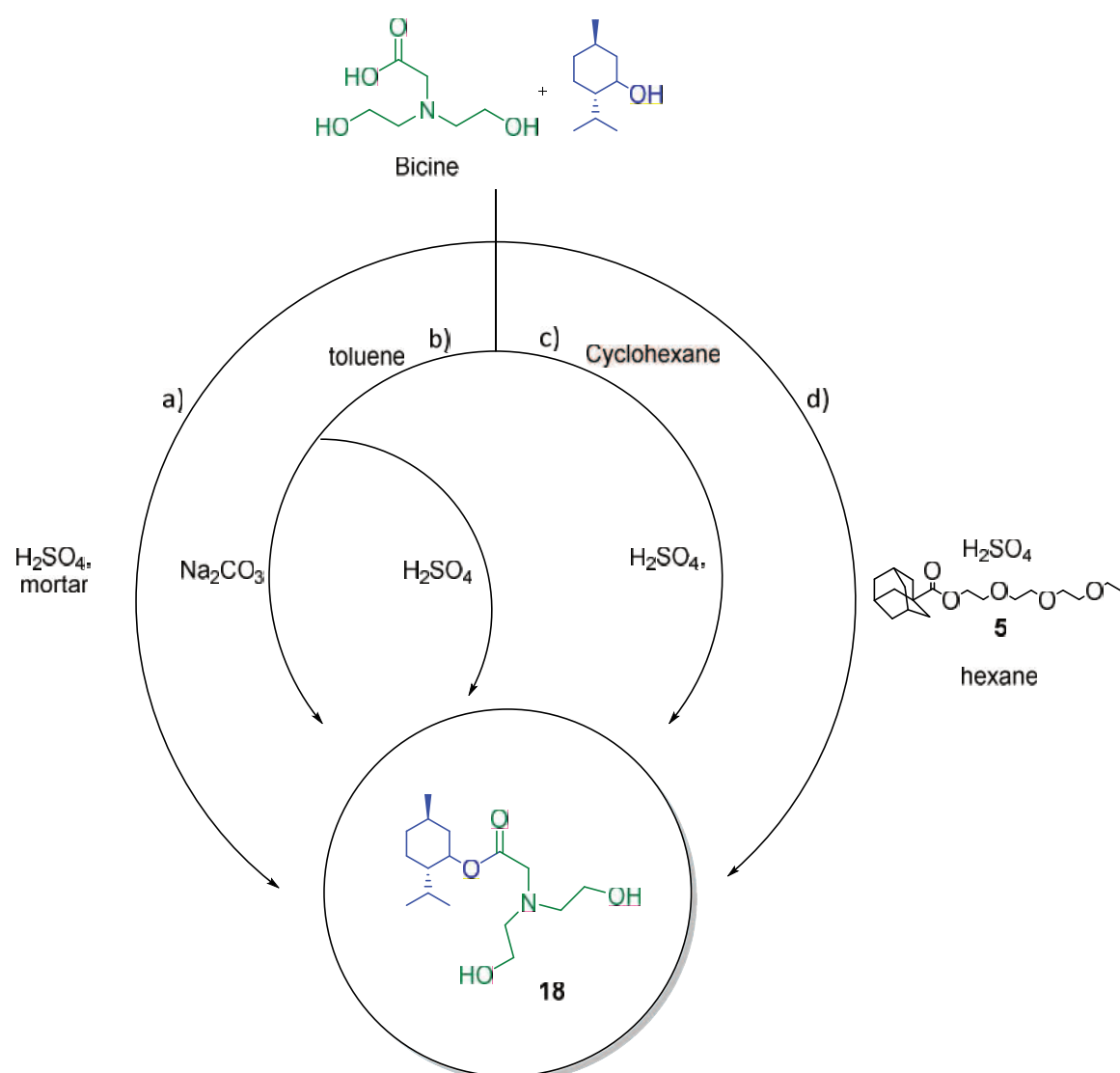


Scheme 2.6 Retrosynthetic route for compound **17**

In scheme 2.7 are reported all the attempts toward the synthesis of compound **18**.

Since the main problem was the solubility of bicine in most common solvents, we carried on the reaction mixing all the reagents and the catalyst in a mortar.

The unsuccessful result lead us to carry on the reaction in different solvents (i.e. cyclohexane, n-hexane and toluene) using different catalyst: an acid (H_2SO_4), a base (Na_2CO_3) and an acid plus compound **5** that may act as surfactant and favour the solubilisation of bicine. All these synthetic routes revealed to be unsuccessful, thus we moved on to solketal instead of bicine.



Scheme 2.7 Alternative synthetic routes for compound **18**

2.4.2. Solketal as linker

Solketal [DL-1,2-Isopropylidenglycerol] was chosen because the hydroxyl group can connect to the head through an esterification, while the acetal can be hydrolysed to give two hydroxyl groups useful for the linkage of the two tails. Its solubility in most common organic solvents made us think that it might be more reactive than bicine.

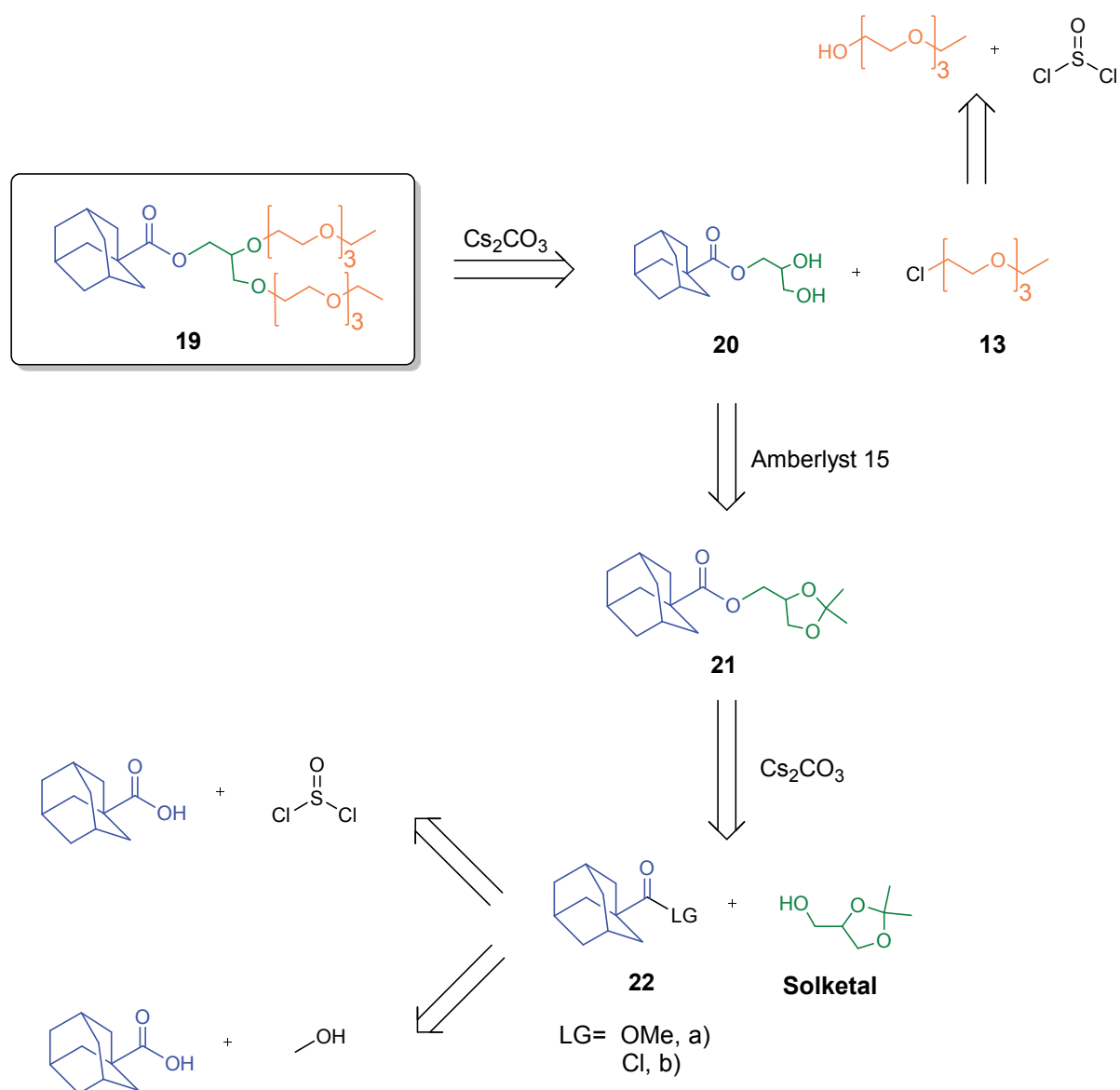
Scheme 3.6 shows the synthetic routes adopted for the synthesis of compound **19**. First step was to convert the carboxylic group on the adamantane into the corresponding methyl ester. This step allowed performing the bond with Solketal under basic conditions avoiding cleavage of the acetal. A second pathway, instead, involved the conversion of the carboxylic group into acyl chloride in order to enhance its reactivity.

These derivatives were then used in the reaction with Solketal. This step involved the substitution of the leaving group on adamantane (*i.e.* chloride or methoxy), by the hydroxyl group on Solketal, under basic conditions.

We tested both derivatives **22a** and **22b** for the reaction with Solketal. In table 3.2 are reported the selectivity, reaction time and isolated yield of compound **21** obtained by reaction of Solketal with both the derivatives. As expected, the acyl chloride derivative is more reactive and lead to a better yield.

Substrate	Selectivity (GC-MS, %)	Time (h)	21 Isolated yield (%)
22a	26	48	13
22b	80	2	36

Table 2.2 GC-MS selectivity, reaction time and isolated yield of compound **21** using as starting material derivatives **22a** and **22b**.



Scheme 2.8 Retrosynthetic route for compound **19**

We then proceeded with the acetal hydrolysis to create two reactive sites to connect the two tails. We carried on this reaction using Amberlyst 15, an acid resin that allowed the complete cleavage of the acetal^[14].

The subsequent step was to convert the hydroxyl group on TEGME into a better leaving group (*i.e.* chloride and mesyl moieties).

We then performed only few attempts of the last step, using a basic catalyst. Although the conversion was quantitative, it was not possible to fully characterise

compound **19** and to determine its purity. Its high molecular weight (*i.e.* 574.75 uma) was not suitable for the characterisation by GC-MS. On the other hand, the high number of atoms having similar magnetic properties on the tails did not allowed the characterisations by NMR. An ESI-MS analysis might allow the complete identification of the product.

2.5. Experimental procedures:

Material. All the reagents were purchased from Aldrich and used without further purification except for phenol and naphthol that were respectively distilled and crystallised.

¹H NMR spectra of compounds were acquired with Varian Unity spectrometer operating at 300 MHz, using chloroform-d as solvent. Chemical shifts are reported downfield from TMS.

GC/MS (EI, 70 eV) analyses were run using a HP5-MS capillary column (30 m) mounted on an Agilent 5975c-7890

General procedure for the Chlorination of PEGs:

In a two neck round bottomed flask topped with a reflux condenser were added 4.2 mmol of PEG, 0.6 mmol of dimethylformamide and 5 mL of chloroform. The mixture was stirred and heated to reflux. A solution of 8.4 mmol of thionyl chloride in dichloromethane was added dropwise (0.5h). The reaction mixture was stirred at reflux for 23 hours. The hydrochloric acid produced was neutralised with a saturated solution of sodium carbonate. The product extracted with dichloromethane and dried under vacuum.

(2-(2-(2-ethoxyethoxy)ethoxy)ethoxy)benzene (1):

In a round bottomed flask topped with a reflux condenser, were added 2.54 mmol of 1-chloro-2-(2-(2-ethoxyethoxy)ethoxy)ethane, 2.34 mmol of phenol, 5.1 mmol of CsCO₃, 0.25 mmol of KI and 5mL of toluene. The reaction mixture was stirred

and heated at reflux overnight under inert atmosphere. The solution was then cooled, dried with sodium sulphate, filtered and dried under vacuum. The crude oil obtained was purified by FCC (silica gel, diethyl ether as eluent).GC/MS (relative intensity, 70 eV) m/z: 254.10 ([M]⁺, 2.0), 121.00 (28.0), 119.95 (47.0), 117.05 (10.0), 103.00 (8.0), 94.10 (15.0), 93.00 (12.0), 77.00 (41.0), 73.05 (37.0), 64.95 (13.0), 59.00 (18.0), 51.00 (7.0), 45.00 (100.0). The product was isolated with a purity of 83%.

(2-(2-(2-ethoxyethoxy)ethoxy)ethoxy)naphthalene (2):

In a round bottomed flask topped with a reflux condenser, were added 2.54 mmol of 1-chloro-2-(2-(2-ethoxyethoxy)ethoxy)ethane, 2.34 mmol of naphthol, 5.1 mmol of CsCO₃, 0.25 mmol of KI and 5mL of toluene. The reaction mixture was stirred and heated at reflux overnight under inert atmosphere. The solution was then cooled, dried with sodium sulphate, filtered and dried under vacuum. The crude oil obtained was purified by FCC (silica gel, diethyl ether as eluent).

GC/MS (relative intensity, 70 eV) m/z: 304.10 ([M]⁺, 23.0), 171.05 (10.0), 170.10 (7.0), 145.00 (9.0), 144.00 (63.0), 143.00 (9.0), 141.05 (9.0), 128.05 (23.0), 127.00 (58.0), 126.10 (11.0), 117.05 (10.0), 116.00 (17.0), 115.10 (85.0), 101.05 (5.0), 89.00 (10.0), 73.05 (50.0), 72.05 (11.0), 62.95 (5.0), 45.10 (100.0). The product was isolated with a purity of 81%.

4-allyl-1-(2-(2-(2-ethoxyethoxy)ethoxy)ethoxy)-2-methoxybenzene (3):

In a round bottomed flask topped with a reflux condenser, were added 2.54 mmol of 1-chloro-2-(2-(2-ethoxyethoxy)ethoxy)ethane, 2.34 mmol of eugenol, 5.1 mmol of CsCO₃, 0.25 mmol of KI and 5mL of toluene. The reaction mixture was stirred and heated at reflux overnight under inert atmosphere. The solution was then cooled, dried with sodium sulphate, filtered and dried under vacuum. The crude oil

obtained was purified by FCC (silica gel, diethyl ether as eluent). The product was isolated with a purity of 87%.

GC/MS (relative intensity, 70 eV) m/z: 324.15 ([M]⁺, 11.0), 164.10 (32.0), 162.95 (9.0), 162.05 (10.0), 161.05 (10.0), 149.00 (9.0), 147.00 (3.0), 131.00 (12.0), 117.05 (17.0), 116.05 (5.0), 114.95 (15.0), 107.00 (7.0), 105.00 (8.0), 104.00 (12.0), 103.00 (17.0), 91.00 (25.0), 88.95 (6.0), 79.00 (7.0), 78.00 (7.0), 77.00 (12.0), 73.10 (64.0), 51.05 (4.0), 45.05 (100.0).

2-(2-(2-ethoxyethoxy)ethoxy)ethyl,2-((2-isopropyl-5-methylcyclohexyl)oxy)acetate(4):

in a round-bottomed flask equipped with a Dean-Stark apparatus topped with a reflux condenser were added 14.03 mmol of menthyloxy acetic acid, 14.03 mmol diethylene glycol monoethyl ether and 0.7 mmol of sulphuric acid in cyclohexane (40mL). The reaction mixture was heated at reflux temperature and stirred for 2h. Then the reaction mixture was cooled at ambient temperature, quenched with saturated K₂CO₃, then extracted with CHCl₃ (6x10 mL). The combined organic layers were dried with anhydrous Na₂SO₄, filtered and evaporated to give a crude oil that was purified by FCC (silica gel, diethyl ether as eluent). Isolated Yield 68%. ¹HNMR (400 MHz, CDCl₃): δ =4.3 (t, 2H), 4.2-4.1 (dd, 2H), 3.7-3.5 (m, 12H), 3.2-3.1 (dt, 1H), 2.3-2.2 (m, 1H), 2.1-2.0 (m, 1H), 1.7-1.6 (m, 2H), 1.4-1.2 (m, 2H), 1.2-1.1(t, 3H), 1.0-0.7 (m, 12H);

GC/MS (relative intensity, 70 eV) m/z: 374.27 ([M]⁺,1.0), 179.10 (26.0), 139.10 (14.0), 138.10 (16.0), 133.10 (10.0), 123.10 (19.0), 117.10 (20.0), 103.00 (59.0), 102.00 (23.0), 97.10 (16.0), 96.10 (10.0), 89.10 (15.0), 87.10 (60.0), 86.00 (25.0), 95.10 (44.0), 83.10 (77.0), 82.10 (18.0), 81.10 (55.0), 73.10 (73.0), 72.10 (76.0), 71.10 (10.0), 69.10(38.0), 67.10 (20.0), 59.10 (54.0), 57.10 (25.0), 55.10 (51.0), 45.10 (100.0), 44.10(10.0), 43.10 (38.0), 42.10 (13.0), 41.10 (33.0); mp = -40.9/-39.7

2-(2-(2-ethoxyethoxy)ethoxy)ethyl adamantane-1-carboxylate (5): in a round-bottomed flask equipped with a Dean-Stark trap topped with a reflux condenser

were added 12 mmol of 1-adamantanecarboxylic acid, 12 mmol di triethylene glycol monoethyl ether and 0.6 mmol of sulphuric acid in cyclohexane (30mL). The reaction mixture was heated at reflux temperature and stirred for 2h. Then the reaction mixture was cooled at ambient temperature, quenched with saturated K_2CO_3 , then extracted with $CHCl_3$ (6x10 mL). The combined organic layers were dried with anhydrous Na_2SO_4 , filtered and evaporated to give a crude oil that was purified by FCC (silica gel, diethyl ether as eluent). Isolated Yield 70%. 1H NMR (400 MHz, $CDCl_3$): δ =4.2 (t, 2H), 3.7-3.5 (m, 12H), 2.1-2 (br, 3H), 1.9 (br, 6H), 1.7-1.6 (br, 6H), 1.3-1.2 (t, 3H); ^{13}C NMR (75 MHz, $CDCl_3$) δ = 178 (C=O), 72.9, 71.1, 71.0, 70.2, 69.6, 67.0, 63.7, 41.1, 39.2, 36.9, 28.3, 15.5.

GC/MS (relative intensity, 70 eV) m/z: 340.20 ([M+],1.0), 208.10 (9.0), 207.10 (59.0), 136.10 (11.0), 135.10 (100.0), 107.10 (10.0), 93.10 (22.0), 92.00 (5.0), 91.00 (13.0), 79.00 (26.0), 78.00 (3.0), 77.00 (11.0), 73.00 (29.0),72.00 (54.0), 59.10 (24.0), 45.00 (39.0), 43.00 (11.0);mp= -45.7 °C

2-(2-(2-hydroxyethoxy)ethoxy)ethyl2-((2-isopropyl-5-methylcyclohexyl)oxy)acetate (6):

in a round-bottomed flask topped with a reflux condenser were added 10 mmol (2.14g) of menthyloxyacetic acid, 25 mmol (3.74g) TEG and 0.7 mmol of sulphuric acid in cyclohexane (10mL). The reaction mixture was heated at reflux temperature and stirred overnight. The reaction mixture was cooled at ambient temperature, quenched with saturated K_2CO_3 and extracted with cyclohexane (5x5 mL). The combined organic layers were dried with anhydrous Na_2SO_4 , filtered and evaporated to give a crude oil that was purified by FCC (silica gel, diethyl ether as eluent). Isolated yield 68%.

1H NMR (400 MHz, $CDCl_3$): δ =4.3 (t, 2H), 4.2-4.1 (dd, 2H), 3.8-3.6 (m, 10H), 3.2-3.1 (dt, 1H), 2.3-2.2 (m, 1H), 2.1-2.0 (m, 1H),1.7-1.6 (m, 2H), 1.4-1.2 (m, 2H), 1.0-0.7 (m, 12H);

¹³C NMR (400 MHz, CDCl₃): δ = 171.0 (C=O), 80.4, 72.7, 70.7, 70.5, 69.1, 66, 63.7, 61.9, 48.2, 40.1, 34.5, 31.6, 25.6, 23.4, 22.4, 21.1, 16.4.

GC/MS (relative intensity, 70 eV) m/z: 346.30 ([M]⁺,2.0), 177.05 (4.0), 151.00 (31.0),149.00 (13.0), 139.15 (18.0), 138.15 (34.0), 133.00 (12.0), 123.10 (23.0), 103 (55.0), 102.00 (20.0),97.10 (15.0), 96.05 (11.0), 95.05 (48.0), 89.05 (37.0), 88.00 (18.0), 87.00 (100.0), 86.00 (30.0), 83.10 (72.0), 82.05 (20.0), 81.05 (60.0), 69.10 (33.0), 67.10 (17.0), 57.10 (21.0), 55.10 (39.0), 45.10 (81.0), 44.05 (10.0), 43.10 (20.0);

d=0.967 g/cm³ at 25 °C.

2-(2-(2-hydroxyethoxy)ethoxy)ethyl adamantane-1-carboxylate (7):

in a round-bottomed flask topped with a reflux condenser were added 10mmol (1.80g) of 1-adamantanecarboxylic acid, 25mmol (3.74g) TEG and 0.7 mmol of sulphuric acid in cyclohexane (10mL). The reaction mixture was heated at reflux temperature and stirred overnight. The reaction mixture was cooled at ambient temperature, quenched with saturated K₂CO₃ and extracted with cyclohexane (5x5 mL). The combined organic layers were dried with anidrous Na₂SO₄, filtered and evaporated to give a crude oil that was purified by FCC (silica gel, diethyl ether as eluent). Isolated yield 74%.

¹H NMR (400 MHz, CDCl₃): δ 4.24 (t, 2H), 3.76 – 3.63 (m, 10H), 2.04 – 1.97 (m, 2H), 1.92 (d, J = 2.9 Hz, 4H), 1.74 – 1.58 (m, 8H).

¹³C NMR (400 MHz, CDCl₃): δ = 177.8 (C=O), 72.6, 70.8, 70.6, 69.4, 63.3, 62.0, 38.9, 36.6, 28.1.

GC/MS (relative intensity, 70 eV) m/z: 312.2 ([M]⁺,1.0), 207.10 (41.0), 136.00 (12.0), 135.05 (100.0), 93.05 (12.0), 91.05 (8.0), 89.10 (28.0), 88.05 (10.0), 79.05 (13.0);

d=1.03 g/cm³ at 25 °C.

(ethane-1,2-diylbis(oxy))bis(ethane-2,1-diyl)

(3r,3'r,5r,5'r,7r,7'r)-

bis(adamantane-1-carboxylate) (10):

in a round-bottomed flask topped with a reflux condenser were added 10mmol of 1-adamantanecarboxylic acid, 4 mmol of TEG and 1 mmol of sulphuric acid in cyclohexane (20mL). The reaction mixture was heated at reflux temperature and stirred overnight. The reaction mixture was cooled at ambient temperature, quenched with saturated K_2CO_3 and extracted with cyclohexane. The combined organic layers were dried with anidrous Na_2SO_4 , filtered and evaporated to give a crude oil. GC-MS yield 87%.

GC/MS (relative intensity, 70 eV) m/z: 474.30 ([M]⁺, 1.0), 266.10 (14.0), 208.10 (9.0), 207.10 (64.0), 206.10 (13.0), 205.05 (9.0), 136.05 (11.0), 135.05 (100.0), 134.00 (18.0), 93.05 (15.0), 91.05 (7.0), 79.10 (17.0), 77.05 (5.0).

References and notes

- [1] J. N. Israelachvili, D. J. Mitchell, B. W. Ninham, *Journal of the Chemical Society, Faraday Transactions 2: Molecular and Chemical Physics* **1976**, 72, 1525-1568.
- [2] J. N. Israelachvili, D. J. Mitchell, B. W. Ninham, *Biochimica et Biophysica Acta (BBA) - Biomembranes* **1977**, 470, 185-201.
- [3] Jacob N. Israelachvili, in *Intermolecular and Surface Forces (Third Edition)* (Ed.: J. N. Israelachvili), Academic Press, San Diego, **2011**, pp. 535-576.
- [4] P.A. FitzGerald, PhD thesis, *Solution behaviour of Polyethylene Oxide, Nonionic Gemini Surfactants*, The University of Sydney **2002**.
- [5] P. Tundo, A. Perosa, M. Selva, L. Valli, C. Giannini, *Colloids and Surfaces A: Physicochemical and Engineering Aspects* **2001**, 190, 295-303.
- [6] S. Krimm, *Journal of Polymer Science: Polymer Letters Edition* **1980**, 18, 687-687.
- [7] J. H. Fuhrhop, T. Wang, *Chem Rev* **2004**, 104, 2901-2938.
- [8] G. D. Sprott, *J Bioenerg Biomembr* **1992**, 24, 555-566.
- [9] A. Gambacorta, A. Gliozzi, M. De Rosa, *World Journal of Microbiology and Biotechnology* **1995**, 11, 115-131.
- [10] K. Yamauchi, K. Togawa, T. Moriya, M. Kinoshita, *Colloid Polym Sci* **1995**, 273, 96-100.
- [11] J. H. Fuhrhop, J. Koenig, *Molecular Assemblies and Membranes, Monographs in Supramolecular Chemistry, Vol. i-xiii*, Royal Society of Chemistry, London, **1994**.
- [12] J. H. Fuhrhop, C. Endisch, *Molecular and Supramolecular Chemistry of Natural Products and Their Model Compounds*, Marcel Dekker, New York, **2000**.
- [13] A. Ulman, *An Introduction to Ultrathin Organic Films, from Langmuir-Blodgett to Self-Assembly* Academic Press, New York, **1991**.
- [14] M. Yakovleva, A. Shayakhmetova, I. Gumerov, G. Ishmuratov, *Chemistry of Natural Compounds* **2004**, 40, 593-594.

3. Introduction: Aggregates analysis methods

3.1. Diffusion Ordered Nuclear Magnetic Resonance Spectroscopy (NMR-DOSY)

The motion of molecules in liquid or solution is a complex system. The translational motion is known as Brownian molecular motion and can be simply called diffusion (or self-diffusion). It depends on several physical parameters such as the sizes and shapes of the molecules as well as on the temperature and viscosity of the solution. If we assume particles having a spherical shape, the diffusion coefficient D can be described by the Stokes-Einstein equation ^[1]

$$D = \frac{k_B T}{6\pi\eta r_H} \quad (3.a)$$

where k_B is the Boltzmann constant, T the temperature, η the viscosity of the solution and r_H is the hydrodynamic radius of the molecule. The latter represents the radius of a hypothetical sphere that diffuses with the same speed as the particle under examination and, thus, provides information on the apparent size of the molecule, including any solvation, ion-pairing or other aggregation effects which may affect its mobility. ^[2]

2D-Diffusion Ordered Spectroscopy (2D-DOSY) is a two-dimensional NMR technique in which one dimension represents the chemical shift data while the second dimension resolves species by their diffusion properties: for this characteristic it has been described as “NMR chromatography”.^[3] For example it has been used for the study of a mixture of different polymers,^[4] the characterization of aggregates^[5] and to determine protein-surfactant bonding. ^[6]

DOSY measurements requires a pulse field gradient that allows measuring the translational diffusion of particles in solution. The use of a gradient is necessary in order to spatially label molecules, *i.e.* it marks molecules depending on their position in the NMR tube. If they move in the diffusion time Δ after the encoding, the new position can be decoded by a second gradient.

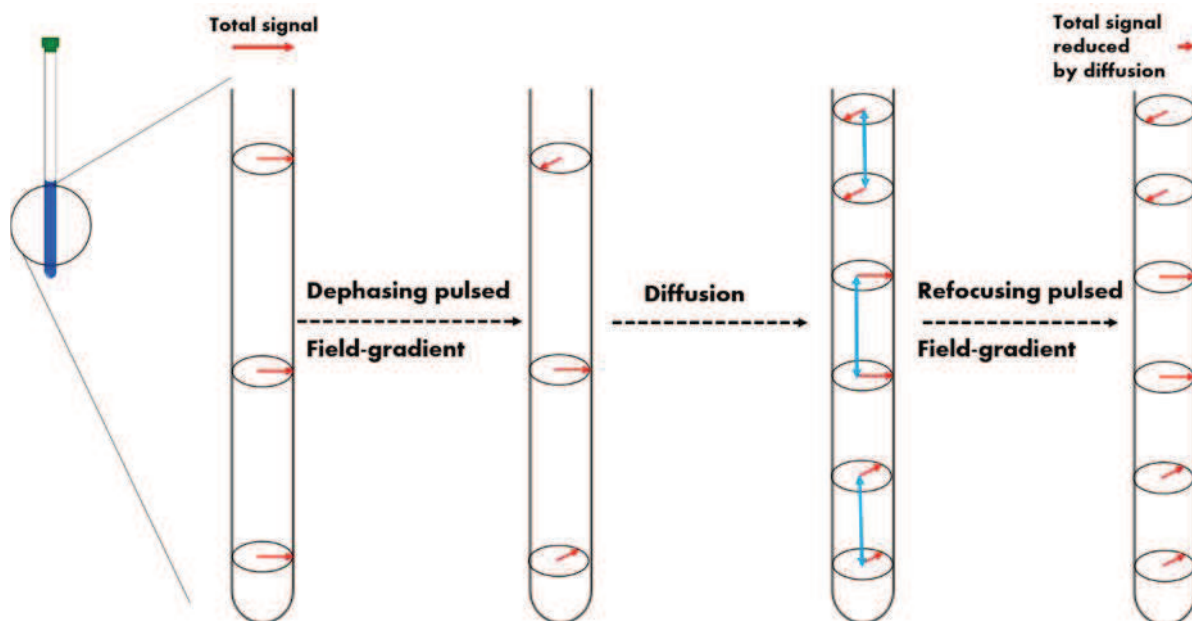


Figure 3-1 Scheme of DOSY experiment

The measured signal is the integral over the whole sample volume, and its intensity is attenuated depending on Δ and the gradient parameters (gradient strength g and gradient length δ). This intensity change is described as

$$I = I(0) e^{-D \gamma^2 g^2 \delta^2 (\Delta - \delta/3)} \quad (3.b)$$

In which I is the observed intensity, $I(0)$ is the unattenuated signal intensity and γ the gyromagnetic ratio of the observed nucleus. [7]

In this project 2D-DOSY NMR was used to study micelle formation using reverse amphiphiles in different hydrocarbon solvents.

3.2. Scattering techniques

In this project we used different scattering techniques *i.e.* Dynamic light scattering (DLS), Small Angle X-Ray Scattering (SAXS) and Small Angle Neutron Scattering (SANS), that are common methods for the determination of a large class of colloids and macromolecules. Examples of such system are polymers, micelles or aggregates, with sizes between 5 and 3000 Å. The range between 5 and 300 Å can be explored by SAXS and SANS, while from 100 to 3000 Å by dynamic light

scattering through the Diffusion coefficient (see eq 3.a). All the scattering information contained in this thesis are discussed in the first two chapters of the book by Lindner and Zemb^[8] and in the book of Glatter and Kratky.^[9]

3.2.1. SAXS and SANS

A small angle scattering experiment involves precise and indispensable stages in the acquisition and treatment of data, which are essential for its quality. During the experiment a well collimated beam of radiation of wavelength λ is sent through the sample, and the scattered intensity at different scattering angle Θ is measured. The total scattering intensity is the sum of all the single scatterings of different particles in solution, with different angles or directions. For simplicity, from here on the scattering will be discussed as single scattering.

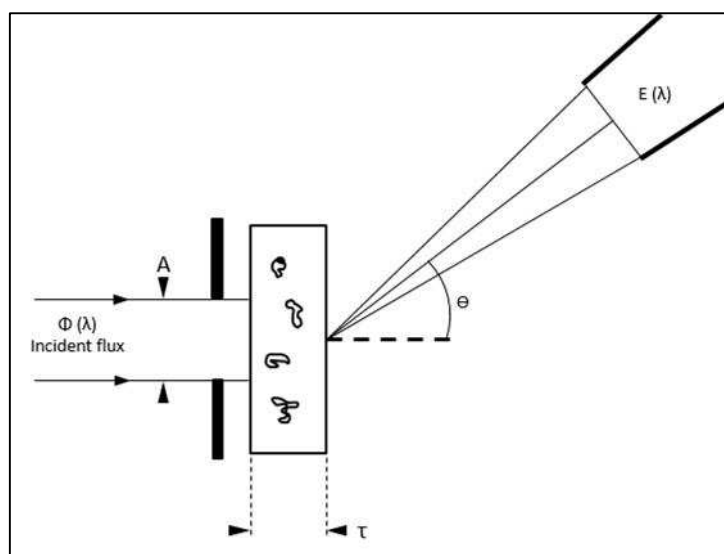


Figure 3-2 general scheme of a scattering experiment

The variation of the scattered intensity is expressed as a function of the scattering vector (q), a physical parameter that allows one to join on the same curve several curves obtained at different λ and Θ values

$$q = \frac{4\pi}{\lambda} \sin\Theta/2 \quad (3.c)$$

The data obtained from these kind of experiments are $I(q)$ at different scattering vector. The useful intensities are those scattered by the samples $I_s(q)$ and by a reference $I_r(q)$ used in order to subtract the background (usually the solvent and sample holder). This aspect will be examined in depth later.

The interpretation of these data consists in the extraction of size, form and organization of particles in solution. General methods are described in the literature: Huglin ^[10] for light scattering, Guinier and Fournet, ^[11] Luzzati and Tardieu ^[12] and Glatter and Kratky for X-Rays, ^[9] while for neutrons Squires ^[13] or Zaccai. ^[14]

3.2.2. Scattering lengths

The scattering length is a parameter that expresses the strength of the interaction of the radiation and the elementary scatterer. This parameter has different characteristics for each type of beam (light, X-Ray or neutron)

- **X-Ray scattering**

The associated particle is a photon of energy of about 10^4 eV, that corresponds to $1 < \lambda < 5$ Å. The interaction takes place on the z electrons of the electronic shell of atoms. The scattering length is given by

$$B = b_0 z ; \quad b_0 = 0.282 \cdot 10^{-12} \text{ cm} \quad (3.d)$$

- **Neutron scattering**

It usually has $1 < \lambda < 20$ Å, and the interaction is nuclear. The b value depends uniquely on the nature of atoms, thus it is sensitive to the isotopes and nuclear spin state.

The scattering length is not easily calculated, but some values are tabulated^[15] and often updated.

A well know example is that of hydrogen: the b value for ^1H is $-0.374 \cdot 10^{-12}$ cm, instead the one for ^2H is $+0.667 \cdot 10^{-12}$ cm. This difference introduces the concept of contrast length and explains the use of deuterated compounds for SANS experiments.

	Light	X-ray	Neutrons	
			incoherent	
H ₂ O	0.0165	2.81	-0.165	3.56
D ₂ O	0.0165	2.81	1.92	0.837

Table 3.1 typical values of b (10^{-12} cm). Values for light were calculated with eq 2 for $\Theta=0$ and $\lambda=5960$ Å.

For neutrons, it is necessary to specify also the value of the incoherent scattering length that is the scattering length of the different isotopes of each atomic species and of nuclear spin states. It is important to subtract the incoherent scattering contribution. To do it, water, thickness 1 mm, can be used as a standard because it gives a strong flat scattering that allows normalising the detector.

In general, the scattering length can be thought as how well the element scatters the incident beam, and it must be measured experimentally.

3.2.3. *Small Angle X-ray Scattering*

SAXS instruments are designed to measure the scattered radiation that is emitted from a sample which is irradiated by a collimated X-Ray beam.

The angles at which the scattered X-Rays are detected can vary between small (SAXS, 0.05 to 10°) and small-and-wide (SWAXS, 0.05 to 41°). SAXS is the most suitable technique to detect micelles, thus in this thesis only SAXS was used.

The geometry of the irradiating beam can be switched between line and point collimation (figure 3.3).

The line collimation has the advantage of achieving higher scattering intensities. It is usually used with liquid and isotropic samples of low scattering power.

The point collimation has the advantage of a two dimensional resolution but produces smaller scattering intensities. It allows to reduce the contribution of multiple scattering because the volume analysed is smaller. It is usually used on samples with high scattering power such as crystals or liquid-crystals.

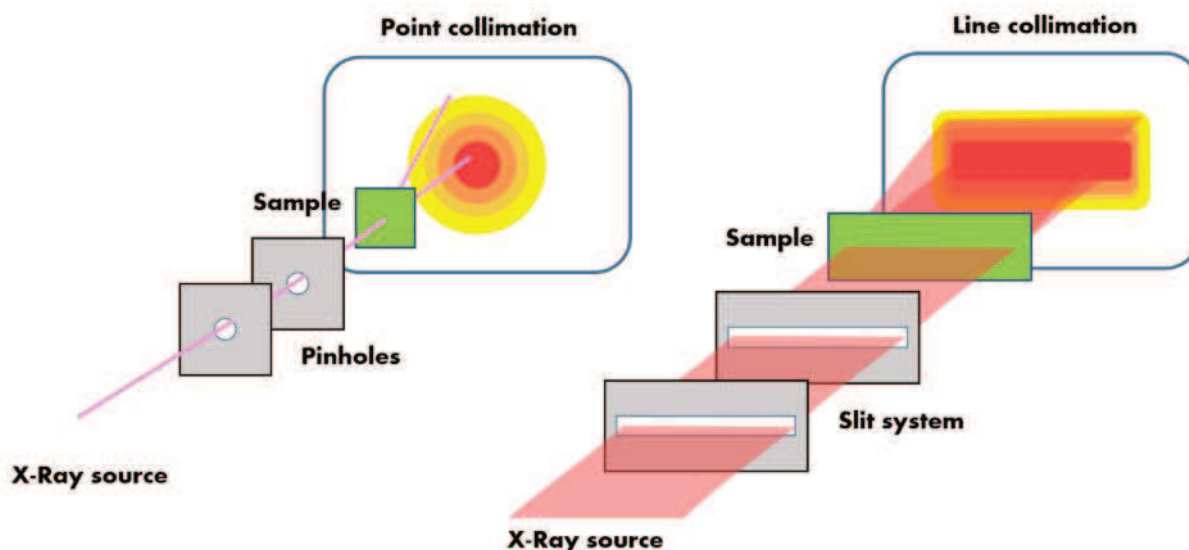


Figure 3-3. General scheme of point and line collimation SAXS

3.2.4. *Small Angle Neutron Scattering: experimental equipment*

The SANS data in this thesis was collected at the Australian Nuclear Science and Technology Organisation (ANSTO), with the Open Pool Australian Lightwater (OPAL) nuclear reactor in Sydney, NSW, Australia, using instrument Quokka. The main features of the instrument are shown in Figure 3.4.

OPAL^[16] is a 20 MW nuclear research reactor, it uses low enriched uranium fuel containing just under 20 per cent uranium-235. In terms of security and nuclear safeguards, this is a distinct advantage over earlier research reactors, some of which required enrichment levels as high as 95 per cent uranium-235 (weapons grade).

The neutrons produced passed through a moderator that give them wavelengths in the range required for SANS. Then, to monochromate the neutron beam a mechanic velocity selector was used. It consisted of a rotating cylinder with helical gaps. Because of the constant velocity of rotation only neutrons with a specific wavelength were able to pass the cylinder. The beam was collimated and then pass through the sample. In order to maximise the scattering but minimising the multiple scattering, was choose a 1mm path length quartz cell. This allowed to have a neutron transmission of more than 90%.^[17]

The scattered beam were then detected by a 2D-detector, and all the data collected were reduced from a 2D to a 1D function of intensity versus scattering angle, and then the scattering angle was converted in q using equation 3.c.

The scattering angle depends on the sample to detector distance and on the maximum distance along the detector.

In this work we used a sample to detector distances of 1.3 and 8 m, that provided in total to a q range of 0.0075 to 0.6439 \AA^{-1} .

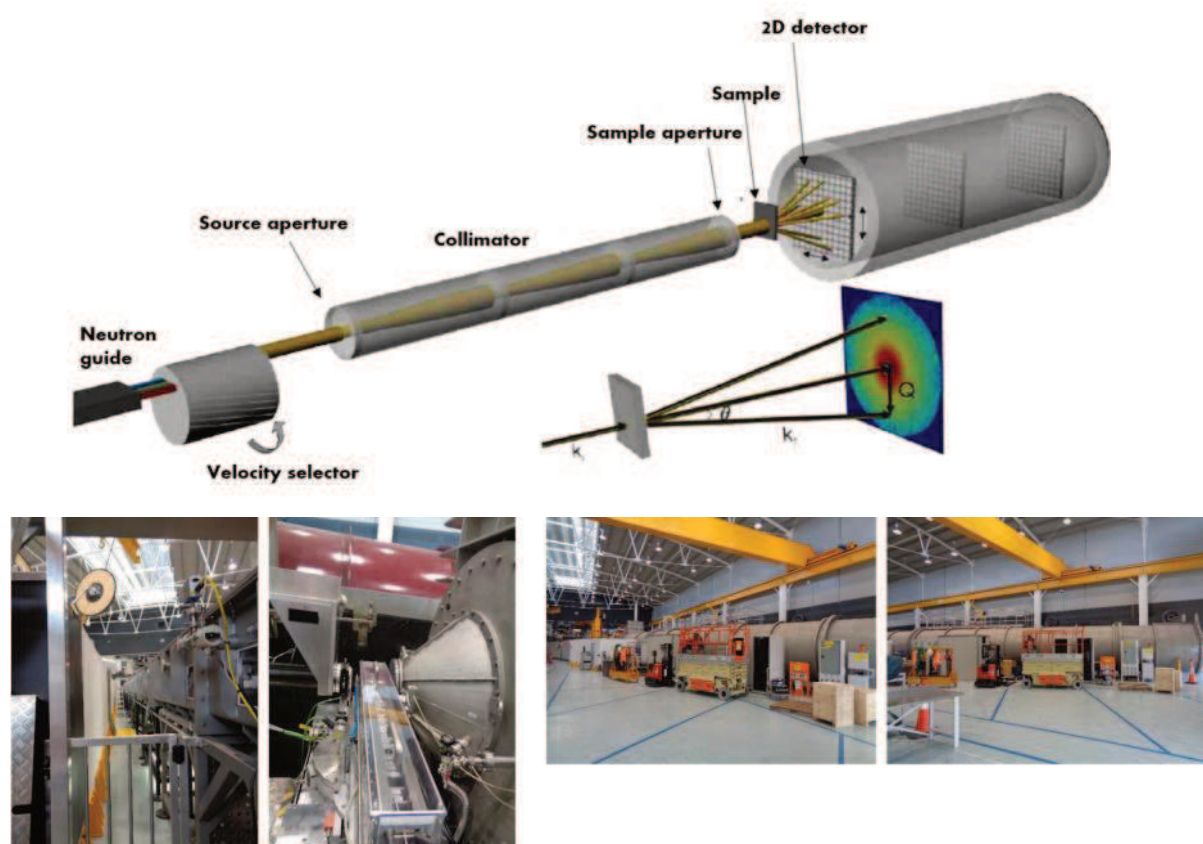


Figure 3-4 Schematic diagram^[18] of SANS instrument Quokka, and pictures of the instrument

The data collected are raw numbers that must be corrected through a mathematical process called reduction. This treatment falls outside the aim of this thesis and will be presented with a non-mathematical approach in order to give an idea of what reduction means.

The raw scattered intensity is a function of the transmission of the cell and the sample, the thickness of the cell, the efficiency of the detector, the flux of the

neutron beam and takes into account the contribution of background due to the electrical noise and imperfections of the detector. This background can be measured by blocking the beam and subtracted from all raw data. In the same way, it is necessary to subtract the contribution of the cell, that can be done simply measuring the scattering of the empty cell.

Next, it is necessary to evaluate the instrument constant that is the number of neutrons striking the sample per second multiplied by the solid angle of the detector element, multiplied by the efficiency of the detector. This constant is measured by recording the intensity of the attenuated direct beam. The attenuation avoid the saturation of the detector.

Finally, the transmissions are measured. The transmission of the attenuated beam is a property of the material used as attenuator and was measured by ANSTO for Quokka prior the experiment. Then, for each detector distance it was measured the intensity of neutrons passing through the empty cell and divided this for the intensity of the direct beam. This procedure was done for all the samples before their acquisition.

3.2.5. Small Angle Scattering data analysis

The scattered intensity collected by SAXS and SANS are visualised as a function of q . Depending on the relative value of q , three specific domains can be defined on the graph, from which different parameters can be determined:

- In the *Guinier region*^[11] ($qR_g \leq 1$) the radius of gyration can be extracted. For very small q the scattering function can be expanded and the R_g can be extracted using the Guinier approximation, applicable on compact particles as spheres or cylinders, and is defined as

$$\ln I(q) = \ln I(0) - (q^2 R_g^2 / 3) \quad (3.e)$$

- In the intermediate range ($R_g^{-1} < q \leq l^{-1}$) the variation of the scattering function depend on the form of the particle and it is possible to distinguish for example between a sphere or a rigid rod.

Recovering all these information from the scattering function is called the inverse scattering problem. The method most used to do it, is to fit the scattering curve for different aggregates shapes. These functions are analytical equations that depend on parameters such as radius of a sphere, shape of the aggregates, length of a rod, etc. Therefore, the data fitting requires a physically reasonable interpretation to ensure that the values extracted are real.

3.3. Dynamic light scattering

Several scattering techniques are typically used to study aggregate formation. In this thesis we used Dynamic Light Scattering (DLS), Small angle X-Ray Scattering (SAXS) and Small Angle Neutron Scattering (SANS).

- **Light scattering**

It is characterised by a $\lambda \approx 5000 \text{ \AA}$, the associated particle is a photon of energy of about 10 eV. The interaction takes place through the polarisability (α) of the elementary scatterer and the scattering length is defined as:

$$b(\Theta, \lambda, \alpha) = f(\Theta) \alpha (2\pi/\lambda)^2 \quad (3.f)$$

from this equation the dependence of b from the scattering angle Θ and from λ is evident. Moreover, the polarisability α can be expressed as function of the refractive index in the case of isotropic scatterers at concentration N/V

$$\alpha = \frac{3}{4\pi} \frac{V}{N} \frac{n^2 - 1}{n^2 + 2} \quad (3.g)$$

3.3.1. Dynamic Light Scattering: experimental equipment

DLS, also known as Photon Correlation Spectroscopy, measures the diffusion coefficient of particles in solution from the scattering of a laser beam, and the size can be calculated using the Stokes-Einstein equation. The laser beam passes through a polarizer and into the sample. The scattered light then goes through a second polarizer where it is collected by a photomultiplier and the resulting image is projected onto a screen. This is known as a speckle pattern.

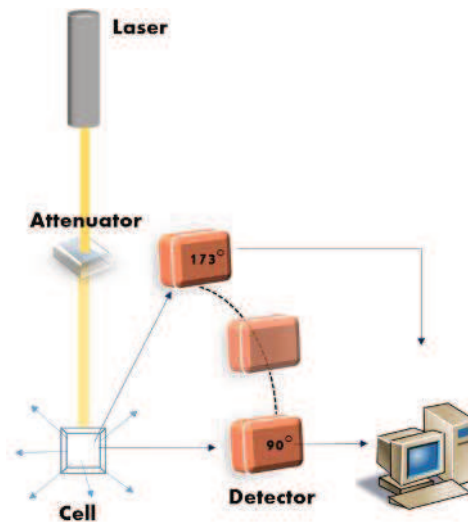


Figure 3-5 scheme of typical DLS systems

Particles in solution are never stationary, they are constantly moving due to Brownian motion governed by the Stokes-Einstein equation (eq 3.a). An important feature of this kind of motion for DLS is that smaller particles move quickly, larger particles move slowly.

As the particles move around, the constructive and destructive phase addition of the scattered light will cause the fluctuation of the intensity of the light on the speckle. The DLS instrument measures the rate of the intensity fluctuation and then uses this to calculate the size of the particles.

The system compares the intensity signal of a particular part of the speckle pattern at time t with the intensity signal a very short time later ($t+\Delta t$). As we can see in fig 3.6 the correlation between the two signals depend on the speed of particles: the rate of decay is much faster for small particles than it is for larger ones.

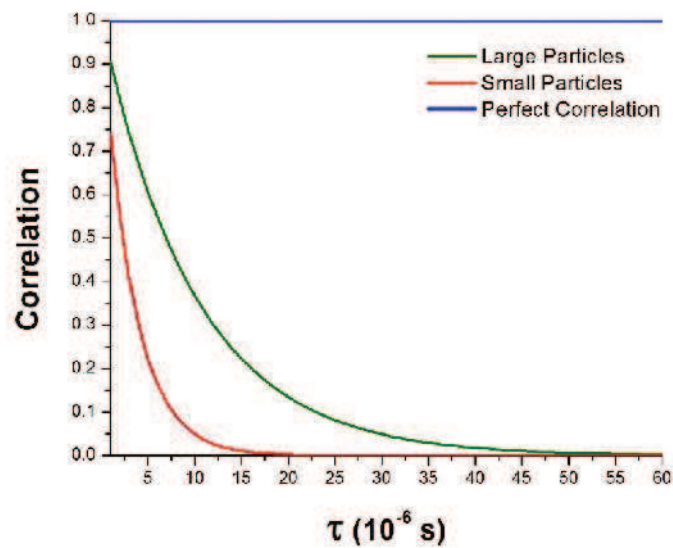


Figure 3-6 Correlation function in DLS

More detailed information are contained in the book by Pecora^[19].

3.3.2. Dynamic Light Scattering: Data analysis

The data collected by DLS are mainly three:

Z-average size (also known as the “cumulants mean”). In dynamic light scattering this is the most important and stable number. This is the size to use if a number is required for quality control purposes. It will only be comparable with other techniques if the sample is monomodal (*i.e.* only one peak), spherical and monodisperse (*i.e.* no width to the distribution), and the sample is prepared in the correct dispersant.

In any other case, the Z-average size can only be used to compare results with samples measured in the same dispersant, by the same technique, *i.e.* by DLS.

The cumulants analysis only gives two values, a mean value for the size, and a width parameter known as the Polydispersity, or the Polydispersity Index (PDI). It is important to note that this mean size (often given the symbol Z or z-average) is an intensity mean. It is not a mass or number mean because it is calculated from the signal intensity.

The cumulants analysis is actually the fit of a polynomial to the log of the G1 correlation function $\ln[G1] = a + bt + ct^2 + dt^3 + \dots$

The value of b is known as the second order cumulant, or the z-average diffusion coefficient. This is converted to a size using the dispersant viscosity and some instrumental constants.

Only the first three terms a, b, c are used in the standard analysis to avoid over-resolving the data; however this does mean that the Z-average size is likely to be interpreted incorrectly if the distribution is very broad (*i.e.* has a high polydispersity).

Polydispersity index. The coefficient of the squared term, c , when scaled as $2c/b^2$ is known as the polydispersity, or polydispersity index (PDI).

Peak means. Displays the size and percentage by either intensity, volume or number for

up to three peaks within the result.

In summary, the cumulants analysis gives a good description of the size that is comparable with other methods of analysis for spherical, reasonably narrow monomodal samples, *i.e.* with polydispersity below a value of 0.1. For samples with a slightly increased width, the Z-average size and polydispersity will give values that can be used for comparative purposes. For broader distributions, where the polydispersity is over 0.5, it is unwise to rely on the Z-average mean, and a distribution analysis should be used to determine the peak positions. ^[20]

3.4. Differential Scanning microCalorimetry (nano DSC)

Differential Scanning Calorimeters (DSC) measures temperatures and heat flows associated with thermal transitions in a material. Common usage includes investigation, selection, comparison and end-use performance evaluation of materials in research, quality control and production applications. The Nano DSC is designed for ultra-sensitive measure of heat absorbed or released by dilute in-solution bio-molecules as they are heated or cooled.

The instrument used for this project was equipped with a capillary platinum cell that

attenuate aggregation and precipitation. Platinum is inert and compatible with strong acids and bases, the small volume (300 μL active cell volume) minimizes sample consumption and minimize trapped air bubbles.

The Thermoelectric Temperature Control ensure an accurate, reproducible temperature control for highest sensitivity in both heating and cooling scans and unmatched baseline reproducibility.

Instrument features were a user-programmable pressurization system (up to 6 atm), a short-term noise of 0.015 μW , a baseline stability of $\pm 0.028 \mu\text{W}$, a response time of 7 seconds, an operating temperature from $-10 \text{ }^\circ\text{C}$ to $130 \text{ }^\circ\text{C}$ or $160 \text{ }^\circ\text{C}$, a temperature scan rate up to $2 \text{ }^\circ\text{C}/\text{minute}$, a fixed capillary platinum cell having an active cell volume of 300 μL and the power compensation heat measurement.

References and Notes

- [1] A. Einstein, *Annalen der Physik* **1905**, 322, 549-560.
- [2] Johnson C. S. Jr, *Progress in Nuclear Magnetic Resonance Spectroscopy* **1999**, 34, 203-256.
- [3] J. S. Gounarides, A. Chen, M. J. Shapiro, *Journal of Chromatography B: Biomedical Sciences and Applications* **1999**, 725, 79-90.
- [4] D. A. Jayawickrama, C. K. Larive, E. F. McCord, D. C. Roe, *Magn Reson Chem* **1998**, 36, 755-760.
- [5] Y. Bakkour, V. Darcos, S. Li, J. Coudane, *Polym Chem-Uk* **2012**, 3, 2006-2010.
- [6] A. Chen, D. Wu, C. S. Johnson, Jr., *The Journal of Physical Chemistry* **1995**, 99, 828-834.
- [7] R. Kerssebaum, *DOSY and Diffusion by NMR, manual for topSpin*, Bruker BioSpin GmbH, **2002**.
- [8] J.P. Cotton, *Neutron, X-Ray and Light-Scattering: Introduction to an Investigative Tool for Colloidal and Polymer Systems*, North Holland delta series, Amsterdam, **1991**.
- [9] O. Glatter, O. Kratky, *Small angle x-ray scattering* Academic Press London, **1982**.
- [10] M.G. Huglin, *Light scattering from polymer solutions*, Academic Press London, London and New York, **1972**.
- [11] A. Guinier, G. Fournet, *Small angle scattering of X-rays.* , John Wiley and Sons, New York, **1955**.
- [12] V. Luzzati, A Tardieu, *Annual Review of Biophysics and Bioengineering* **1980**, 9, 1-29.
- [13] G.L. Squires, *Introduction to the Theory of Thermal Neutron Scattering*, Cambridge University Press, Cambridge, **1978**.
- [14] G. Zaccai, B. Jacrot, *Annual Review of Biophysics and Bioengineering* **1983**, 12, 139-157.
- [15] W. B. Yelon, in *Interstitial Intermetallic Alloys* (Eds.: F. Grandjean, G. J. Long, K. H. J. Buschow), Springer Netherlands, Dordrecht, **1995**, pp. 225-248.
- [16] <http://www.ansto.gov.au/AboutANSTO/OPAL/index.htm>;
- [17] O. Glatter, *Neutron, X-Ray and Light-Scattering: Introduction to an Investigative Tool for Colloidal and Polymer Systems*, North Holland delta series, Amsterdam, **1991**.
- [18] P.A. FitzGerald, PhD thesis, *Solution behaviour of Polyethylene Oxide, Nonionic Gemini Surfactants*, The University of Sydney **2002**.
- [19] R. Pecora, *Dynamic Light Scattering: Applications of Photon Correlation Spectroscopy*, Plenum Press, New York, **1985**.
- [20] H. Wilczura-Wachnik, *DLS Manual*, University of Warsaw, Faculty of Chemistry.

5. Conclusions

"As the search for life in the solar system expands, it is important to know what exactly to search for". ^[1] We started this thesis work with this sentence and presenting different ideas of how life on Titan's methane lakes could be. This project doesn't claim to be a proof of the existence of life in extreme hydrocarbon environments, but rather an experimental work to prove that life can be constituted by different bricks than those that build the life as-we-know-it-on-Earth. Thus, the principal aim of this project was to synthesise new reverse amphiphiles and to detect their aggregation in an organic solvent that acted as model for hydrocarbon environment. There is a lack in the definition of typical micelle and reverse micelle, though. What we obtained is a new kind of aggregate in hydrocarbons, made of amphiphilic molecules that differ from common surfactants for the inverted polarity, but at the same time are different from amphiphilic block co-polymers that bear a long lipophilic chain and are generally one or two orders of magnitude larger. ^[2] For these reasons we called them reverse amphiphiles.

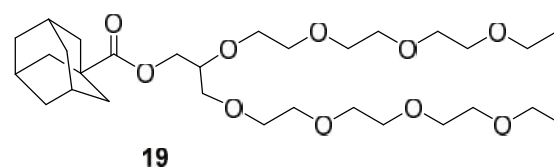
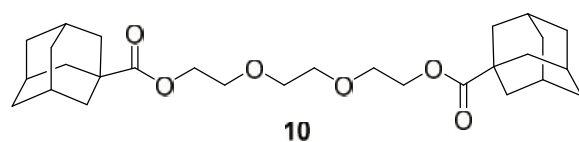
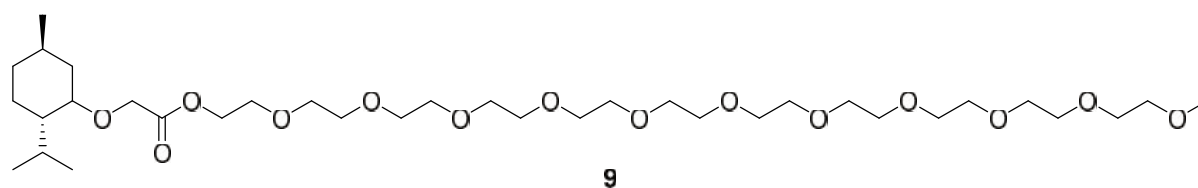
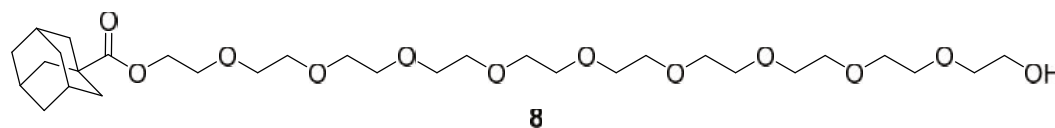
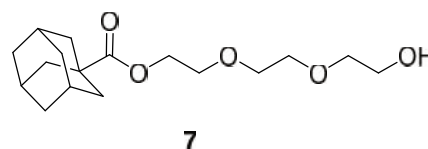
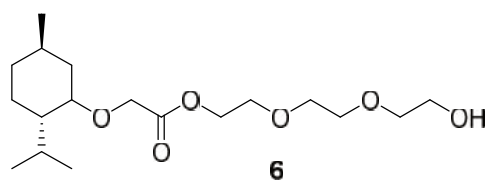
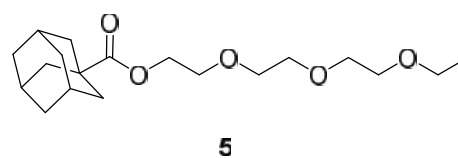
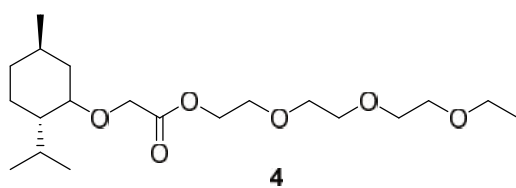
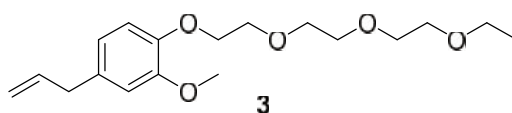
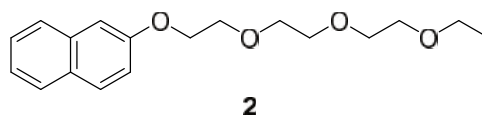
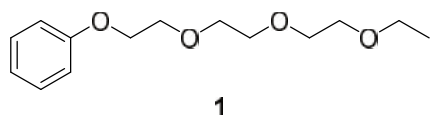
It must be stressed that this is the first experimental work in which micelles with the same geometric configuration of typical micelles in water, are formed in hydrocarbons.

The project started with the design and synthesis of nine new reverse amphiphiles. Two others- *i.e.* **10** and **19**- are currently issue of synthesis (see figure 5.1).

Their designed was based on the geometry and dimensions of the final molecule as well as the electronic configuration of each part. We used different kind of headgroups, while for the tails we used PEGs with different lengths and terminal groups.

Seven reverse amphiphiles were obtained in high yield and purity (*i.e.* **1-7**). Purity is an important parameter for the aggregation process. Since this was the first attempt to obtain typical micelles in hydrocarbons, we wanted to avoid the

presence of impurities that might influence the micelle formation. Compounds **8** and **9** were obtained as a mixture of amphiphiles with different tail length, thus their behaviour in hydrocarbons was not analysed.



For the same reason a particular attention was put on the dehydration of both solvents and reverse amphiphiles, although it was not possible to determine the water content. This analysis, in fact, is commonly done with a Karl-Fisher titration, that implies the solubilisation of the compound under examination in methanol. Reverse amphiphiles **4-7** though, are not soluble in this organic solvent.

We started analysing the aggregation of reverse amphiphiles using one of the most common technique for aggregates detection that is DLS.

This instrument is a powerful tool with aqueous solutions, but failed with hydrocarbons.

The high polydispersity of micelles and their very small size, limited the accuracy of DLS measures and thus it wasn't possible to determine the size and volume of aggregates. DLS though, allowed the discrimination between solutions containing aggregates and those without.

Compounds **1-3** didn't show any aggregation ability, while compound **4** and **5** were found to aggregate only in n-hexane and cyclohexane.

Although DLS measures didn't allow the characterisation of the aggregates formed, the results obtained were really important. We found that an aromatic ring in the headgroup is not enough hydrophobic, and doesn't give to the final molecule the necessary amphiphilic nature to permit the aggregation in hydrocarbons. Thus the electronic configuration of each part of the amphiphilic molecule is fundamental. Another important feature obtained with DLS, is the role of the solvent. While for conventional surfactants typical micelle can form only in water, for reverse surfactants the geometry and polarity of solvent influence dramatically the aggregation process. The result is that while in hexane and cyclohexane compounds **4** and **5** showed aggregation abilities, in a mixture of alkanes like

petroleum ether the aggregation was not permitted. Thus, aggregation is not possible with all reverse amphiphiles and not in all hydrocarbon solvents.

We then used calorimetric methods to confirm DLS results. The instrumental limits, though, didn't allowed the complete acquisition of nano-DSC scans. As DLS, nano-DSC is design for the analysis of aqueous solutions and not for solvents that are more volatile. DSC measure was insufficient to calculate micelle formation enthalpy, but enough to confirm the aggregation of free amphiphiles in cyclohexane. We attempted also the determination of the CAC of compounds **4** and **5** with Isothermal Titration Calorimetry, but all the attempts were unsuccessful. A deep study of the thermodynamic of the aggregation process is planned using compounds **6** and **7** in methylcyclohexane.

The complexity of self-aggregation of reverse amphiphiles in hydrocarbons partly relies on the fact that there are more factors to consider than in water.

From this point, we decided to study both these aspects starting with the synthesis of reverse amphiphiles similar to compound **4** and **5**, but with an enhanced lipophobicity on the tail.

Compounds **6** and **7** were then designed and synthesised using TEG as tail precursor. The first evidence of the amphiphilic nature of compounds **6** and **7** was the different solubility of them and TEG in cyclohexane. While TEG itself is not soluble in it, the reverse amphiphiles **6** and **7** form clear colourless solutions up to a 50/50 volume ratio.

The aggregation was studied with an NMR technique- *i.e.* 2D-DOSY – that calculated the diffusion coefficient of particles in solution. This method is usually adopted to analyse the formation of big aggregates in water ^[3] since the measure is a weighted average between $\text{Log}[(D)_{\text{free amphiphile}}]$ and $\text{Log}[(D)_{\text{aggregate}}]$.

2D-DOSY was done on solutions at different concentrations of amphiphiles **6** and **7** in cyclohexane. The difference of D between a dilute solution and a concentrated one for both amphiphiles was not really marked. This suggested a high

polydispersity of aggregates size, a multi-equilibrium process of micelle formation and aggregates size in the same order of magnitude of amphiphile length. Although 2D-DOSY was not a suitable technique for the study of reverse amphiphiles aggregation, it was sufficient to detect aggregates.

From all these results, it is evident that more sophisticated techniques are necessary for the characterisation of micelles from reverse amphiphiles in hydrocarbons.

SAXS measures were performed both at Università Cà Foscari Venezia and at The University of Sydney. With this technique it was possible to calculate the radius of gyration of aggregates applying the Guinier law. It must be pointed out that R_g is, for definition, independent from the aggregate shape. Once calculated the R_g it was possible to advance some hypothesis about the aggregates shape. The most plausible assumption was the sphere, thus we calculated the geometrical aggregate radius for each amphiphile at each concentration. It's not possible, though, to distinguish between a system of polydisperse spheres and a system of ellipsoids (these results were collected in a first communication that is currently under revision). The only consideration that can be advanced, is to exclude the formation of vesicles. This hypothesis was actually confirmed by preliminary studies performed with solvent penetration experiments that was done using the Polarizing Optical Microscopy, available at The University of Sydney. Solvent penetration experiments were performed to examine lyotropic phase formation over a range of concentrations. This method is well established for identifying vesicle formation.^[4-6] The procedure was to place a spot of reverse amphiphile on a microscope slide with a cover slip. A drop of the solvent was then placed on the outer edge of the cover slip where it was drawn into contact with the amphiphile via capillary action.^[7] This creates a concentration gradient. Using the solvent penetration, we tested also the effect of the addition of D-Glucose, $C_{12}E_3$ (triethylene glycol monododecyl ether), TEG, TEGME and ethylene glycol monobuthyl ether at molar ratio with the reverse amphiphiles **4-7** of 1, using

cyclohexane as solvent. These compounds were supposed to act as co-surfactants, and favour the formation of vesicles. Since all these attempts were unsuccessful, we didn't report any measure to avoid a tedious lecture.

So far, the aggregation of reverse amphiphile in hydrocarbons was detected, we calculated the R_g and the CAC of each amphiphile, thus the aim of the project was satisfied. There are though, some other aspects that must be study in deep.

With DLS we saw the importance of the solvent in the aggregate formation, in particular it was found that petroleum ether did not permit the micellisation. We then collected SAXS measures of compounds **4-7** at 200mM in methylcyclohexane, ethylcyclohexane, benzene, toluene and water. We already saw that compounds **6** and **7** that bear a terminal hydroxyl group were not soluble in n-hexane while compounds **4** and **5** are soluble and aggregates in it. Benzene and toluene are not sufficiently apolar to permit the aggregation, while cyclic hydrocarbons allow the aggregation of all four compounds. The hypothesis is that a cyclic conformation rather than the linear or branched ones, might permit the insertion of solvent molecules between the heads stabilising the micelle. This supposition might be confirmed with the SANS data treatment.

One of the most obvious questions at this point, is to confirm the geometry of the micelle obtained. The target was a micelle in hydrocarbon with the same configuration of typical micelle in water. Thus next step was to confirm the lipophobic nature of the micelle core.

Common techniques in water implies the use of a probe like a chromophore or a fluorophore. Such compounds usually change their luminescent (or fluorescent) properties once incorporated in the micelles. ^[8-10] In the same way we used Fluorescein, Reichardt dye, Rhodamine B and Brilliant Green as probes. These common dyes are insoluble and inactive in hydrocarbons. In the solutions containing a concentration of 200mM of reverse amphiphiles, the dyes were solubilised in the solution. This behaviour suggested their incorporation in the aggregates. We then performed UV-VIS or Fluorescence measures on the solutions,

but without success. The explanation may rely on the dimensions of dyes compared to micelles. Although positive interactions were established between amphiphiles and dyes, the latter couldn't fit in the micelle, with the consequent quenching of the dye.

We then opted for another kind of measure, using water as probe and SAXS as analytic technique. With this procedure it was possible to determine not only the polar core of micelles, but also the influence of the terminal hydroxyl group in the aggregation and the role of the headgroup in the stability of aggregates. Preliminary measures were performed with SAXS, but the proposal for SANS measures at ANSTO was accepted and funded for a value of 47.000 aud.

Although we are still performing SANS data analysis, it's possible to claim that:

- hydroxyl group at the end of the amphiphile tail is necessary for water incorporation, since compounds **4** and **5** cannot solubilise water in hydrocarbon solutions;
- Water is packed in the core of micelle, that confirmed the desired geometrical configuration of the micelle, *i.e.* the lipophilic heads are directed toward the apolar solvent and are distributed on the external surface of the micelle, while PEG tails are packed into the core of the micelle.
- Although both compounds **6** and **7** bear the terminal hydroxyl group, they behave in a different way in a water in oil system. Our hypothesis about the different behaviour is based on the geometry of these reverse amphiphiles. Headgroup shapes influenced the packing properties of amphiphiles in the micelle, *i.e.* a flat rounded headgroup (**6**) lead to a more stable micelle than a spherical one (**7**). Perturbing the system with water addition, made this difference in stability more evident.

Moreover, it was found that the lowering of temperature to -20°C, has no effects on micelles composed only by reverse amphiphiles, while lead to an enhancement of micelle size once water is incorporated.

SANS results are subject of a paper in preparation.

Lastly, some attempts were done for the study of solubility and aggregation abilities of amphiphiles **4-7** in liquid methane, with the aim of reconnect this project with the idea of life on Titan's methane lakes. Since all the problems we encountered during the acquisition were due to technical aspects, we are working on a proposal for new SANS measures. There are, in fact, no other techniques that allow to detect the micelle formation at such extreme conditions.

Future prospective

This thesis work opened a new branch in the field of soft matter. The possible studies that could be done now are many.

With conventional surfactants, there are a lot of different techniques used for the detection and characterisation of aggregates in solution, but we saw that not all are applicable in hydrocarbons. Thus, it would be interesting to find a probe such as a chromophore or a fluorophore suitable for this kind of system, and use them as detector of aggregation.

Another aspect that can be develop is the geometry of amphiphile. We are currently synthesising compound **10** and **19**, with the aim of obtain bigger micelles or lyotropic phases. The main target in this sense is to obtain a double layer vesicle. Another way to produce bigger aggregates is the use of molecules that can be inserted between amphiphiles. A preliminary study was performed at The University of Sydney, but more attempts should be done.

Lastly, we aim to find an application of reverse amphiphiles, as for example as dehydrating agents for apolar solvents, or nano-reactors. This last target, though, will require a long and extensive research.

References and notes

- [1] *The Limits of Organic Life in Planetary Systems*, Nature Publishing Group, **2007**.
- [2] Raoul Zana, Carlos Marques, Albert Johner, *Advances in Colloid and Interface Science* **2006**, 123–126, 345-351.
- [3] L. Klíčová, P. Šebej, P. Štacko, S. K. Filippov, A. Bogomolova, M. Padilla, P. Klán, *Langmuir* **2012**, 28, 15185-15192.
- [4] L. S. Hirst, *Fundamentals of Soft Matter Science*, Taylor and Francis, FL, **2013**.
- [5] F.B. Rosevear, *Journal of the American Oil Chemists' Society* **1954**, 31, 628-639.
- [6] W. J. Benton, *Physics of Amphiphilic Layers*, Springer, Berlin, **1987**.
- [7] S. J. Bryant, R. Atkin, G. G. Warr, *Soft Matter* **2016**, 12, 1645-1648.
- [8] L. Basabe-Desmonts, D. N. Reinhoudt, M. Crego-Calama, *Chem Soc Rev* **2007**, 36, 993-1017.
- [9] K. A. Fletcher, I. A. Storey, A. E. Hendricks, S. Pandey, S. Pandey, *Green Chemistry* **2001**, 3, 210-215.
- [10] C. Reichardt, *Chem Rev* **1994**, 94, 2319-2358.

4. Results Measurement of phase behaviour

In chapter 3 we introduced several techniques that are commonly used to study the aggregation behaviour of amphiphilic molecules in water. In this project these methods were used to detect and analyse the aggregation of our reverse amphiphile in hydrocarbons. It must be stressed that all these techniques are usually used for aqueous systems and often the instruments are designed for aqueous samples and not for hydrocarbons. For this reason, every instrument had to be calibrated and the acquisition methods optimised for each solvent, where possible.

4.1. Dynamic Light Scattering (DLS)

DLS is one of the most used techniques for the study and characterisation of aggregates in solution. DLS is easy to use, doesn't require a high amount of sample and its cost make this instrument affordable and used for routine measurements. Particle sizing in the submicrometer size-range is nowadays performed on a routine basis using DLS. The scattering of the laser beam is due to a different refractive index of the particle respect to the solvent. The instrument used for this project was a Malvern Zetasizer Nano ZS90, located at University of Verona, Italy. This particular instrument has a measurement range of 0.3 nm – 5.0 microns (diameter, sample dependent), it uses a 90° optics and has a sensitivity of 10 mg/L (tested with lysozyme)^[1]. These features are common in most of DLS instruments.

DLS was used to analyse the aggregation behaviour of amphiphiles **1-5** in different apolar solvents, such as hexane, cyclohexane, and petroleum ether (b.p. 40°- 60°C). All measures were acquired using a 10 mm optical glass fluorescence cuvette. The choice was dictated by the fact that disposable cuvettes are made of polystyrene, a polymer that is soluble in organic solvents. A fluorescence cell, moreover, allowed the acquisition with the detector at 90 degrees because all faces are transparent to light.

We first ran measures of pure solvents at RT, in which no particles were detected. For each amphiphile were prepared stock solutions at the concentration of 500 or 200mM of amphiphile in different solvents (i.e. hexane, cyclohexane and petroleum ether 40-60°C). Concentrations in the range of 10-500 mM were prepared by further dilution of the stocks.

All solutions and pure solvents were filtered before the acquisition in order to lower the dust content in solution that can affect the intensity distribution. However, any signal due to the presence of particles bigger than 1000 nm was ignored since considered as dust.

The first order result from a DLS experiment is an intensity distribution of particle sizes. The intensity distribution is naturally weighted according to the scattering intensity of each particle fraction or family. For biological materials or polymers the particle scattering intensity is proportional to the square of the molecular weight. As such, the intensity distribution can be somewhat misleading, in that a small amount of aggregation/ agglomeration or presence of a larger particle species can dominate the distribution^[2-4]. However, this distribution can be used as a sensitive detector for the presence of particles in the sample.

Although the fundamental size distribution generated by DLS is an intensity distribution, this can be converted, using the Mie theory^[5], to a volume distribution or a distribution describing the relative proportion of multiple components in the sample based on their mass or volume rather than based on their scattering (Intensity.) When transforming an intensity distribution to a volume/mass distribution, four assumptions are made.

- All particles are spherical
- All particles are homogeneous
- The optical properties of the particles are known, *i.e.* the real and imaginary components of the refractive index
- There is no error in the intensity distribution

An understanding of these assumptions is particularly important since the DLS technique itself produces distributions with inherent peak broadening, so there will always be some error in the representation of the intensity distribution. As such, volume and number distributions derived from these intensity distributions are best used for comparative purposes, or for estimating the relative proportions where there are multiple modes, or peaks, and should never be considered absolute.

Amphiphile	conc (mM)	size (nm)	vol (%)	PDI	conc (mM)	size (nm)	vol (%)	PDI
		<i>cyclohexane</i>				<i>hexane</i>		
4	300	51.0	83	0.8	300	0.7	100.0	0.9
	200	7.0	100	1	200	0.7	100	0.8
	100	10.0	87	0.9	100	0.7	100	1.0
	50	7.9	97	1	50	1	100	1.0
	10	8.0	83	1				
5	300	0.7	100	1	300	0.7	100.0	1
	200	0.9	100.0	1.0	200	0.7	100.0	0.9
	100	0.7	100.0	1	100	0.7	100.0	1
	50	0.8	100	1				
	10	1.2	100	1				

Tab 4.1: size of particle in solution detected with DLS of compounds **4** and **5** in cyclohexane and hexane at different concentrations, RT

In table 4.1 are reported the size and their relative volumetric percentage abundance of the most abundant particles in solution. For amphiphiles **1**, **2** and **3** no sign of aggregation was detected. On the contrary the analysis of amphiphiles **4** and **5** in hexane and cyclohexane showed the presence of aggregates in the range between 0.5-60 nm. No aggregation was detected in petroleum ether. All the analysis, though, were characterised by a high polydispersity index (PDI). PDI is calculated by a simple two-parameter fit to the correlation data (the cumulants analysis), it is dimensionless and scaled such that values smaller than 0.05 are rarely seen other than with highly monodisperse standards. Values greater than 0.7 indicate that the sample has a very broad size distribution and is probably not suitable for DLS. The various size distribution algorithms work with data that fall between these two extremes^[6-8].

By DLS we didn't detect aggregates in any of the solutions of the reverse amphiphiles **1-3**, but with compounds **4** and **5** we detected a highly polydisperse system of reverse surfactants aggregates in hydrocarbons. For all acquisitions the PDI value was higher than 0.7.

4.1.1. DLS data discussion:

The study carried out using DLS was focused on the self-assembly of reverse amphiphiles **1-5** in hexane, cyclohexane and petroleum ether (b.p. 40°- 60°C) at different concentrations. From the data collected with this technique, two important features were deduced. Foremost, compounds **1-3** didn't show any self-aggregation property in any solvent. The main difference between these compounds and amphiphiles **4-5** lies in the electronic configuration of the headgroups. Compounds **1-3**, in fact, beared an aromatic ring (two for compound **2**) that lended a more polar nature to the headgroup while **4** and **5** possess aliphatic headgroups. These observations may indicate that a requirement for the aggregation of reverse amphiphiles in oil is the presence of a highly lipophilic headgroup.

Compounds **4** and **5** showed different behaviour in petroleum ether compared to n-hexane or cyclohexane. DLS of compounds **4** and **5** in hexane and cyclohexane revealed the presence of particles in solution at all concentrations. The data collected though, were characterised by a PDI greater than 0.7, thus this technique was not suitable for the determination of the particle size. Although these data cannot be considered as the real size of particle in solution, we used them as indicator of aggregation. One possible explanation for the poor quality of the data is that the DLS instrument built for routine measures of aqueous solutions was not suitable for the detection of aggregates in hydrocarbon solvents.

For what concern compounds **1-3**, no aggregate was detected, so their behaviour was not studied further. Compounds **6-19**, instead, were synthesised after the aggregates described above and thus their aggregation in hydrocarbons was not

investigated by DLS but rather studied by using the different and more suitable techniques outlined later.

4.2. Nano DSC

Nano-DSC is a specific kind of DSC instrument designed to characterize the molecular stability of biomolecules in water. Because of its high sensitivity it can measure the tiny heat absorption of micelle formation.^[9]

This instrument is commonly used for the analysis of aggregation in aqueous samples. The standard acquisition method is 10 minutes of stabilisation time before the scan, 1°C/min scan rate and 3 atm of pressure perturbation (N₂).

This method was used for a first scan of pure hexane, giving a baseline not suitable for the analysis for the presence of several broad peaks and a high initial perturbation heat (see fig 4.1 a). The method was thus optimised taking into account the higher vapour pressure of this solvent compared to water (*i.e.* 124 mmHg for hexane^[10] compared to 17.5 mmHg^[11] for water at 20°C). We raised the pressure perturbation and slowed the scan rate in order to minimize the bubble formation in the capillary. The optimized acquisition method was found to be 30 minutes of stabilisation time before the scan, 0.2 °C/min scan rate and 6 atm of pressure perturbation (gas used N₂), that are the instrumental limits of the available nano-DSC (see figure 4.1 b). Because of the high vapour pressure of hydrocarbon solvents, the maximum temperature reached in all the acquisitions was 30 °C. Above this temperature it was impossible to avoid bubble formation. The acquisition of the pure solvent was necessary because its contribution must be subtracted to the heat capacity curve of the samples. For this reason, the curve of pure solvents should be linear.

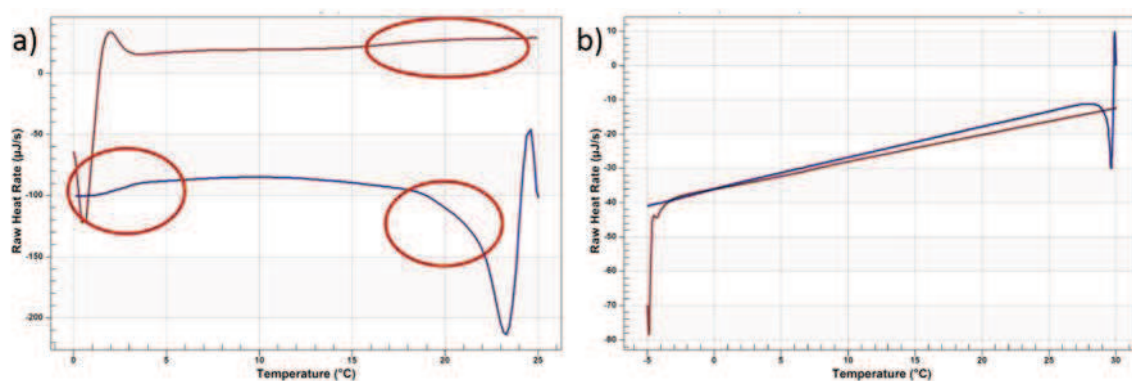


Figure 4.1: DSC scans of hexane in cooling mode (blue) and heating mode (red), standard acquisition method a) and optimised acquisition method b)

The enthalpy of the micelle formation could be obtained from a DSC experiment by integration of the heat capacity curve between two temperatures.

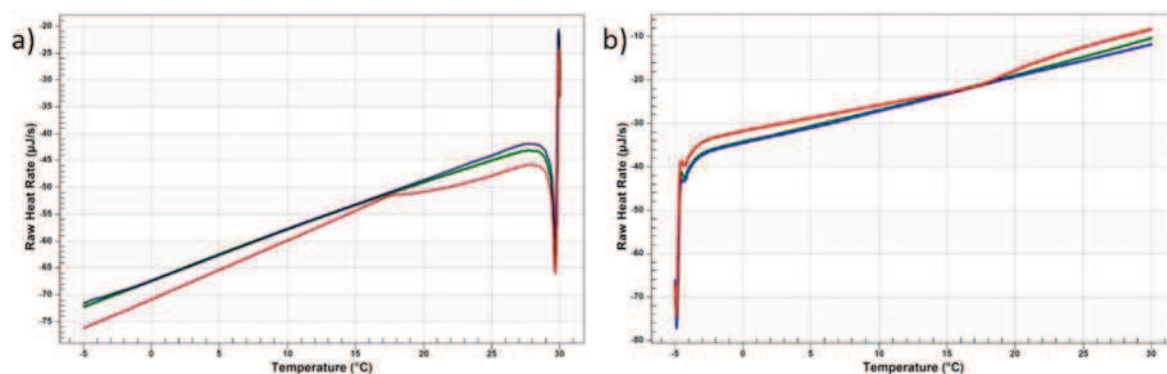


Figure 4.2: comparison of heat capacity curves of hexane (blue) and compound 4 in hexane at 20mM (green) and 50 mM (red). Cooling mode scan (a) and warming mode scan (b).

In figure 4.2 are shown nano-DSC curves (cooling and heating scans) of 20 and 50 mM solutions of compound 4 compared to hexane. The DSC trace of the solution at 50 mM shows a thermal transition between 17.6 and 28 degrees with a broad peak. Instrumental limits didn't allow to reach higher temperatures in order to collect the entire peak.

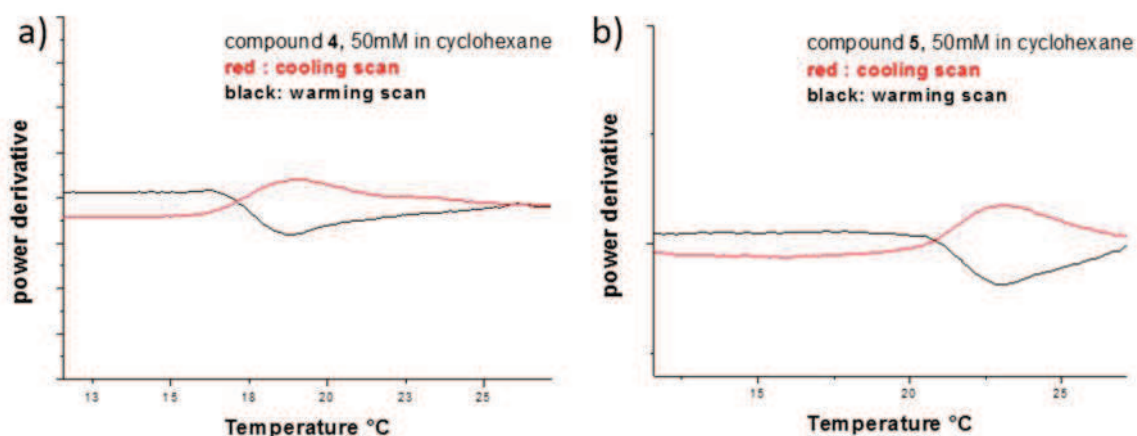


Figure 4.3 derivative curves of DSC measures for surfactant **4** (a) and surfactant **5** (b) at 50mM after solvent subtraction

Figure 4.3 shows derivative curves of DSC measures for both surfactants at 50mM. Deriving the heat capacity curve (solvent subtracted) allows visualisation of the temperature at which the aggregation take place at constant concentration. Since the instrumental limits did not permit a deeper and more accurate study of the thermodynamics of the system, no other measures were performed.

4.2.1. Nano DSC data discussions:

The aggregation heat capacity of compounds **4** and **5** in hexane and cyclohexane was measured by DSC scans. We studied two different concentrations, *i.e.* 20 and 50 mM of reverse amphiphile in hydrocarbon solvent, for both molecules. At the concentration of 50 mM, monomeric species and aggregates were hypothesized to be both present in solution, thus the transition around 25 degrees is due to aggregation/disaggregation of free surfactant. It was not possible to measure the aggregation temperature on a solution containing only monomeric species because the required low concentration of the solution (< 20mM) is characterised by a very low heat of transition.

The shape of the transition depends on the cooperativity of the process. Highly cooperative processes, such as micellisation of conventional amphiphiles in water give very sharp transitions, whereas less cooperative changes show much broader

transitions. In water, the formation of micelles is due to two different contribution: the hydrophobic effect and Van der Waals interactions .^[12] For a reverse amphiphile such as **4** and **5** in a lipophilic solvent, the hydrophobic effect is lacking and micelle formation is driven only by the attractive forces established between the polar tails. This is confirmed by the broad transition recorded with nano-DSC. It is therefore possible to deduct that critical aggregation temperature (CAT), *i.e.* the temperature in which aggregates are formed, is comprised between 18 and 25 °C for both amphiphiles.

These curves show that the transition occurred at the same temperature in both directions: cooling as well as warming. This suggested that the process of aggregation in hydrocarbon solvents is reversible.

4.3. 2D-Diffusion Ordered Spectroscopy Nuclear Magnetic Resonance (2D-DOSY NMR)

Since DLS was not sufficient to study reverse amphiphile aggregation, the self-assembly of compounds **6-7** in cyclohexane was studied by measuring the diffusion coefficient of the species in solution using 2D-DOSY NMR (2-Dimensional Diffusion Ordered Spectroscopy).

4.3.1. 2D-DOSY experiments acquisition and processing

2D-DOSY was run on freshly prepared solutions of the two amphiphiles at different concentrations in the range 5-260 mM in cyclohexane. Locking was performed on residual protons of dms_o-d₆ contained in a coaxial tube. Before running the 2D DOSY experiment, simple 1D DOSY were recorded for each sample in order to optimize the magnetic field pulse gradients (δ) and diffusion time (Δ) values to ensure proper signal abatement during the 2D experiment.

¹H-NMR were recorded at 303 K, unless otherwise stated, on a Bruker AVANCE 300 spectrometer operating at 300.15 MHz. δ values in ppm are relative to SiMe₄. 2D-

DOSY spectrum were recorded on the same instrument equipped with a PABBO BB-1H Z GRD probe head. Pulse sequence used was ledbpgp2s 2D sequence for diffusion measurements using stimulated echo and LED using bipolar gradient pulses using 2 spoil gradients. The amplitude of the field gradient was varied from 2 to 95% of its maximum value over 32 increments, while the gradient recovery delay (τ) and the eddy current delay (t_e) were fixed at 0.1 and 5 ms, respectively. The diffusion delay (Δ) was set to 50 ms and the corresponding gradient pulse duration (δ) 1-1.5 ms, in order to achieve an intensity attenuation range of at least 95%. The number of scans was set in the range 8-32 depending on the concentration of the amphiphile, with a recycling delay D1 of 5 s. Without sample spinning, a series of 32 spectra on 16K data points were collected with 32 transients, total measuring time was ca. 1 h. After Fourier transformation and baseline correction, the diffusion dimension was processed with the Bruker Xwin-NMR software package.

4.3.2. 2D-DOSY results

We performed 2D-DOSY analyses on solutions of reverse amphiphiles **6** and **7** in cyclohexane in the concentration range 5-260 mM. For each sample, the diffusion coefficients of the resonances of the amphiphile and of the solvent were determined at 303 K and plotted as a function of the concentration of each amphiphile.

Measurements of $\text{Log}(D)$ of amphiphile **6** at different concentrations by 2D-DOSY NMR are reported in fig 4.4. In the range of concentrations considered, the solvent showed a rather constant diffusion coefficient, indicating that the viscosity of the solution was not affected significantly by changing the concentration of **6**. The diffusion coefficients of cyclohexane in itself (\diamond) and of amphiphile **6** (\bullet) at increasing concentrations of **6** showed that the ratio between the hydrodynamic radii of **6** and cyclohexane was about 2.0. This behaviour is indicative of aggregation, albeit weak.

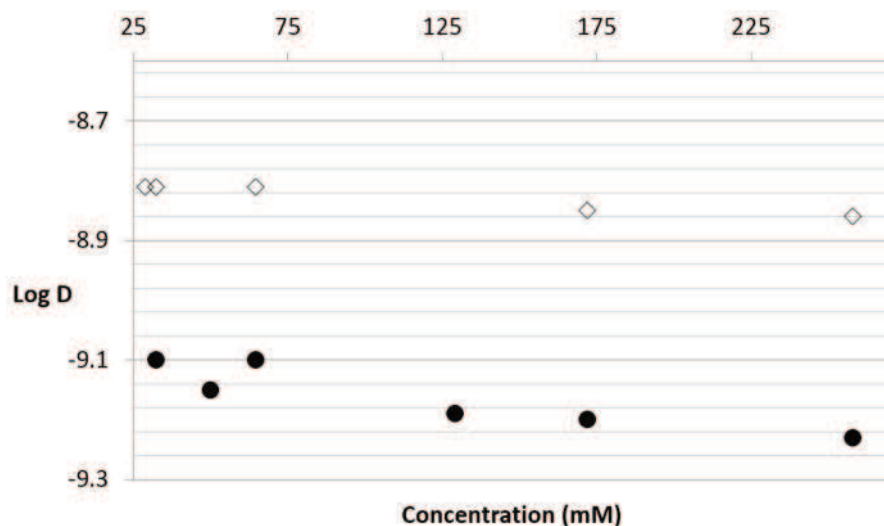


Figure 4.4 Plot of $\text{Log}(D)$ vs. concentration of **6** measured by 2D-DOSY experiments. ●amphiphile **6**, ◇ cyclohexane.

Since 2D-DOSY does not distinguish between the diffusion coefficients of the amphiphiles and of the aggregates, thus an underestimated average hydrodynamic radius of the aggregates was probably obtained.

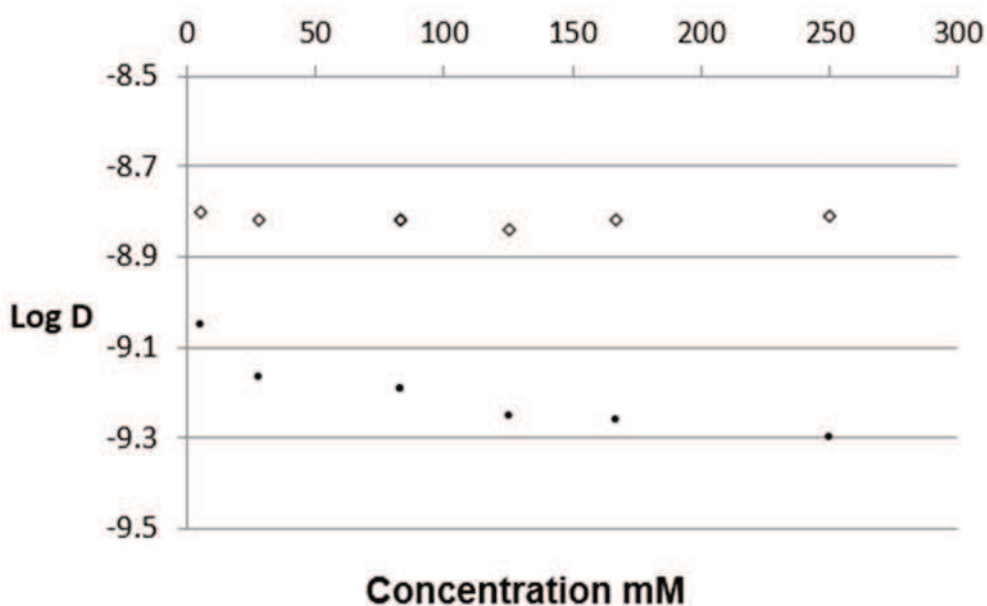


Figure 4.5 Plot of $\text{Log}(D)$ vs. concentration of **7** measured by 2D-DOSY experiments. ●amphiphile **7**, ◇ cyclohexane.

Figure 4.5, instead, shows the diffusion coefficients of cyclohexane in itself (◇) and of amphiphile **7** (●) at increasing concentrations of **7**. As clearly observed in figure 3, while the diffusion coefficient of cyclohexane remained constant, the profile of

Log(D) for the amphiphile **7** as a function of the concentration (5-250 mM) decreased monotonically down to the value of -9.3 at 250 mM. At a concentration of 250 mM the ratio between the hydrodynamic radius of **7** and that of the solvent cyclohexane was about 2.

4.3.3. 2D-DOSY data Discussions

The 2D-DOSY NMR experiments provided diffusion coefficients of the aggregates with respect to the solvent that were consistent with the magnitude of the proposed self-assembled structures. However, it should be kept in mind that these measures afforded experimental Log(D) values that are a weighted average between Log[(D)_{free amphiphile}] and Log[(D)_{aggregate}] because the aggregates are in equilibrium with each amphiphile **6** and **7** in solution and because the aggregation equilibrium was fast with respect to the NMR timescale.

The diffusion coefficient for cyclohexane at 25°C observed by direct DOSY measurements as an average value among the different solutions of **6** and **7** was $1.48 \cdot 10^{-5} \text{ cm}^2/\text{s}$ which is in good agreement with the value reported in the literature corresponding to $1.43 \cdot 10^{-5} \text{ cm}^2/\text{s}$.^[13]

No clear change in the diffusion coefficient of **6** was observed up to 100 mM as indicated by the minimal slope of log(D). The average ratio between the diffusion coefficients of **6** and of cyclohexane is inversely proportional to the ratio of the hydrodynamic radii of the two species. Calculation in the range 17-260 mM led to an average hydrodynamic ratio about two times larger for **6** compared to that of cyclohexane.

For compound **7**, considering the ratios between the diffusion coefficients of **7** and of the solvent cyclohexane for the different solutions, it is clear that the average hydrodynamic radius of the amphiphile tends to increase with increasing concentration, up to about $5.0 \cdot 10^{-10} \text{ cm}^2/\text{s}$ for 250 mM. Moreover, at a concentration of 250 mM the ratio between the hydrodynamic radius of **7** and that

of the solvent cyclohexane was about 3.5. Both these results are a strong indication of aggregation.

At a concentration of 250 mM the ratio between the hydrodynamic radius of **7** and that of the solvent cyclohexane was about 2, that is a clear indication of micelle formation.

4.4. Small Angle X-ray Scattering (SAXS) results

4.4.1. Micelle detection

Having obtained evidences of aggregation of our reverse amphiphiles **4-7** by DLS, DSC and NMR, we then focused on SAXS measurements for a more detailed characterization of the aggregates. We therefore investigated the behaviour of **4-7** in cyclohexane by SAXS at different concentrations (50, 75, 100, 200, 300, 500 mM). All the intensities are reported in arbitrary units and subtracted of the solvent contribution.

We first searched for organised structures of **4** and **5** over a range of concentrations in cyclohexane using small angle X-ray scattering spectroscopy (SAXS). These measures were run in order to confirm the presence of the aggregates detected by DLS and DSC. Moreover, SAXS allowed to estimate the size of particles in solution. The SAXS intensities relative of compound **4** at different concentrations in cyclohexane (see figure 4.6 a) were indicative of the presence of self-assembled structures as indicated by the increasing of the intensity of the scattering curve in the region $0.01 - 1.0 \text{ nm}^{-1}$. In figure 4.6 b are shown the Guinier plots of the intensities (see equation 3.e).

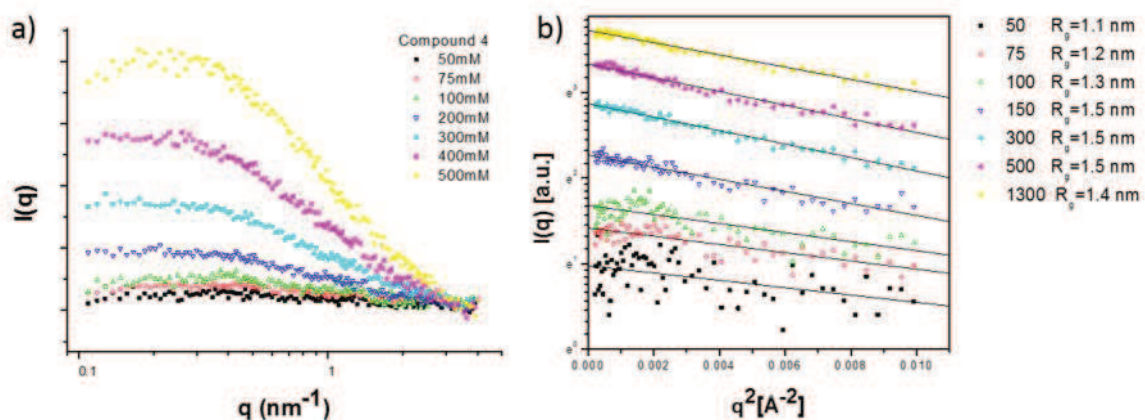


Figure 4.6: SAXS intensities (arbitrary units, solvent subtracted) of compound **4** in cyclohexane at different concentrations (a) and Guinier plot of SAXS intensities (b).

The slopes of the linear fit, that gives $-R_g^2/3$, were all very similar and independent of concentration and assuming spherical particles this allowed the estimation of the radii ($R^2 = (5/3) R_g^2$). Since the particle size did not increment with increasing concentration, the increase of intensity of scattering curves was due to the number of particles.

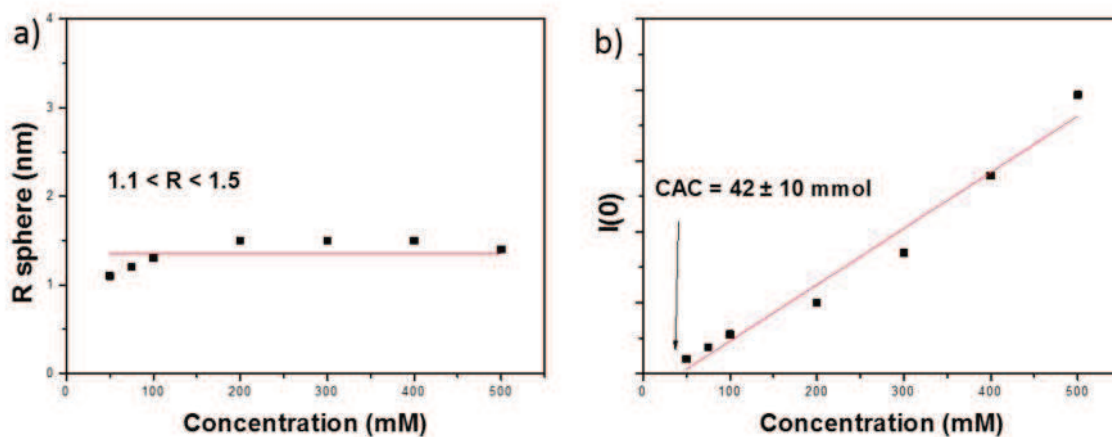


Figure 4.7 geometric radii of aggregates and CAC extrapolation by linear fit of $I(0)$ for compound **4**.

The calculated radii were plotted as a function of surfactant concentration. The aggregate sizes complied with the consistence restrain for the Guinier Plot that requires that the linear fit must be done in the region $q^2 < 1/R_g^2 \approx 0.35$ nm⁻². The radii of the aggregates were about 1.5 nm and were almost independent of the

concentration in the investigated range (50-500 mmol). The estimated length of surfactant **4** was approximately 2 nm by molecular mechanics, therefore the size of the aggregates was consistent with the one of the surfactant.

Using the Guinier plot it was evident that aggregate size didn't change with concentration, as indicated in figure 4.7 a.. Although there's no evident changing in the intensity of scattering curves, the Critical Aggregate Concentration (CAC) was obtained by linear extrapolation of these intensities to $I(0)=0$. The CAC obtained for surfactant **4** is 42 ± 10 mM (see figure 4.7 b).

Very similar results were obtained with surfactant **5** and figure 4.8 a shows the increase of the intensity of the SAXS signal with the concentration. The slope of the Guinier plot in figure 4.8 b does not change significantly for the studied concentrations and the average radius, obtained assuming a spherical shape of the aggregates, was 1.3 ± 0.2 nm.

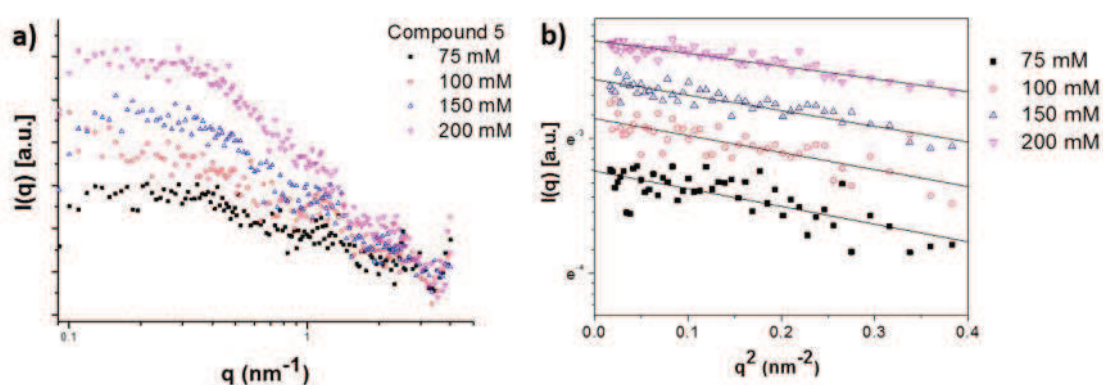


Figure 4.8: SAXS intensities (arbitrary units, solvent subtracted) of compound **5** in cyclohexane at different concentrations (a) and Guinier plot of SAXS intensities (b).

CAC was estimated with the same plot used for compound **4**, and a value of CAC = 22 ± 5 mM was obtained. Sizes and CAC of compound **5** were both comparable to the results obtained for **4** within the experimental error.

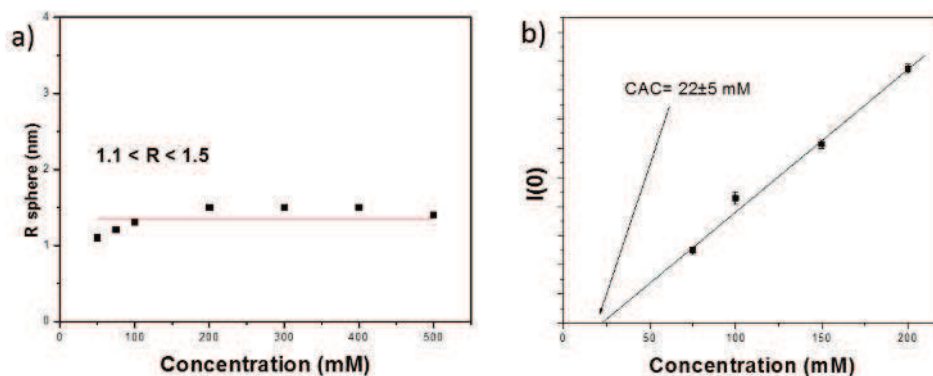


Figure 4.9.: geometric radii of aggregates and CAC extrapolation by linear fit of $I(0)$ for compound 5.

We then measured the scattering spectra of reverse amphiphile analogous to compound 4 and 5, but bearing a tail with an enhanced polar nature. Compound 6 and 7, in fact, are characterised by a terminal hydroxyl group that should allow the formation of hydrogen bonds and thus favour the self-aggregation.

SAXS measures were performed in the same conditions used for compounds 4 and 5.

The SAXS intensities of compound 6 were concentration-dependent and showed the presence of self-assembled structures as indicated by the increase in intensity of the signal in the region $0.1 - 1.0 \text{ nm}^{-1}$ (figure 4.10 a), while in figure 4.10 b are reported the respective Guinier plots.

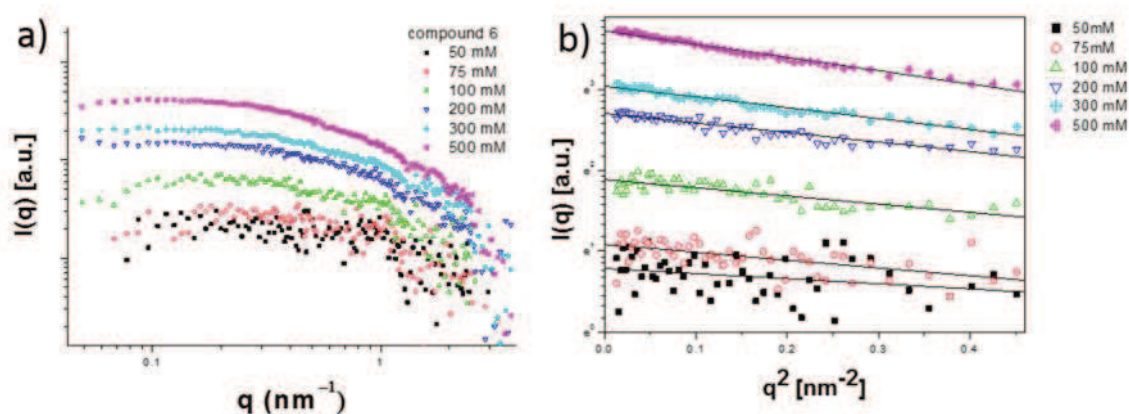


Figure 4.10. SAXS intensities (arbitrary units, solvent subtracted) of compound 6 in cyclohexane at different concentrations (a) and Guinier plot of SAXS intensities (b).

The calculated radii were plotted as a function of surfactant concentration (figure 4.11 a) and it was found to be comprised between 1.8 and 2.6 nm over the concentration range of 50-300 mM.

A plot of $I(0)$ vs concentration allowed to estimate a CAC by extrapolating the concentration at $I(0) = 0$. The CAC appeared to be comprised between 20 and 40 mM (Figure 4.11 b).

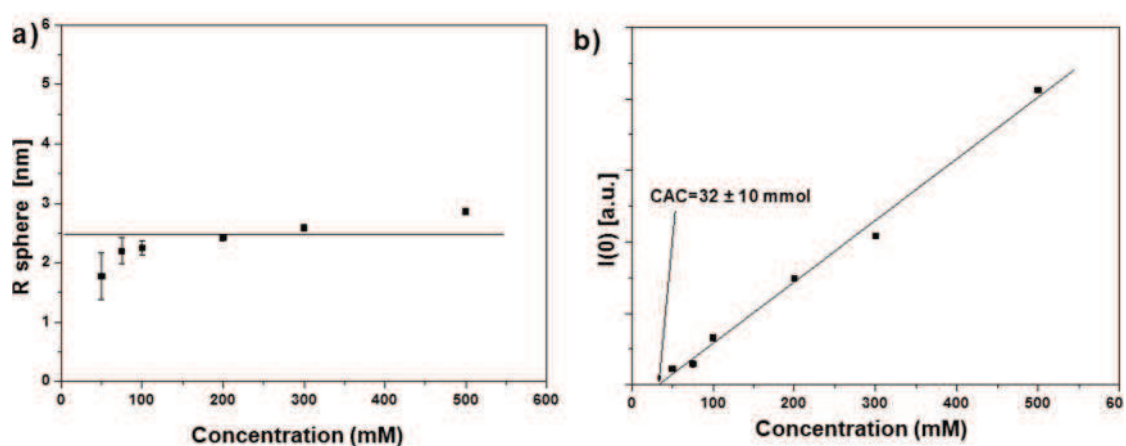


Figure 4.11: geometric radii of aggregates and CAC extrapolation by linear fit of $I(0)$ for compound 6.

The scattering spectrum of amphiphile 7 in cyclohexane at different concentrations is reported in figure 4.12a while the Guinier plot of the intensities subtracted of the solvent contribution are shown in Figure 4.12 b.

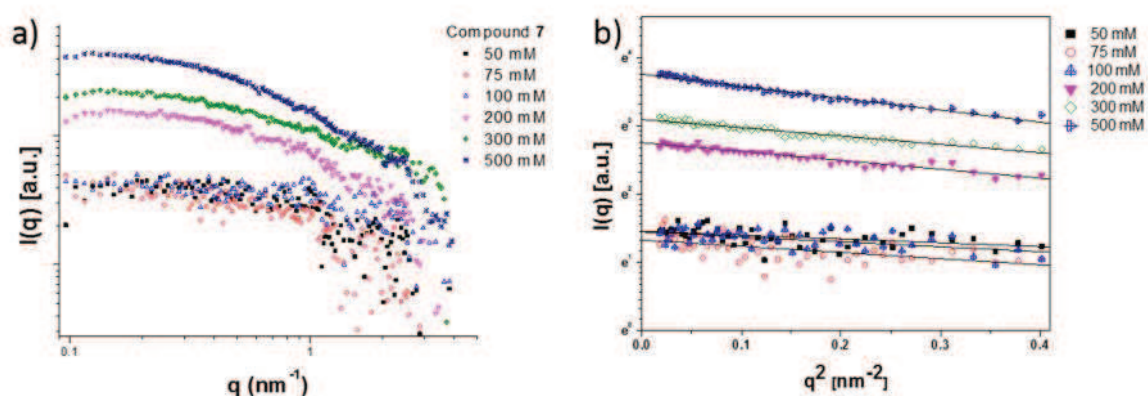


Figure 4.12 SAXS intensities (arbitrary units, solvent subtracted) of compound 7 in cyclohexane at different concentrations (a) and Guinier plot of SAXS intensities (b), 25°C

Over the range of concentrations, all the slopes and therefore the R_g 's of **7** were very similar. The geometric radii (R) were calculated using equation $R^2 = 5 R_g^2/3$, and the values obtained were plotted in Figure 4.13 a as a function of amphiphile concentration and, assuming a spherical shape of the aggregates, averaged around 1.7- 2.5nm.

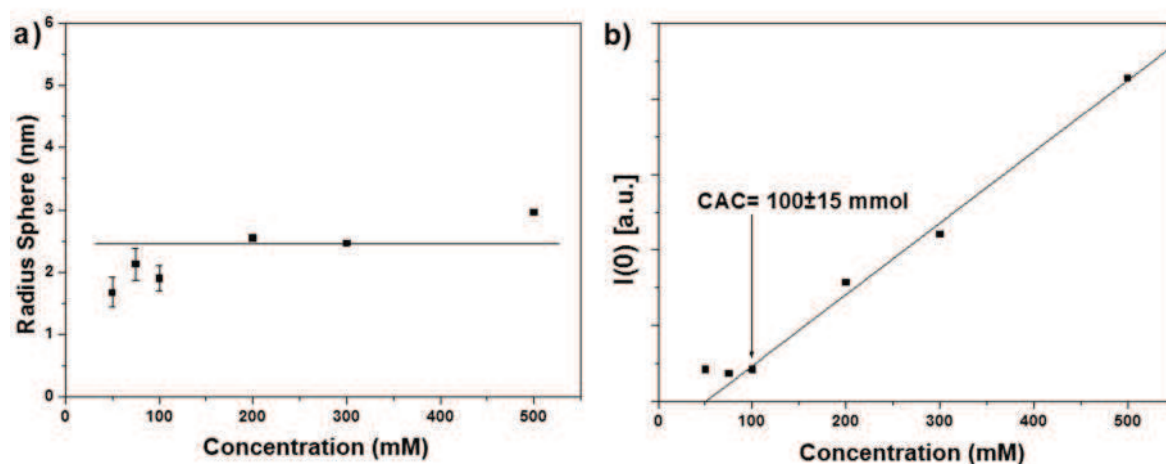


Figure 4.13 geometric radii of aggregates and CAC extrapolation by linear fit of $I(0)$ for compound **7**.

The self-aggregation of compound **7** in cyclohexane is more evident than the other amphiphiles, and in figure 4.13 b it is clear that the aggregation took place after 100mM.

To the best of our knowledge, these results provided the first experimental evidence of self-assembly of reverse amphiphiles in hydrocarbons to form typical micellar structures.

Once obtained the proof of micelle formation in cyclohexane using our new reverse amphiphiles, the project was carried on at the University Of Sydney, where there was the possibility to acquire SAXS and SANS data. All the results collected are presented below.

Firstly, all data presented above were confirmed. Then the effects of solvent, water addition and temperature on the self-aggregation were analysed.

4.4.2. Solvent effect

As presented above, compounds **4-7** were found to be soluble in cyclohexane at all concentrations up to a 50/50 volume ratio and gave evidences of aggregation. The analysis of those aggregates by SAXS allowed to establish an aggregates size of around 4 nm of diameter and to speculate about their possible spherical shape.

Different hydrocarbons were then used in order to study the behaviour of reverse amphiphiles in solvents having different geometry and electronic features.

The aim of this study was on one hand to establish a correlation between the terminal group of the tail - *i.e.* ethyl or hydroxyl - and the electronic features of the solvent, while on the other hand we searched for a relation between the geometry of solvent and the one of the headgroup.

The solvents used were n-hexane, methylcyclohexane, ethylcyclohexane, isooctane, toluene, benzene and water

- ***n-hexane***

Hexane is a six-carbon hydrocarbon like cyclohexane, but linear. The difference in the geometry of these two compounds was very important, because the interaction with amphiphiles both in the packing process and in the stabilisation of the aggregate was different.

Hexane and cyclohexane differs also for polarity, vapour pressure, melting point and boiling point. For details see appendix B.

The result of all these differences was a different interaction with reverse amphiphiles, that strongly influenced their solubility and aggregation capacity.

Compound **4** and **5** were characterised by a terminal ethyl group that diminished the polarity of the tail. These compound were soluble in hexane up to 50/50 volume ratio. Solutions of 200 mM in hexane for both compound were studied by SAXS. The profiles obtained are indicative of the presence of aggregate in solution (fig 4.14).

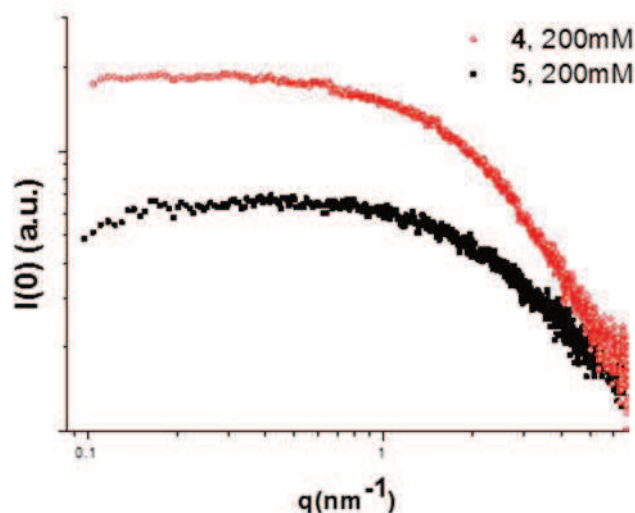


Figure 4.14. SAXS intensities (arbitrary units, solvent subtracted) of compound 4 and 5 at 200mM in *n*-hexane, 25°C

The size of aggregates was calculated using the Guinier law, and the R_g s found were around 1.5 and 2 nm for compound **4** and **5** respectively. The profiles were fitted using the sphere model and the ellipsoid model. Both models gave a good fitting only using a polydispersity index comprised between 0.3-0.7 (Shultz distribution). On the contrary reverse amphiphiles **6** and **7** were not soluble in *n*-hexane. The terminal hydroxyl group lend such a polar nature to the tail, that the solubilisation in this solvent was not permitted.

- ***Methylcyclohexane and ethylcyclohexane***

These two solvents are characterised by a cyclic but asymmetric geometry - due to the alkyl chain on the ring - a very low melting point and are both immiscible in water.

In both solvents compounds **4-7** were soluble and self-assembled in aggregates.

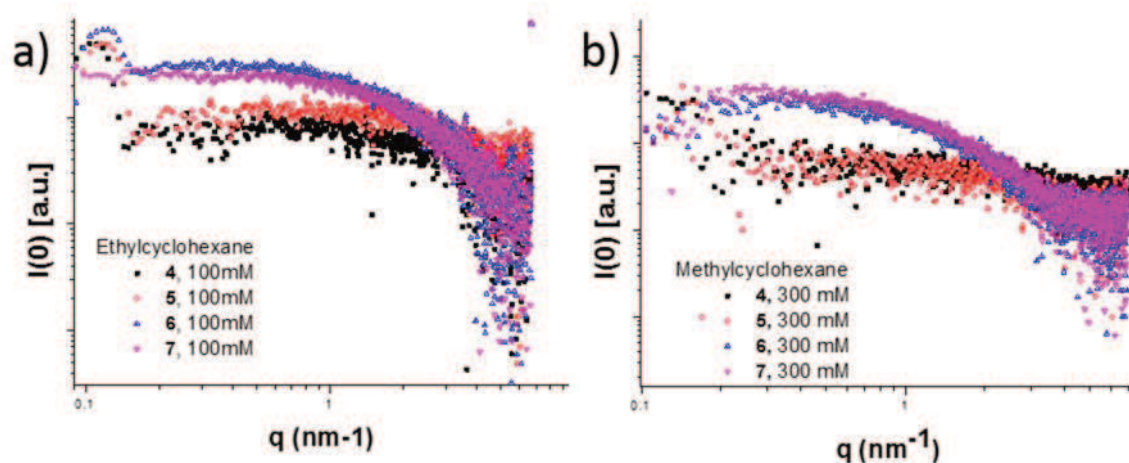


Figure 4.15 SAXS intensities (arbitrary units, solvent subtracted) of compounds **4-7** in ethylcyclohexane at 100mM (a) and in methylcyclohexane at 300mM (b), 25°C

In figure 4.15 are reported the SAXS intensities of compounds **4-7** in ethylcyclohexane at 100mM (a) and in methylcyclohexane at 300mM (b). The scattering curves of compounds **4** and **5** were less intense than those of compounds **6** and **7** in both solvents. For all amphiphiles, also in this case it was not possible to establish the shape of aggregates between sphere or ellipsoids, because of the high polydispersity index of the size of aggregates, that were comprises between 0.3 and 0.8 (Shultz distribution).

For this it was not possible to give an accurate size for the aggregates formed. Average radii (see table 4.2) were calculated fitting the profiles with sphere models instead using the Guinier plot because data points were smeared, especially for compounds **4** and **5**.

	4	5	6	7
<i>Ethylcyclohexane</i>	0.5± 0.7 nm	0.6± 0.8 nm	1.3± 0.8 nm	1.2± 0.9 nm
<i>Methylcyclohexane</i>	0.3 ± 0.8 nm	0.4 ± 0.7 nm	1.4 ± 0.8 nm	1.3 ± 0.7 nm

Table 4.2 average radii of aggregates in hydrocarbons of compound **4-7**, calculated by fitting with sphere model.

- **Isooctane**

The main difference between the other solvents tested so far and isooctane (2,2,4-trimethylpentane) is the geometry. This is a linear branched alkyl hydrocarbon

immiscible with water and with a very low melting point (*i.e.* -107.4°C, see appendix B)

At 25°C, compounds **4-6** are soluble in these solvents up to 100 mM, concentration after which all the solutions became turbid. Compound **7**, instead, was soluble up to 75 mM, while at around 100 mM it was possible to appreciate a clear phase separation.

For all compounds the formation of particles in solution was detected by SAXS. It was not possible, though, to establish the nature of the scatterer because the SAXS curves were not reproducible. The hypothesis that could explain this behaviour is that the scattering might be originated by the self-aggregation of amphiphiles, as well as by the formation of very small drops of amphiphiles that at concentration higher than 100 mM caused the macroscopic turbidity of solutions.

- ***Benzene and Toluene***

Benzene and Toluene were chosen to determine the effect of a planar geometry and a more polar nature of the solvent respect to cyclohexane. Compounds **4-7** were soluble up to 50/50 volume ratio, but no aggregates were detected at any concentration.

- ***Water***

Analogously to conventional surfactants that self-assemble in reverse micelles in hydrocarbons, reverse amphiphiles in water were expected to aggregate in reverse micelles. Compound **4** and **5**, were instead insoluble in water and formed a separate clear phase at all concentrations, while compounds **6** and **7** gave turbid solutions once mixed with water.

4.4.3. Addition of water effect

By using SAXS it was possible to observe the formation of typical micelles in hydrocarbons using reverse amphiphiles. In this system, the micellar core was lipophobic, while lipophilic heads were arranged on the external surface toward the hydrocarbon solvent. Our hypothesis was that water should be incorporated in

the core of micelle thanks to the positive polar interactions with the triethylene glycol tails.

The choice of the solvent was based on the previous SAXS results: cyclohexane, methylcyclohexane and ethylcyclohexane were solvents in which all amphiphiles examined formed aggregates. Methylcyclohexane, though, was chosen because it has a melting point that allowed to study the process also at low temperature (see appendix B), and it was more easily available than ethylcyclohexane.

Solutions of the amphiphiles **6** and **7** at 200mM in methylcyclohexane and water/amphiphile ratios of 0.6, 3 and 5 were prepared mixing the amphiphile with water and subsequently diluting the mixture with the solvent. All solutions were then mixed overnight and analysed by SAXS.

In the solutions of compounds **4** and **5** water separated out as a different phase. SAXS of the organic phase were performed to confirm the absence of water in solution. For both amphiphiles the profiles collected at different w/a ratio (r) were compared with the one in absence of water. Figure 4.16 reported the example of compound **4**.

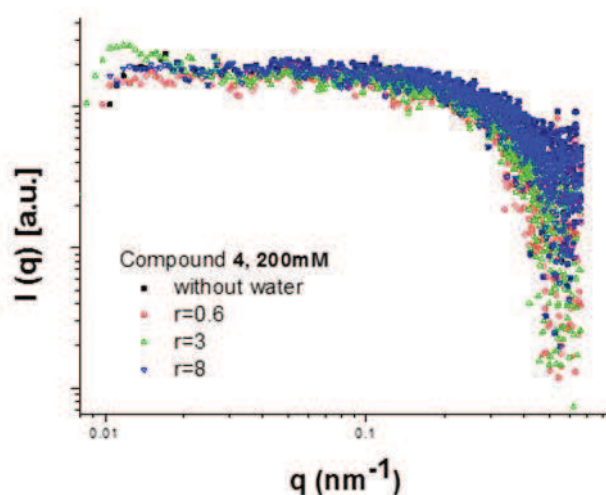


Figure 4.16: SAXS intensities (absolute units, solvent subtracted) of solution containing compound **4** at 200mM in methylcyclohexane and at different w/a ratios (r): without water in black, $r=0.6$ red, $r=3$ blue, $r=5$ magenta.

SAXS curves plotted in figure 4.16 are relative to a water/amphiphile ratio (r) of 0, 0.6, 3 and 5. Those curves are superimposable, thus aggregates in solutions are not influenced in number or size by the addition of water. An analogous result was obtained with compound 5.

A completely different scenario was obtained with compounds 6 and 7.

In figure 4.17 are compared SAXS intensities of solution containing amphiphile 6 at 200 mM in methylcyclohexane without water and with water/amphiphile ratios of 3 and 5.

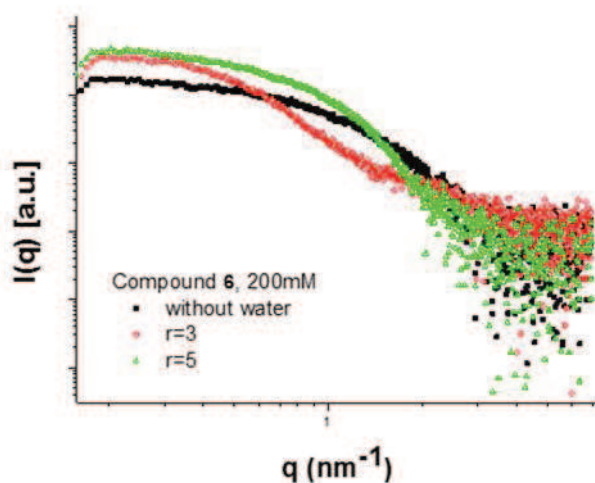


Figure 4.17 SAXS intensities (absolute units, solvent subtracted) of solution containing compound 6 at 200mM in methylcyclohexane and at different w/a ratios (r): without water in black, $r=3$ red, $r=5$ blue.

For all SAXS profiles the aggregate sizes were calculated by fitting the scattering curves with a sphere model (table 4.2).

Water/amphiphile ratio		
0	3	5
1.4 ± 0.8	2.6 ± 0.06	3.9 ± 0.08

Table 4.1 aggregate sizes at different water/amphiphile ratio (r) calculated by sphere model fitting

The effect of water on the aggregation of reverse amphiphile 7 was more complicated.

Water was added without any phase separation up to 0.6 water/amphiphile ratio at an amphiphile concentration of 200 mM. SAXS measures were performed on this solution and compared to the profile of a solution of amphiphile at the same concentration without the addition of water.

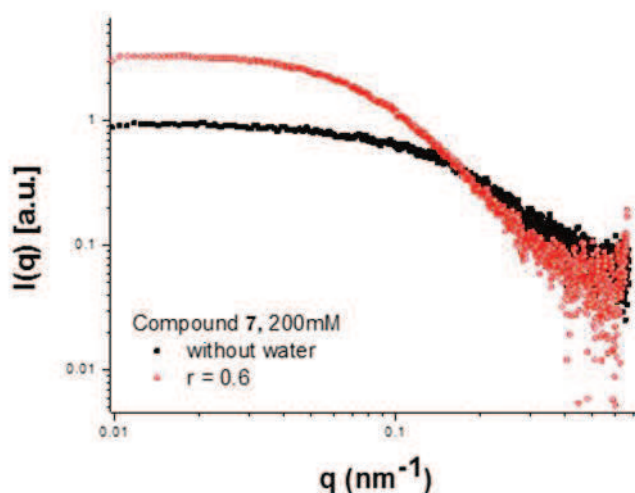


Figure 4.18: SAXS intensities (absolute units, solvent subtracted) of solution containing compound **7** at 200mM in methylcyclohexane without water (black) and with a water/amphiphile ratio (r) of 0.6 (red).

The aggregate size formed by addition of water was calculated fitting the scattering curve with a sphere model. The value of the radii found was 2.1 ± 0.6 nm.

At a water/amphiphile ratio of 3 the solution separated into two different phases. SAXS measures were performed on both phases.

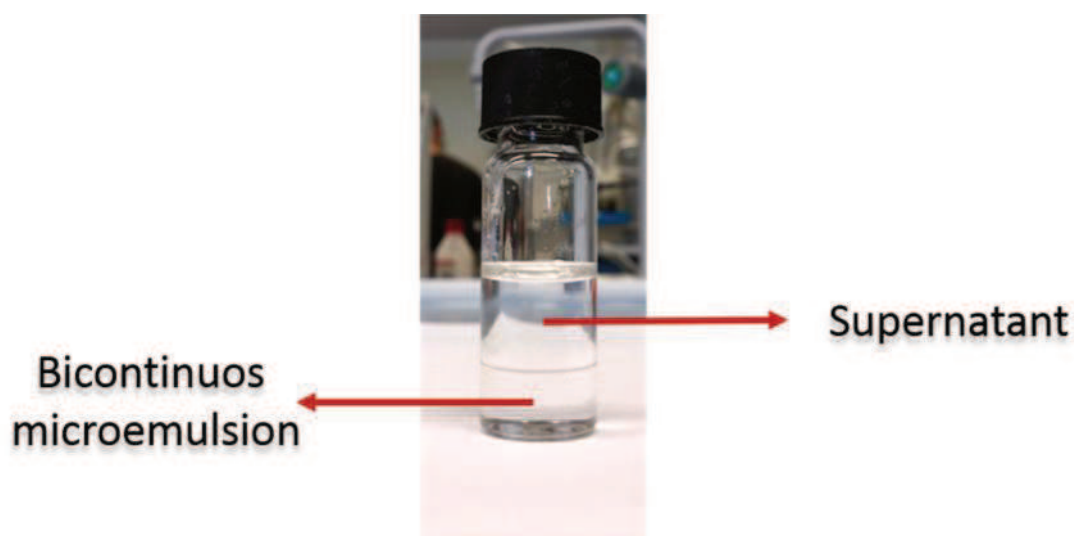


Figure 4.19 phase separation of a solution containing amphiphile **7** at 200 mM and water at 600mM in methylcyclohexane.

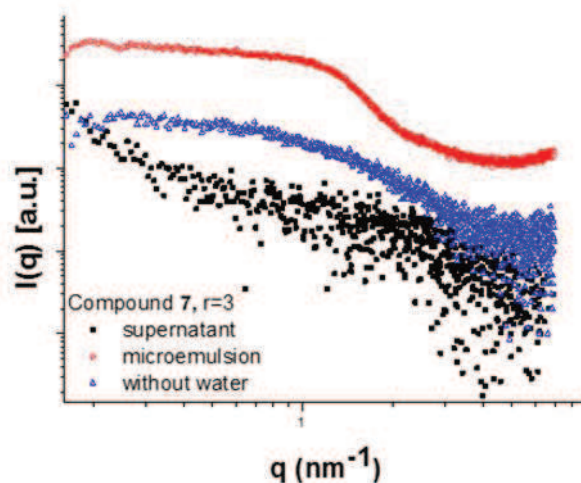


Figure 4.20 SAXS intensities of solution containing compound **7** at 200mM in methylcyclohexane without water (blue, absolute units, solvent subtracted) and with a water/amphiphile ratio (r) of 3: supernatant (black, absolute units, solvent subtracted) and microemulsion (red).

In figure 4.20 are compared SAXS profiles of the two phases and of a solution with the same content of amphiphile **7** without water. The SAXS curve relative of the supernatant is almost flat and points are spread. On the contrary, the profile relative of the lower phase is intense and well defined.

4.4.4. SAXS Data discussions

SAXS is a more sensitive technique than 2D-DOSY NMR, thus it allowed a more detailed and accurate study of the behaviour of reverse amphiphiles in hydrocarbons.

Compounds **4-7** in cyclohexane were measured by SAXS at different concentrations to determine size and CAC of aggregates in solution. Compounds **6** and **7** were found to form bigger aggregates than compounds **4** and **5**. The terminal hydroxyl group of the formers, increased the polar nature to the lipophobic part of the reverse amphiphiles, favouring their aggregation in hydrocarbons. This behaviour was clearer in ethylcyclohexane and methylcyclohexane. The intensity of scattering measured on solutions containing the amphiphiles bearing a terminal ethyl group was weaker than that of amphiphiles **6** and **7**. Radii dimensions suggested that for

compounds **4** and **5** only very small and few oligomers were formed, while for reverse amphiphiles **6** and **7** micelles of about 1.5-2 nm radii were detected.

The difference in polarity due to the terminal group influenced also the solubility of reverse amphiphiles. This behaviour was macroscopically evident in n-hexane. Compound **4** and **5**, characterised by a less lipophobic tail, were soluble in this solvents and seemed to aggregate in small and very polydisperse aggregates. On the contrary, compounds **6** and **7** were insoluble at any concentration.

A different scenario was observed for isooctane. Although it is immiscible with water as cyclohexane, its dielectric constant is indicative of a different electronic configuration. In this solvent compounds **4-7** were all apparently soluble up to 75-100 mM. However, SAXS measures were not reproducible, and this suggested that the scattering observed in solution was due to small drops rather than aggregates. The difference between a drop of amphiphile and an aggregate lies on the solubility of the molecule in the solvent: if the amphiphile is completely insoluble, a phase separation take place, and drops are formed. Within the drop the molecules are not ordered. On the other hand, although the aggregate formation it is considered as a microphase separation, molecules are packed with a precise order and the process of formation is reproducible.

The aromatic nature of benzene and toluene was found to be enough to hinder the aggregation of reverse amphiphiles.

Lastly, the aggregation of reverse amphiphiles in water was analysed. The formation of reverse micelles was expected, at least for amphiphiles **6** and **7**, which could hydrogen bond with water. The results, instead, indicated a clear phase separation for compounds **4** and **5** at all concentrations, and the formation of turbid solutions for compounds **6** and **7**. The explanation for this might be due to the fact that the hydroxyl group present on **6** and **7** did hydrogen bond water, but the interactions (*i.e.* repulsions with heads and attraction with tails) were not sufficient for micelle formation.

The effect of the presence of water in the system was studied. Our hypothesis was that water should be incorporated in the core of micelle by positive interactions with the polar tails. SAXS results suggested that water molecules interacted only with the reverse amphiphiles **6** and **7** that are able to hydrogen bond. Although those amphiphiles had the same tail, the effect of water on their micellar solutions was different: spherical aggregates with an increased radius were observed for compound **6** at all water/amphiphile ratios, while a phase separation took place at a water/amphiphile ratio of 3 for compound **7**. For the latter, SAXS measures were performed on both phases. The SAXS intensity of the supernatant phase was weaker than the one of the solution containing the amphiphile at 200 mM, and almost comparable to the profile of the pure solvent. This meant that almost the entire amount of reverse amphiphile **7** was confined in the heavier bottom phase. The SAXS profile of the latter was fitted with several models, but without any conclusive results. Our hypothesis was that the amphiphile **7** formed with water and methylcyclohexane a bicontinuous microemulsion in which the three components coexisted in a clear and thermodynamically stable phase. For this system the subtraction of solvent would be a wrong procedure, since methylcyclohexane was probably not the most abundant component. Furthermore the shape of SAXS profile suggested the formation of an ordered phase but different from aggregates obtained so far. The accurate study of this system should be carried on by building a ternary phase diagram.

Our hypothesis to explain the different behaviour of compounds **6** and **7** in a water-in-oil system, is based on the geometry of these reverse amphiphiles. Headgroup shapes influenced the packing properties of amphiphiles in the micelle. Thus a flat rounded headgroup (**6**), that resemble the shape of a spoon, might lead to a more stable micelle than a spherical one (**7**) that looks like an air balloon (see figure 4.21).

Perturbing the system with water addition, made this difference in stability more evident.

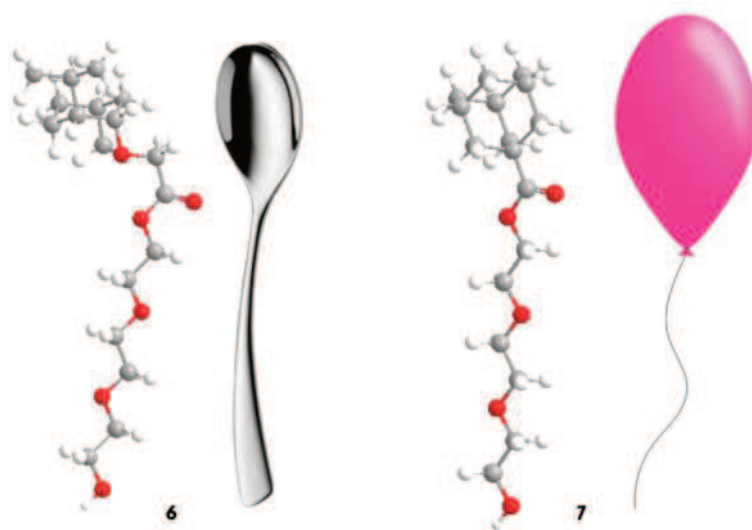


Figure 4.21 3D structure of compound 6 and 7, associated to a spoon and a balloon respectively

4.5. Small Angle Neutron Scattering (SANS) results

As explained in chapter 3, all SANS measures presented in this thesis were collected at the nuclear facility ANSTO, using QUOKKA SANS instrument.

The proposal for SANS acquisitions included two different studies. The first part was to confirm the results collected by SAXS, while the second part aimed to study the behaviour of reverse amphiphiles **4-7** in liquid methane.

4.5.1. Micelle detection: water and temperature effect

This part of the project was performed with a 20 sample holder, equipped with a temperature controller (fig 4.22, indicated by a red arrow) that allowed to reach the temperature of -20°C.

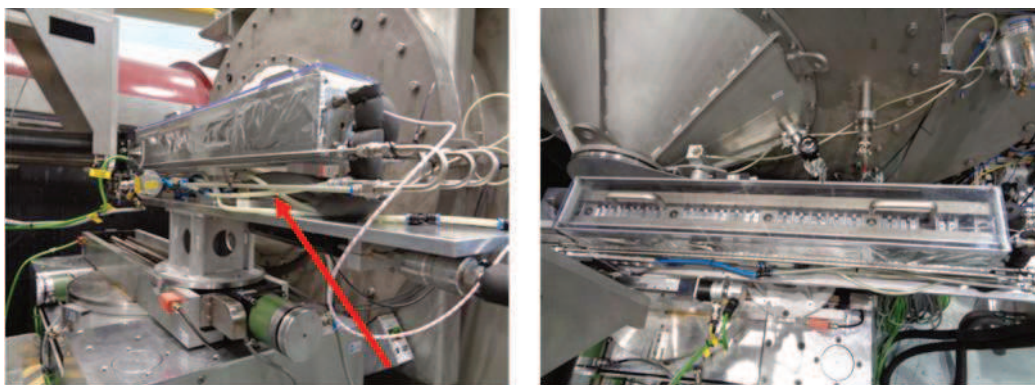


Figure 4.22: 20-samples holder on Quokka instrument, temperature controller indicated by the red arrow.

The cell used was a 1mm, round quartz cell mounted on an aluminium support (see figure 4.23).



Figure 4.23 pictures of the 1mm quartz cell (left) and of the cell mounted on the aluminium support (right).

SANS measures required the use of deuterated solvents that often are very expensive. For this reason, the number of solvents and samples investigated are limited. For example deuterated ethylcyclohexane is not commercially available and thus it was excluded.

Compounds **4** and **5** were analysed in deuterated hexane, cyclohexane and methylcyclohexane in the range of concentration of 50-200 mM at different temperatures (25, 0, -10 and -20 °C).

Compounds **6** and **7**, instead, were analysed in deuterated cyclohexane and methylcyclohexane in the same range of temperature and concentration. Just as was done for SAXS, water influence on a solution 200mM of compound **6** was studied.

- **Compounds 4 and 5**

SANS curves of compound **4** and **5** were acquired in hexane, cyclohexane and methylcyclohexane. Figure 4.24 reports all SANS curves acquired for compound **4**.

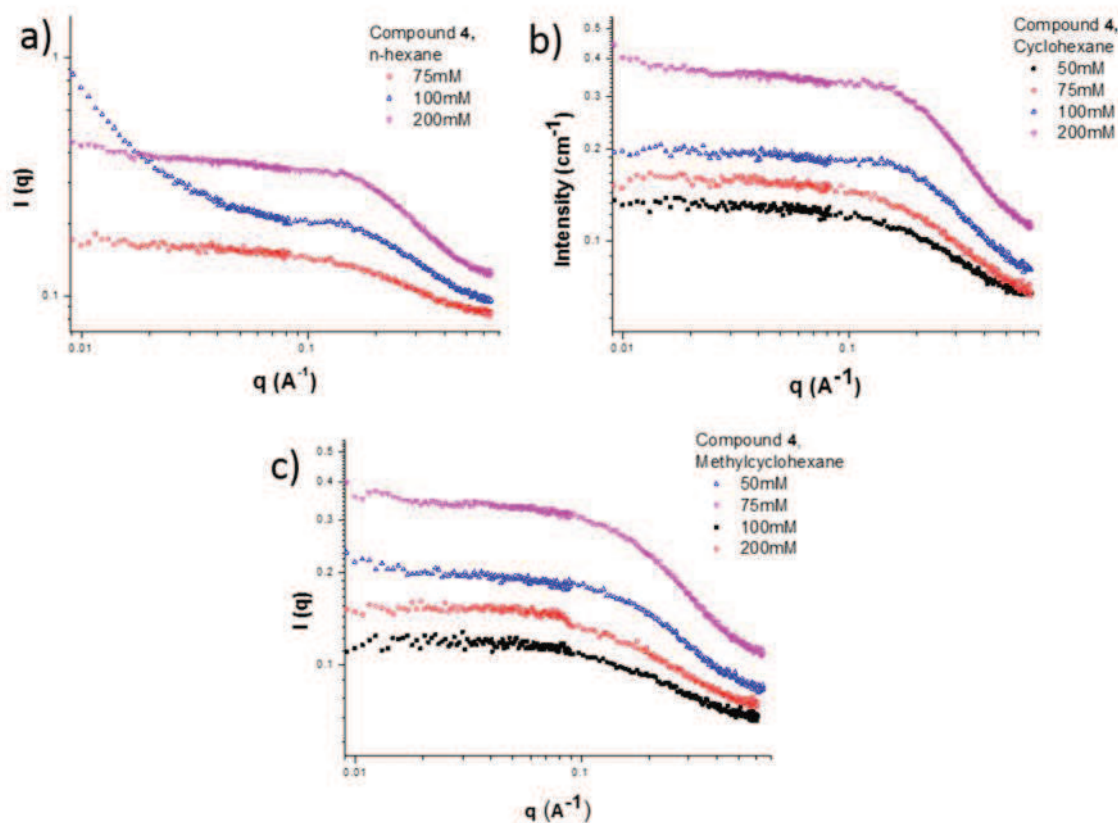


Figure 4.24: SANS intensities of compound **4** in n-hexane (a), cyclohexane (b) and methylcyclohexane (c) in the concentration range of 50-200 mM, at 25 °C.

SANS curve of compound **4** in n-hexane at 100 mM (fig 4.24 a, blue) was affected by humidity condensing on the aluminium surface of the sample holder. It was possible to limit this phenomenon by a constant flux of nitrogen on the surface of the holder, but it could not be completely avoided.

Analogous SANS curves were collected for compound **5** (see appendix C).

The samples were analysed at 25°C, 0°C, -10 °C and -20°C. The aim of this study was to determine the correlation between micelle formation and temperature.

Figure 4.25 reports the effect of temperature on samples at 200mM. This concentration was well above the CAC, thus we were sure to analyse the effect on

aggregates already formed. For samples in cyclohexane, SANS intensities under 0 °C were not collected because that was below its solidification point.

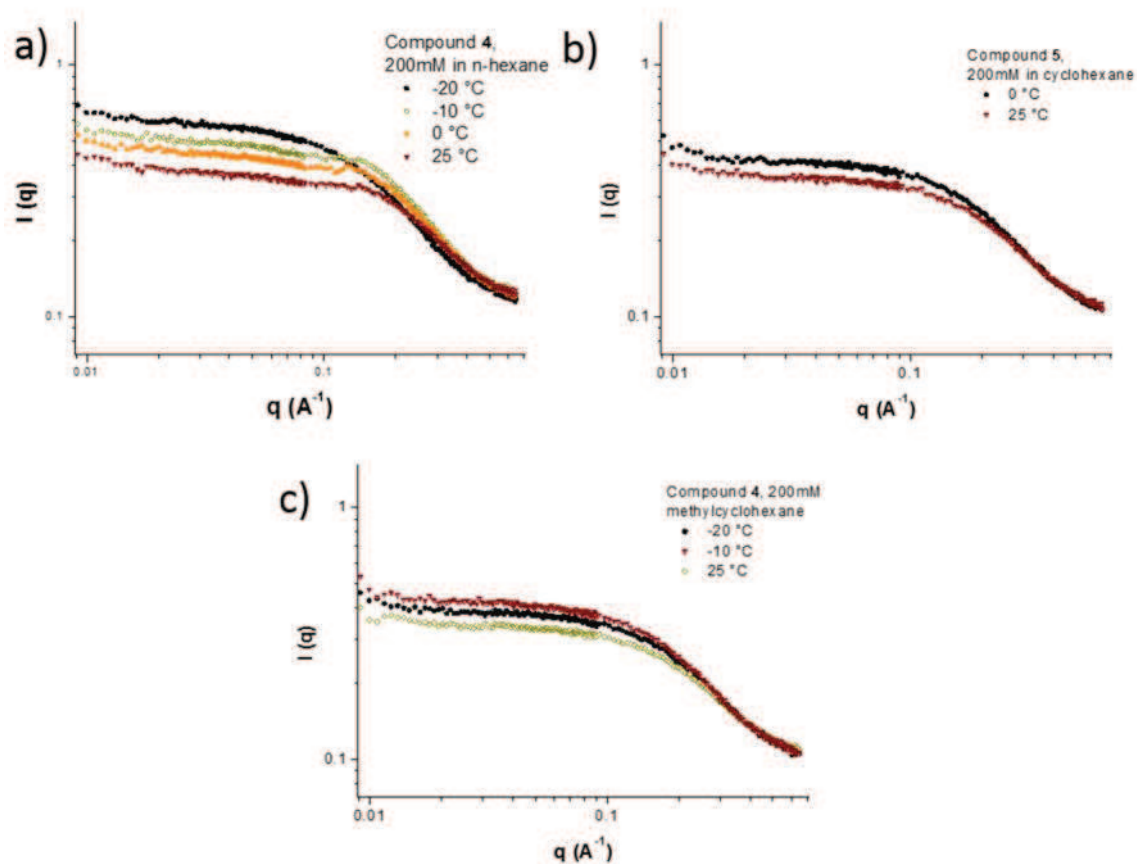


Figure 4.25 SANS intensities of compound 4 in n-hexane (a), cyclohexane (b) and methylcyclohexane (c) at the concentration of 200 mM at different temperatures

In all cases SAXS curves were almost superimposable. The profiles collected in n-hexane, instead, showed an increasing of the scattered intensity with the temperature lowering. Analogous results were obtained for amphiphile 5 and reported in appendix C.

- **Compounds 6 and 7**

SANS intensities of compounds 6 and 7 were collected in cyclohexane and methylcyclohexane at 50, 75, 100 and 200 mM. The profiles obtained at 25°C were plotted and compared as reported in figure 4.26.

As also previously observed for the SAXS measurements, SANS profiles were intense and well defined. A first estimation of size of the aggregates was conducted using both a sphere model and an ellipsoid model, and the average radius of

gyration was found to be around 2 nm, the same value previously calculated for as calculated with SAXS. More accurate fittings are currently being studied with the aim of discriminate between these two micelle geometries. In the same way, the evaluation of a precise value of the geometric radius (or radii in the case of ellipsoids) is still object of study as it depends on the shape.

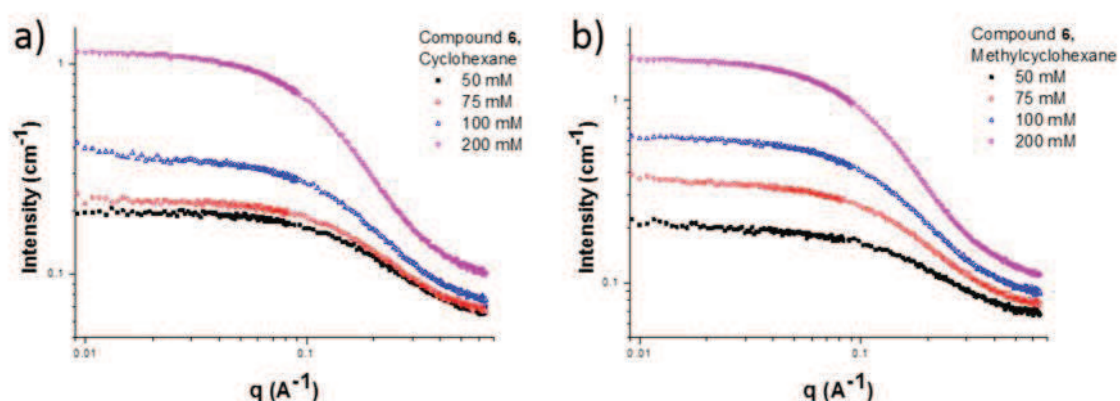


Figure 4.26: SANS intensities of compound 4 in cyclohexane (a) and methylcyclohexane (b) in the concentration range of 50-200 mM, at 25 °C.

As for compounds 4 and 5 the effect of the temperature was studied.

In cyclohexane at the temperature of 0 °C, the curve might be affected by the solidification of cyclohexane (figure 4.27 a, orange curve). In methylcyclohexane SANS profiles showed an increasing of the scattered intensity with the temperature lowering.

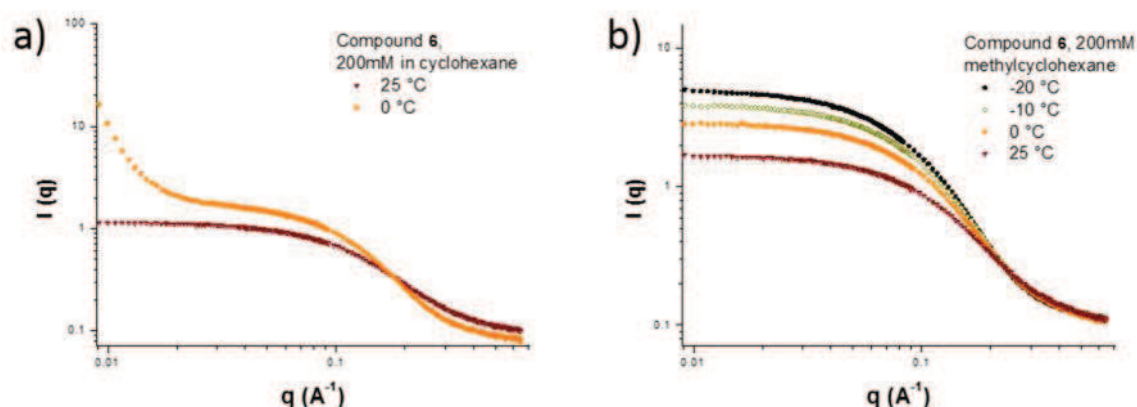


Figure 4.27 SANS intensities of compound 6 in cyclohexane (a) and methylcyclohexane (b) at the concentration of 200 mM at different temperatures

Analogous results were collected for amphiphile **7** and are reported in fig C.5 (see appendix C).

For compound **6** the effect of the addition of water was studied. A preliminary study of the water-in-oil system was performed with SAXS (see paragraph 4.4.3). The different contrast length between H₂O and D₂O, in fact, allowed the acquisition of a more detailed analysis (for the theory of contrast length see paragraph 3.2.2). 200 mM solutions of compound **6** were prepared in deuterated methylcyclohexane without water and with a water/amphiphile ratio of 3, using H₂O and D₂O separately. These three solutions were analysed at 25, 0, -10 and -20 °C. The aim of lower the temperature was to analyse the behaviour of water in the micelle under 0°C, since water should freeze.

The SANS profiles of the 200 mM solutions of compound **6** without water, with H₂O and with D₂O (both at water amphiphile ratio of 3) at 25°C are plotted and compared in figure 4.28.

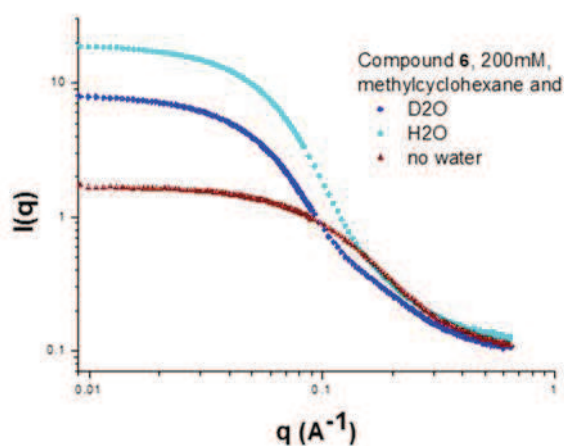


Figure 4.28 SANS profiles of solutions of compound **6** at 200 mM without water (brown), with H₂O (light blue) and with D₂O (both at water: amphiphile ratio of 3) at 25°C

As expected, the intensity of the SANS curves increased with water addition, and it was more intense with H₂O rather than with D₂O. The most interesting thing was the shape of the profile relative to the solution with D₂O, that is typical of spherical

micelles. This effect was more evident at $-20\text{ }^{\circ}\text{C}$. At this temperature, the scattering curve did not present any variation due to the D_2O freezing. The SANS profile, though, suggest an increasing of D_2O density, that highlight more details of micelle structure thanks to the contrast length (figure 4.29).

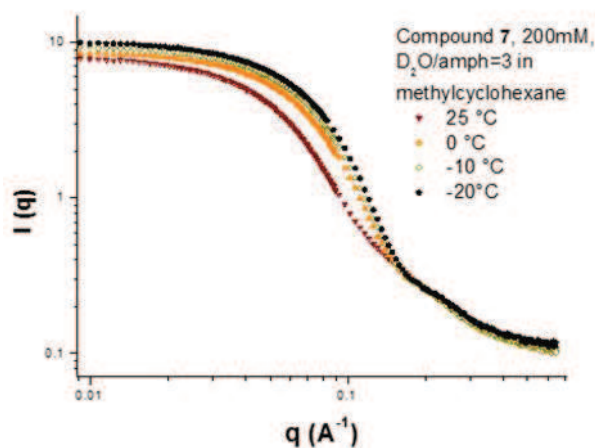


Figure 4.29 SANS profiles of solutions of compound 6 at 200mM with D_2O / amphiphile ratio of 3 at 25, 0, -10 and $-20\text{ }^{\circ}\text{C}$.

The SANS profile acquired on the solution containing D_2O at $-20\text{ }^{\circ}\text{C}$, was fitted using the most plausible shape that micelle can adopt to minimize the superficial tension: the sphere. The curve of a sphere with 2.7 nm radii fit the SANS curve with a good agreement, taking into account that at high q the polydispersity of the real system affects the correspondence between the real and the ideal systems (see figure 4.30).

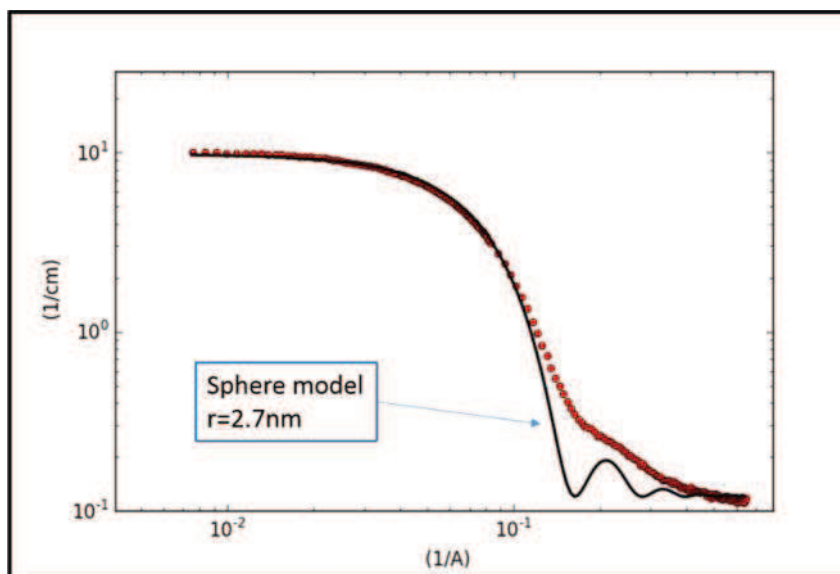


Figure 4.30 SANS intensity of compound **6** at 200 mM with D₂O (red dots) and of a sphere of 2.7 nm radius in a ideal monodisperse system.

4.5.2. SANS: Micelles in liquid methane

As anticipated at the beginning of paragraph 4.5, the second part of the proposal presented to ANSTO was the study of the behaviour of reverse amphiphiles in liquid methane. This part of the project was based on the possibility of life on Saturn's moon Titan and it required a special equipment, designed to work at -170°C and with the possibility to completely fill the cell with deuterated methane. The cell was built in aluminium with an O-ring of Indium. This element has the characteristic to expand at low temperatures, thus it was supposed to be the best candidate to seal the cell.

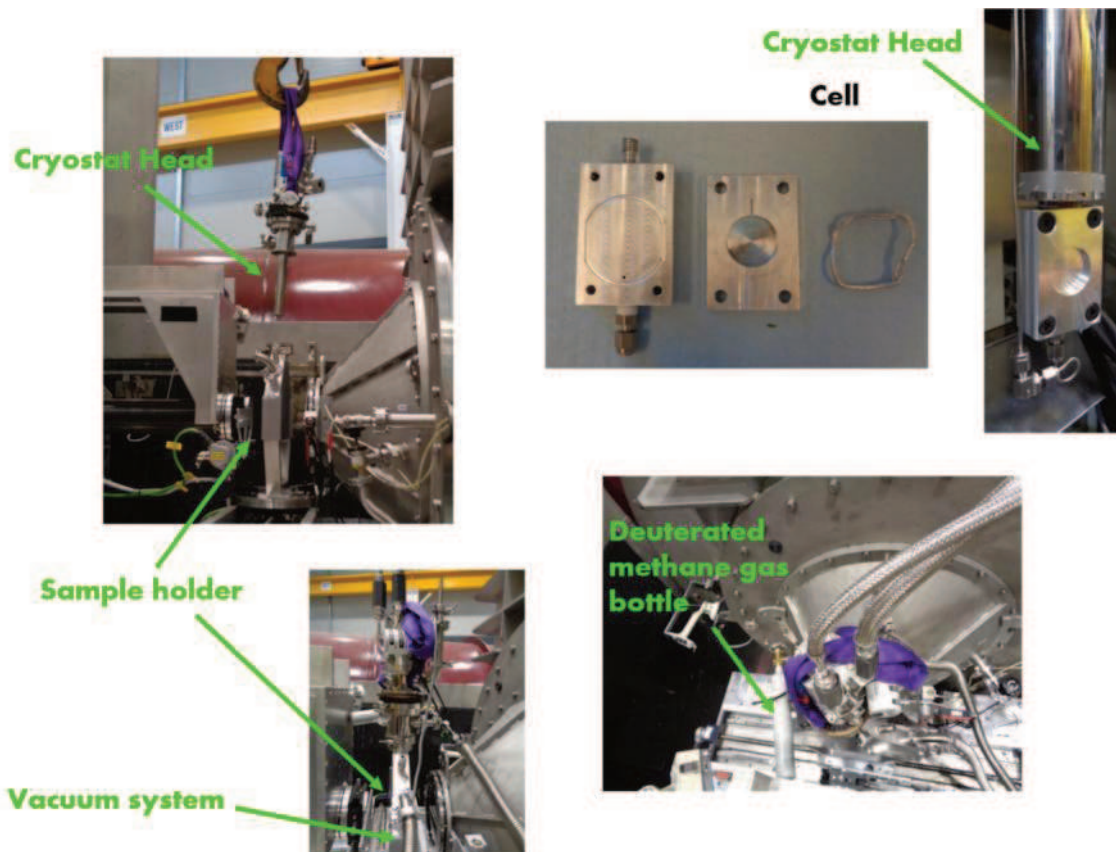


Figure 4.31 pictures of the equipment adopted for SANS acquisitions in liquid methane.

The cell was built with a direct connection to the cryostat, which assured the temperature control of the cell. The inner part of the cell was connected both to a vacuum pump and to the D4-methane bottle, through a T-shape valve. The experiment required the dissolution of the amphiphile in the cell before its solidification. To fulfil this requirement the amphiphiles were weighted directly in the cell, the cell was closed and evacuated with a vacuum pump and then filled with gaseous methane at room temperature. The cell holder was then put under vacuum and the entire system chilled to -170°C .

Unfortunately, the attempts were unsuccessful because the O-ring didn't seal the cell, and once the vacuum was applied the amphiphile was sucked out the cell.

4.5.3. SANS data discussion

Although the determination of an accurate value of size and shape at each temperature is an issue still under study, it was still possible to make some considerations.

As observed via SAXS, amphiphiles **4** and **5** aggregated in small polydisperse oligomers. Because of the high polydispersity it was not possible to determine an accurate value of the size, neither the shape of the aggregates. It was possible though, to exclude the formation of more complex and bigger structures. The accurate determination of these parameters is still one of the issues currently being studied.

For what concerns the screening of temperature effect on solutions containing compounds **4** and **5** in cyclohexane and methylcyclohexane, SANS curves were almost superimposable. The profiles collected in n-hexane, instead, showed an increasing of the scattered intensity with the temperature lowering. Furthermore, the flex points of the curves were approximately at the same q value, except for the one collected at $-20\text{ }^{\circ}\text{C}$.

The hypothesis was that at lower temperature the aggregate size remained constant, while the number of aggregates increased. At $-20\text{ }^{\circ}\text{C}$ instead a change in shape or dimensions might have happened. To confirm this hypothesis further data analysis needs to be done.

Although a more accurate determination of size and shape of aggregates in solution is still under examination, SANS measures confirmed the micelle formation in methylcyclohexane from compounds **6** and **7**. Their radius of gyration is comparable with those calculated by SAXS.

It was not possible to analyse the effect of low temperature in cyclohexane because the measure was performed just under its melting point. It was not possible to determine the reason why the SANS intensity increased at very low q , since it was

not possible to check the solution during the acquisition. The reason could be the solidification of the sample or its cloudiness.

The profiles collected in methylcyclohexane, instead, showed an increasing of the scattered intensity with the temperature lowering. This behaviour suggested an increasing of the number as well as the size of particle in solution. It was possible though, to exclude the formation of more complex and bigger structures.

Once the micelle formation was ascertained, the most obvious concern was to determine the shape of such micelles. The target was to determine the polar nature of the micelles core by adding water. The results confirmed the formation of micelles in hydrocarbons with the same geometric configuration of typical micelles in water.

In literature are reported several methods for the detection of micelles in water and to establish their core nature.

A more sophisticated analysis like SAXS allowed us to collect preliminary measures using water as probe. But the most useful and reliable technique was SANS.

We took advantage of the contrast length of H₂O and D₂O to determine the position of water molecules in the micelle and we were able to confirm the lipophobic nature of micelle core.

With a more accurate analysis of SANS data, it will might be possible to determine the shape of micelles and thus their averaged dimensions. The high polydispersity might affect seriously this analysis.

We had the possibility to run some SANS measures in liquid methane. The design of such delicate system was really complicated, and many factors has to be taken into account. We still don't know if reverse amphiphiles **4-7** are soluble in liquid methane, neither if they self-assemble in it. SANS is probably the only technique that can be used for such analysis, but it's obviously not easily available.

References and notes

- [1] [http://www.malvern.com/en/products/product-range/zetasizer-range/zetasizer-nano-range/zetasizer-nano-zs90/;](http://www.malvern.com/en/products/product-range/zetasizer-range/zetasizer-nano-range/zetasizer-nano-zs90/)
- [2] International Organisation for Standardisation (ISO), *International Standard ISO 13321 Methods for Determination of Particle Size Distribution Part 8: Photon Correlation Spectroscopy* **1996**.
- [3] International Organisation for Standardisation (ISO), *International Standard ISO22412 Particle Size Analysis - Dynamic Light Scattering* **2008**.
- [4] W. T. Winter, *Measurement of suspended particles by quasi-elastic light scattering*, , John Wiley & Sons, Inc., **1983**.
- [5] A. J. Stratton, *Electromagnetic Theory*, McGraw Hill Book Company, New York and London, **1941**.
- [6] R. Pecora, *Dynamic Light Scattering: Applications of Photon Correlation Spectroscopy*, Plenum Press, New York, **1985**.
- [7] C. Washington, *Particle size analysis in pharmaceuticals and other industries : theory and practice / Clive Washington.*, CRC Press, England, **1992**.
- [8] C.S. Jr. Johnson, D.A. Gabriel, *Laser Light Scattering*, Dover Publications, New York, **1981**.
- [9] A. Román–Guerrero, E. J. Vernon–Carter, N. A. Demarse, *TA Instruments – Applications Note* **2010**.
- [10] C.B. Williamham, W.J. Taylor, J.M. Pignocco, F.D. Rossini, *J. Res. Natl. Bur. Stand. (U.S.)* **1945**, 35, 219-244.
- [11] O. C. Bridgeman, E. W. Aldrich, *Journal of Heat Transfer* **1964**, 86, 279-286.
- [12] E. Fisicaro, C. Compari, E. Duce, M. Biemmi, M. Peroni, A. Braibanti, *Phys Chem Chem Phys* **2008**, 10, 3903-3914.
- [13] Nishi Akio, Kamei Yoshinobu, Oishi Yasumichi, *B Chem Soc Jpn* **1971**, 44, 2855-2856.

Appendix A

A.1 Chemical Potential

The chemical potential for a surfactant in solution is given by^[1]:

$$\mu_i = \mu_i^\circ + RT \ln x_i + RT \ln \gamma_i$$

where μ_i° is the standard chemical potential, R is the ideal gas constant, x_i is the concentration of solute in solution and γ_i is called the activity coefficient.

The standard chemical potential (μ_i°) includes all interactions between the solute and the solution as well as the solute internal energy. All solute-solute interactions are accounted for in $RT \ln \gamma_i$, which can often be set equal to zero at low concentrations, or more precisely as the solute concentration approaches infinite dilution. $RT \ln x_i$ is a purely statistical term arising from the entropy of mixing solute and solvent. The great advantage of using mole fraction units is that all of the entropy is accounted for in this term and the standard chemical potential contains only the solute-solvent free energy and the solute internal free energy.

- [1] C. Tanford, *The hydrophobic effect: formation of micelles and biological membranes*, Wiley, New York, **1973**.

Appendix B

	n-hexane	Cyclohexane	Methylcyclohexane
density (g/cm³)^[1]	0.66 (20°C)	0.7781	0.77 (25°C)
solubility in water (g/L)^[1]	0.0095 (20°)	immiscible	immiscible
m.p. (°C)^[2]	-94	4-7	-126.3
b.p. (°C)^[2]	69	80.7	101
dielectric constant^[3]	1.89 (20°C)	2.023 (20°C)	2.020 (20°C)

	Ethylcyclohexane	Isooctane	Benzene	Toluene
density (g/cm³)^[1]	0.788 (25°C)	0.692	0.8765 (20°C)	0.867 (20°C)
solubility in water (g/L)^[1]	immiscible	immiscible	1.84 (30 °C)	0.52 (20°C)
m.p. (°C)^[2]	-111	-107.38	5.53 °C	-95
b.p. (°C)^[2]	131	99	80.1	110.6
dielectric constant^[3]	N.A.	1.94	2.284 (20°C)	2.379 (25°C)

[1] [http://www.sigmaaldrich.com/;](http://www.sigmaaldrich.com/)

[2] C.B. Willingham, W.J. Taylor, J.M. Pignocco, F.D. Rossini, *Journal of Research of the National Institute of Standards* **1945**, 35, 219-244.

[3] NIST, *NBS Circular 514*, **1951**.

Appendix C

C.1 SAXS data

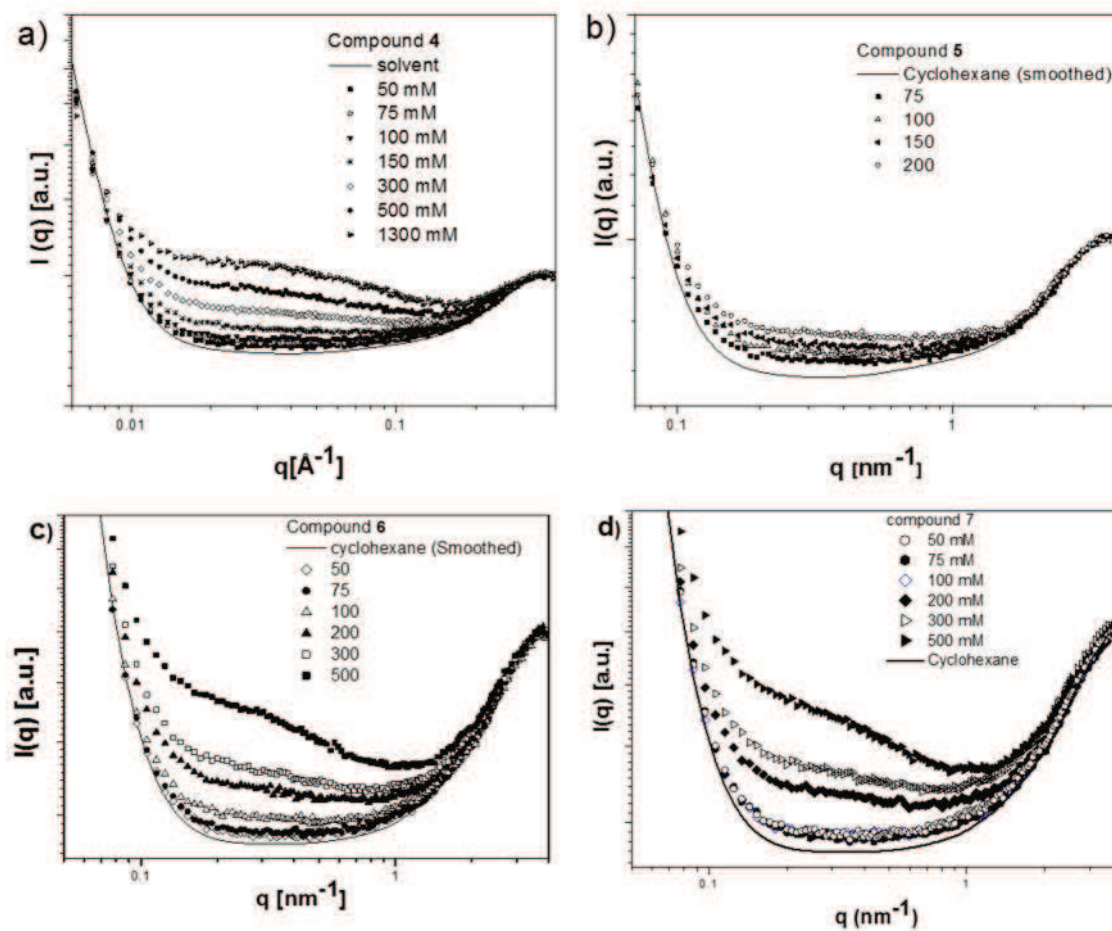


Figure C.1: SAXS intensities of compounds 4-7 (a-d respectively) at different concentrations in cyclohexane, compared to cyclohexane

C.2 SANS $q^2 I(q)$ at 25°C

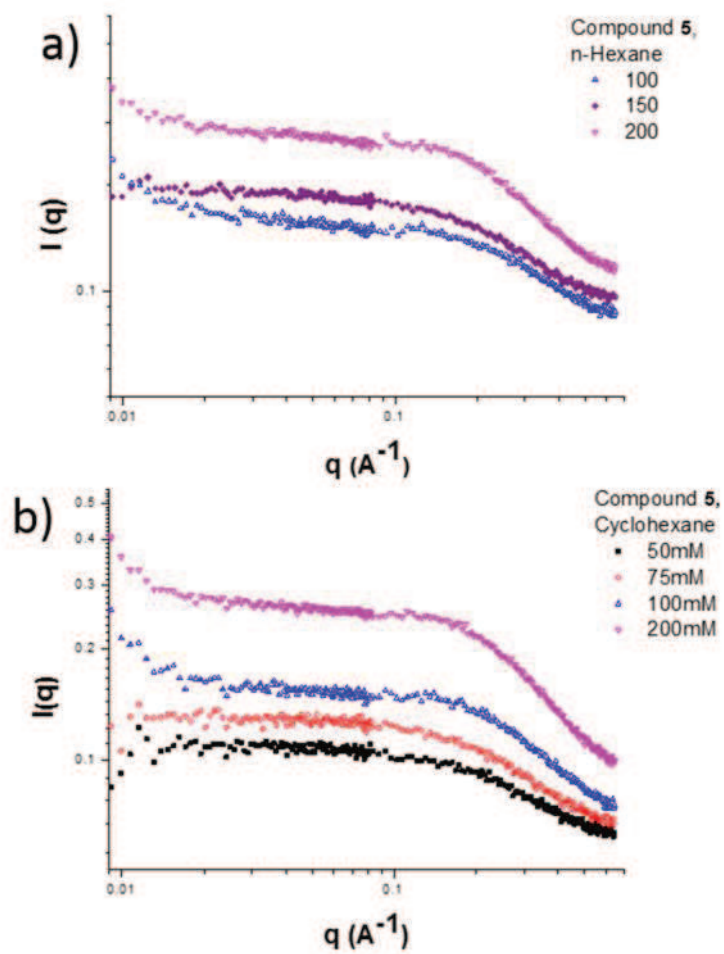


Figure C.2 SANS intensities of compound 5 in n-hexane (a) and cyclohexane (b) in the concentration range of 75-200 mM, at 25 °C.

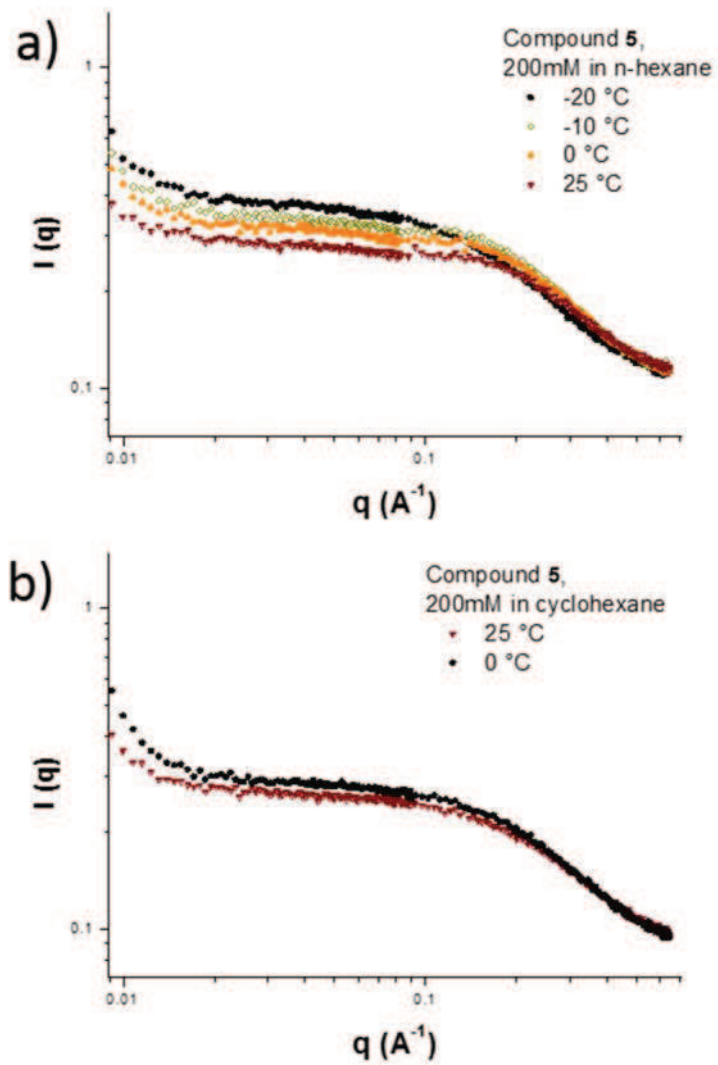


Figure C.3 SANS intensities of compound 5 in n-hexane (a) and cyclohexane (b) at the concentration of 200mM at different temperatures.

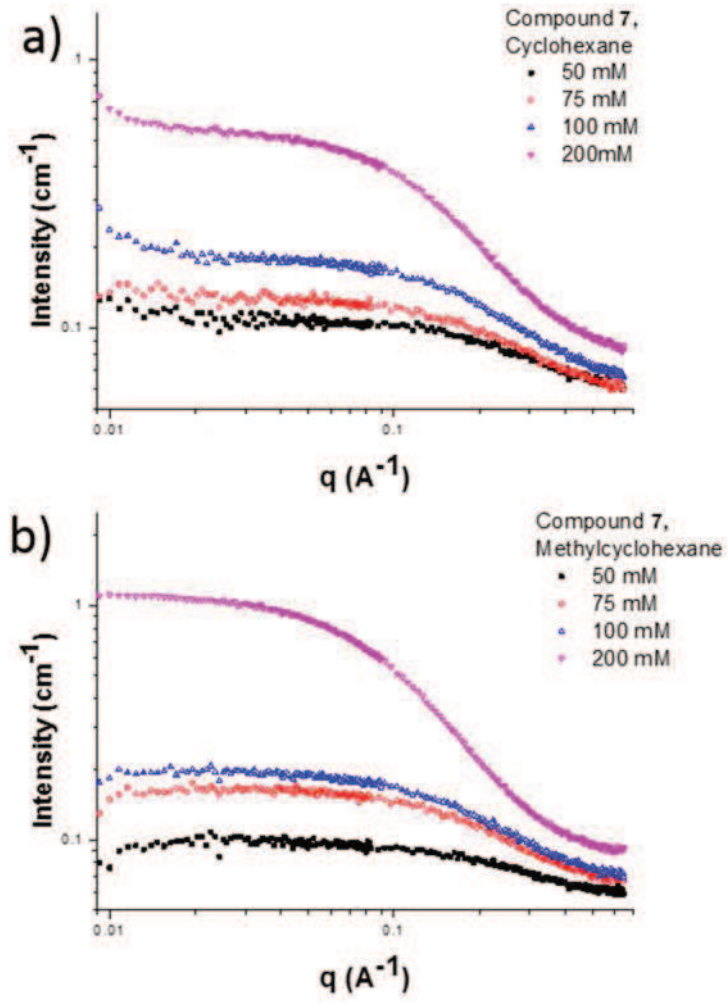


Figure C.4 SANS intensities of compound 7 in cyclohexane(a) and methylcyclohexane (b) in the concentration range of 75-200 mM, at 25 °C.

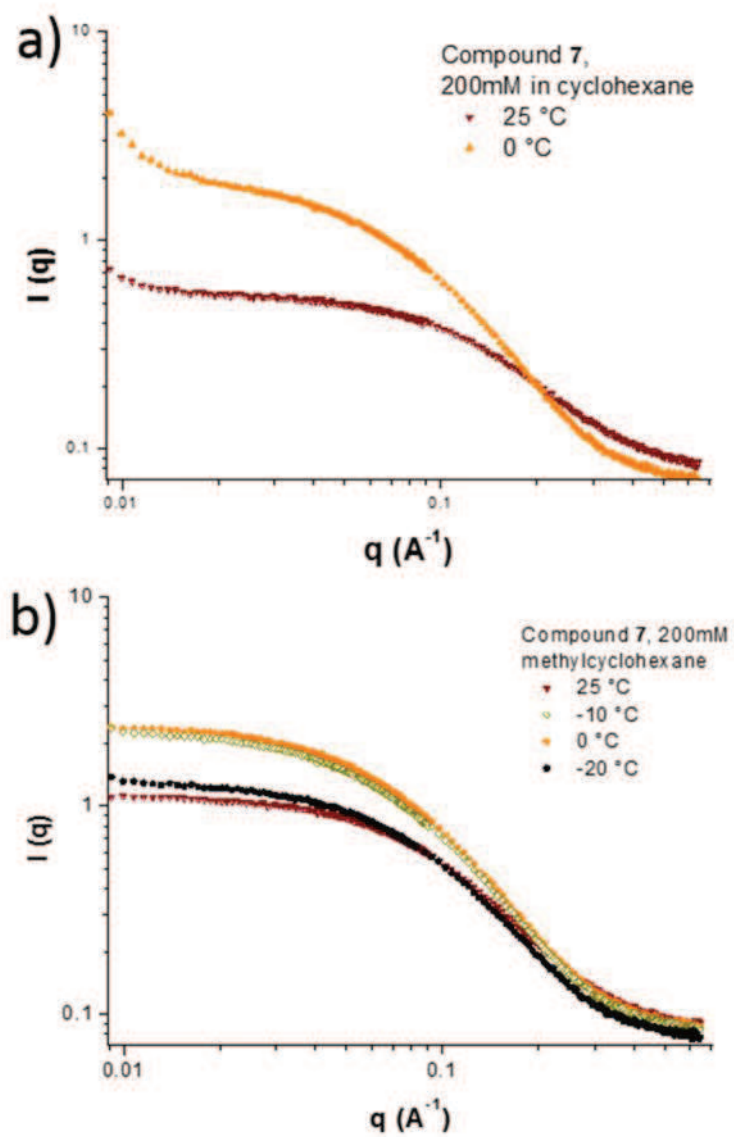


Figure C.5 SANS intensities of compound **7** in cyclohexane (a) and methylcyclohexane (b) at the concentration of 200mM at different temperatures.

Abbreviations List

- DLS Dynamic Light Scattering
- DOSY Diffusion Ordered Spectroscopy
- DSC Differential scanning calorimetry
- FCC Flash Column Chromatography
- MOA Menthyloxyacetic acid
- NMR Nuclear Magnetic Resonance
- PEG Polyethylene glycol
- SANS Small Angle Neutron Scattering
- SAS Small Angle Scattering
- SAXS Small angle X-Ray scattering
- TEGME Triethylene glycol monoethylether

Dottoranda: Manuela Facchin

Tutors: Alvise Perosa, Pietro Riello

Titolo della tesi: Life in Hydrocarbons: typical micelles in oil

Abstract

La scoperta dei laghi di idrocarburi presenti sulla superficie di Titano ha sollevato la questione dell'esistenza di membrane in grado di auto-assemblarsi in idrocarburi che potrebbero essere alla base della vita extraterrestre.

In questa tesi vengono descritti design, sintesi e aggregazione di una nuova classe di anfifili inversi in solventi idrocarburici. Questi anfifili inversi di nuova sintesi hanno una geometria simile a quella dei surfattanti tradizionali ma con configurazione topologica opposta, vale a dire testa lipofila e coda lipofobica.

La loro aggregazione in idrocarburi è stata studiata mediante una serie di tecniche diverse, tra le quali ¹H DOSY-NMR, SAXS, SANS, DSC, DLS. È stato dimostrato che gli anfifili inversi sintetizzati in questa tesi hanno la capacità di aggregarsi in solventi idrocarburici e di formare strutture micellari.

Abstract

The hydrocarbon lakes discovered on Titan prompted the question on the existence of membranes able to self-assemble in hydrocarbons that would be at the basis of life in such extra-terrestrial environments. This thesis describes the design, synthesis and the self-assembly behavior of a new class of reverse amphiphiles in a hydrocarbon solvent. The synthesised reverse amphiphilic molecules possess a geometry similar to conventional amphiphiles but with an opposite topological configuration: lipophilic heads and lipophobic tails. Their self-assembly in hydrocarbons was studied by using a number of techniques, including ¹H DOSY-NMR, SAXS, SANS, DSC, DLS. It was demonstrated that the reverse amphiphiles synthesized in this project are capable of self-assembly in a hydrocarbon solvent and that they form organized micellar-like structures.

Attività Scientifica:

Durante il triennio di dottorato di ricerca, Manuela Facchin ha sviluppato un progetto di ricerca il cui tema è stato la sintesi e lo studio del comportamento di nuovi anfifili inversi in solvente idrocarburico. Manuela ha condotto la propria ricerca scientifica con un alto grado di entusiasmo, autonomia e spirito di iniziativa in tutte le fasi: dall'identificazione del soggetto della ricerca, alla ricerca bibliografica, alla progettazione ed esecuzione delle sintesi, all'impiego delle tecniche di indagine delle strutture autoassemblate, all'interpretazione dei dati per finire con la scrittura dei lavori scientifici. Ha saputo interagire in maniera positiva e propositiva sia con noi come tutors così come con il gruppo di ricerca dimostrando spiccata capacità critica e di lavorare in team. Ha svolto tenacemente la sua ricerca anche quando alcuni risultati sembravano sfuggirle riuscendo a completare un corpo di lavoro omogeneo e di alto valore scientifico.

Il lavoro di ricerca è stato molto articolato e complesso, principalmente perché si è trattato di un lavoro completamente nuovo in un campo inesplorato della scienza. Non esistevano, infatti, altre pubblicazioni riguardanti la *self-assembly* di anfifili inversi in idrocarburi.

Nel corso del triennio la dottoranda Manuela Facchin ha svolto un periodo di ricerca all'estero della durata di 7 mesi presso The University of Sydney con il prof. Gregoy Warr. Ha esposto i risultati del suo lavoro a 6 convegni presentando personalmente le sue ricerche, ha pubblicato 1 lavoro scientifico su 1 rivista internazionale con sistema di referee (*Phosphonium-based tetrakis dibenzoylmethane Eu(III) and Sm(III) complexes: synthesis, crystal structure and photoluminescence properties in a weakly coordinating phosphonium ionic liquid RSC ADVANCES, vol. 5, pp. 60898-60907 (ISSN 2046-2069)*), e 1 lavoro scientifico è in via di pubblicazione.

Nel suo curriculum ha raggiunto un numero di crediti pari a 91 in accordo con quanto richiesto dal regolamento della Scuola di Dottorato. Ha partecipato attivamente a diverse attività formative quali conferenze, congressi e scuole, in particolare:

- 1° Scuola di Soft Matter, San Servolo, Venezia
- 20th International Symposium on Surfactants in Solution (SIS 2014), Coimbra, Portogallo
- Green Solvents Conference, Dresda, Germania
- Convegno: Life in a Cosmic Context, Italian Astrobiology Society, Trieste
- 30th Australian Colloid and Surface Science Student Conference, Kioloa, Sydney, Australia
- XLI International Summer School on Organic Synthesis "A. Corbella", Gargnano, Bs

Premi e riconoscimenti:

- Best poster award, Green solvents conference, Dresda;
- Endeavour Fellowship and Scholarship, Australian government

Elenco pubblicazioni, anche quelle in preparazione:

- Phosphonium-based tetrakis dibenzoylmethane Eu(III) and Sm(III) complexes: synthesis, crystal structure and photoluminescence properties in a weakly coordinating phosphonium ionic liquid RSC ADVANCES, 2015, vol. 5, pp. 60898-60907
- Typical micelles of reverse amphiphiles in liquid hydrocarbons, submitted to Angewandte Chemie.